CHARLES UNIVERSITY IN PRAGUE

FACULTY OF SCIENCE

Program of study: Mikrobiologie

Study branch: Microbiology

Blanka Jurková

Testing of anti-microbial and anti-adhesive properties of nanodiamond materials

Testování antimikrobiálních a antiadhezních vlastnostní nanodiamantových materiálů

Diploma thesis

Supervisor: RNDr. Jana Beranová, PhD

Consultant: Mgr. Halyna Kozak, PhD

Praha 2015

Prohlášení:

Prohlašuji, že jsem diplomovou práci zpracovala samostatně a že jsem uvedla všechny použité informační zdroje a literaturu. Tato práce ani její podstatná část nebyla předložena k získání jiného nebo stejného akademického titulu.

Declaration:

I declare that I have compiled my diploma thesis independently and that I have properly cited all the resources used. This thesis, nor its substantial part has not been submitted elsewhere with the aim of obtaining the same or another academic degree.

Prague, August 14th, 2015

Signature:

Firstly, I would like to thank my supervisor, RNDr. Jana Beranová, PhD., for her guidance, valuable remarks and patience during processing my diploma thesis.

I am very grateful to my consultant, Mgr. Halyna Kozak, PhD., for her numerous advices and valuable consultations in the field of nanomaterial physics.

My thanks go also to Ing. Alexander Kromka, PhD., for his support and many constructive discussions.

I would also like to thank to Ing. Oleg Babchenko, PhD., Ing. Anna Artemenko, Ph.D, Ing. Tibor Ižák, PhD., Ing. Egor Ukraintsev, PhD, Ing. Karel Hruška and Ing. Vlastimil Jurka for their technical support in the field of nanocrystalline diamond deposition and characterization.

Last, but not least, I would like to thank my family for their support during my studies.

This work was supported by grants GACR project P108/12/0910 and GACR 15-01687S from Czech Science Foundation.

Index

Abbreviations

a. u.	arbitrary units
AFM	atomic force microscopy
ATP	adenosin triphosphate
CFU	colony-froming unit
CLSM	confocal laser scanning microscopy
DAPI	4’,6-diamidino-2-phenylindole
DIC	differential interference contrast
EHT	extra high tension
NCD	nanocrystalline diamond
NCD-H	hadrogenated nanocrystalline diamond
NCD-O	oxidized nanocrystalline diamond
PGA	Poly-β-1,6-N-acetylglukosamine PGA
PI	propidium iodide
r. l. u.	relative luminescence unit
RMS	root mean square
sccm	standard cubic centimetre
SDS	sodium dodecyl sulphate
SEM	scanning electron microscopy
TEM	transmission electron microscopy
UV	ultra violet (light)
θ	contact angle
CVD	chemical vapour deposition
XPS	X-ray photoelectron spectroscopy

Abstract

Nanocrystalline diamond (NCD) films possess great mechanical properties (low friction coefficient, high hardness etc.), chemical properties (e.g. low corrosivity or chemical inertness) and good biocompatibility. This makes them perspective materials for protective coatings of medical implants and devices. As bacteria biofilms are often very resistant to antibacterial treatment, materials with anti-bacterial or at least anti-adhesive properties are needed. The interaction of NCD films with bacteria has not been properly examined yet. The aim of this thesis was to introduce and optimize the methods for routine bacterial biofilm cultivation and analysis, use them to investigate the ability of NCD films to inhibit the attachment and biofilm formation of *Escherichia coli* and correlate it with the NCD surface hydrophobicity.

The materials used for the study were hydrogenated NCD (hydrophobic), oxidized NCD (hydrophilic) and uncoated glass. For bacterial biofilm growth, cultivation in six-well plates and continuous cultivation in CDC Bioreactor was used. Several methods were tested for quantitative biofilm detachment and analysis. The putative anti-bacterial properties of NCD material were not confirmed in this work. Higher bacterial attachment to NCD films in comparison to the uncoated glass was observed. This effect may be caused by higher roughness of NCD films. The hydrogenated NCD films were more attractive for bacterial attachment than the oxidized NCD.

Key words:

Bacterial biofilms, adhesion, nanocrystalline diamond, surface hydrophobicity, continuous cultivation

Abstrakt

Nanokrystalické diamantové (NCD) filmy se vyznačují výbornými mechanickými vlastnostmi (nízkým koeficientem tření, velkou tvrdostí atd.), chemickými vlastnostmi (např. nízkou korozivitou či chemickou neaktivitou) a dobrou biokompatibilitou. Díky tomu se jeví jako perspektivní materiály pro ochranné vrstvy lékařských implantátů a pomůcek. Jelikož bakteriální biofilmy jsou často velmi rezistentní vůči léčbě, materiály s antibakteriálními nebo alespoň antiadhesivními vlastnostmi jsou velmi žádoucí, nicméně interakce bakterií s NCD nebyla doposud do hloubky zkoumána. Cílem této práce je představit a optimalizovat metody pro rutinní kultivaci bakteriálních biofilmů a jejich analýzu, pomocí těchto metod zjistit, zda jsou NCD schopné inhibovat adhezi a tvorbu biofilmu u *Escherichia coli,* a případně korelovat tuto schopnost s mírou hydrofobicity NCD povrchů.

Materiály užité v této práci byly hydrogenovaný NCD (hydrofobní), oxidovaný NCD (hydrofilní) a čisté sklo. Pro růst biofilmů byla využita kultivace v šesti jamkových destičkách a v CDC Bioreaktoru. Pro odloučení bakteriálních biofilmů z povrchu bylo testováno hned několik metod.

Domnělé antibakteriální vlastnosti NCD nebyly v této práci prokázány, naopak byla pozorována vyšší adheze k NCD filmům než ke sklu. Tento efekt by mohl být zapříčiněn vyšší drsností NCD filmů. Hydrogenované NCD filmy byly pro adhezi bakterií atraktivnější než oxidované.

Klíčová slova:

Bakteriální biofilmy, adheze, nanokrystalický diamant, hydrofobicita povrchu, kontinuální kultivace

1. Introduction

In nature, bacteria can live in planctonic form or in biofilms. The biofilms are studied from many points of view: the structure and morphology, composition of extracellular matrix and physiology of bacteria, environmental signals and signalization networks leading to maturation or detachment, etc. One of the aspects, which influence bacterial adhesion to solid surfaces and consequent biofilm formation is the interaction of cells with solid surface.

Living in biofilms is very beneficial for bacteria because it protects them from drying out, provides them protection against toxic agens or host immune system. Therefore bacterial biofilms might cause several problems in industry or serious infections in medicine. Curing secondary infections of surgery implants is very difficult and almost always results in operation and implant removal. Thus, the investigation and development of anti-adhesive and/or antibacterial coatings of these medical devices and implants or various industrial applications is a very perspective field of study. Finding new materials, which would help to solve these problems with resistant bacteria contamination and fouling is of great importance nowadays.

A perspective material for the use in medicine should combine chemical and physical inertness with good biocompatibility. Also, these materials should support eukaryotic cell attachment and hamper bacterial adhesion or even release bactericide agens.

Nanocrystalline diamond (NCD) films are materials of perfectly suitable properties for use in this area.

They can be deposited on great range of substrate materials with reasonable costs and exhibit similar properties to those of bulk diamond. They are hard with high durability and great optical properties. Also, they are physically and chemically inert, and they were also reported to be highly biocompatible with eukaryotic cells. This all makes them favourable for their use in medicine.

The surface of NCD films can be easily terminated by various elements or functional groups resulting in change of their electrical properties or easy modification by biomolecules such as proteins or nucleic acids. Therefore NCD films are very promising for biosensors or other electronic applications used in medicine such as electrodes or diodes etc. While interaction of NCD films with eukaryotic cells is quite well investigated, their interaction with bacteria is still unsolved question.

My work was a part of the cooperative project of the Laboratory of Bacterial Physiology (Dpt. of Genetics and Microbiology, Faculty of Science, Charles University in Prague) with the Laboratory of diamond thin films and carbon nanostructures (Dpt. of Optical materials, Institute of Physics, Academy of Science of the Czech Republic, v. v. i.). One of the aims of this project is to investigate the antibacterial potential of different carbon materials. In my work, I focused on nanodiamond, a material with unique physical and chemical properties. My task was to characterize the tested material, introduce a cultivation and quantification method for testing of the adherence of bacteria on different surfaces and finally to use

these methods to investigate the tendency of *Escherichia coli* to adhere to glass surface coated by nanocrystalline diamond films with different hydrophobicity.

2. Aims of the thesis

- To prepare and characterize nanocrystalline diamond films with hydrophobic and hydrophilic surface properties

- To optimize and implement new basic methods to our laboratory to enable:
  - Cultivation of bacterial biofilms on various solid surfaces
  - Quantification of bacteria grown in these biofilms
  - Observation of grown biofilms and their qualitative analysis

- To investigate possible anti-adhesive properties of nanocrystalline diamond films against *Escherichia coli* and correlate them with their surface hydrophobicity

3. Literature review

3.1. Bacterial growth and biofilm formation on solid surfaces

3.1.1.Bacterial growth in biofilms

In nature, bacteria commonly live in two states: in planctonic form or they can aggregate, attach to solid surface and form so-called bacterial biofilm.(Costerton *et al.*, 1999; Stewart, P. S. and Costerton, 2001; Donlan, R. M., 2002; Ploux *et al.*, 2007; Lewis *et al.*, 2010).

This chapter briefly reviews the basic knowledge on bacterial growth in biofilms, especially the mechanisms of primal adhesion of bacteria to solid surfaces, the factors that may promote or inhibit formation of bacterial biofilm and available methods for bacterial biofilm growth and quantification. The main attention is payed to bacterium *E. coli* because this bacterium was used in this study.

3.1.1.1. General structure and location of biofilms

Bacteria have strong tendency to attach to solid surfaces, accumulate there and form structured aggregates called biofilms. Biofilms are defined as multicellular communities which consist of bacterial cells (of one or more species) embedded in extracellular matrix (3.1.1.2) (Figure 1) (J.William Casterton, 1995; O'Toole George, 2000).

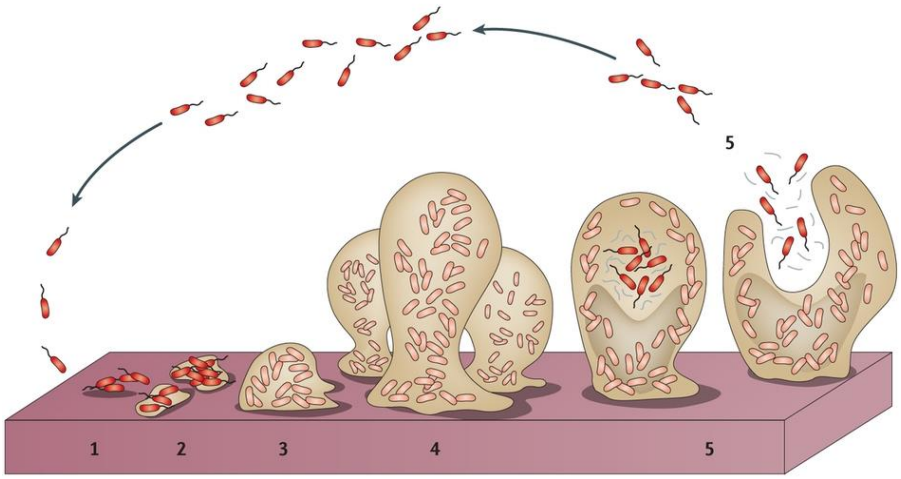

Figure 1 The biofilm development. The individual stages are depicted from left to right. (Lappin-Scott et al., 2014)

This way of living brings several advantages compared with planctonic growth. These are, for example, higher resistance to antibiotics and other antibacterial agents (J.William Casterton, 1995; Costerton *et al.*, 1999; Watnick, P. and Kolter, 2000; Stewart, P. S. and Costerton, 2001; Donlan, R. M., 2002; Ploux *et al.*, 2007), protection against drying, antibodies or phagocythosis (Costerton *et al.*, 1999; Stewart, P. S. and Costerton, 2001; Lacqua *et al.*, 2006; Beloin *et al.*, 2008). Due to increased resistance,

bacterial biofilms present serious problems in healthcare (Passerini *et al.*, 1992; Costerton *et al.*, 1999; Morris *et al.*, 1999; Stewart, P. S. and Costerton, 2001). ECM also prevents the washing-out of nutrients, digestive enzymes and signalling molecules from the proximity of the cells (Redfield, 2002; Flemming and Wingender, 2010).

3.1.1.2. Composition of extracellular matrix

Extracellular matrix (ECM) is a three-dimensional scaffold formed by hydrated extracellular substances excreted by biofilm-forming bacteria. ECM is composed of highly hydrated and viscous layers of slime. The chemical composition of ECM is highly variable and depends on bacterial genus, species or even strain and also on the growth conditions and various environmental signals (Flemming and Wingender, 2010).The main components of ECM (Figure 2) are saccharides (glucose, galactose, mannose, fructose, rhamnose, alginate, amino-sugars etc.), which are usually polymerised, various bacterial proteins (adhesins, curli, pili or fimbriae), uronic acid, extracellular DNA (Figure 3) and extracellular RNA, lipids and ions (Sutherland, 2001; Das *et al.*, 2010; Flemming and Wingender, 2010). These components all contribute to the shape and structural stability of whole biofilm and enhance the adhesion and immobilization of the cells (Das *et al.*, 2010; Flemming and Wingender, 2010).

In *E. coli* biofilms, the key polysaccharides are poly-β-1,6-N-acetylglukosamine (PGA) and cellulose. It was shown, that PGA plays a role in cell-cell and cell-surface adhesion (Agladze *et al.*, 2005). Concerning the cellulose, *E. coli* wild type strains are endowed with genes for cellulose production

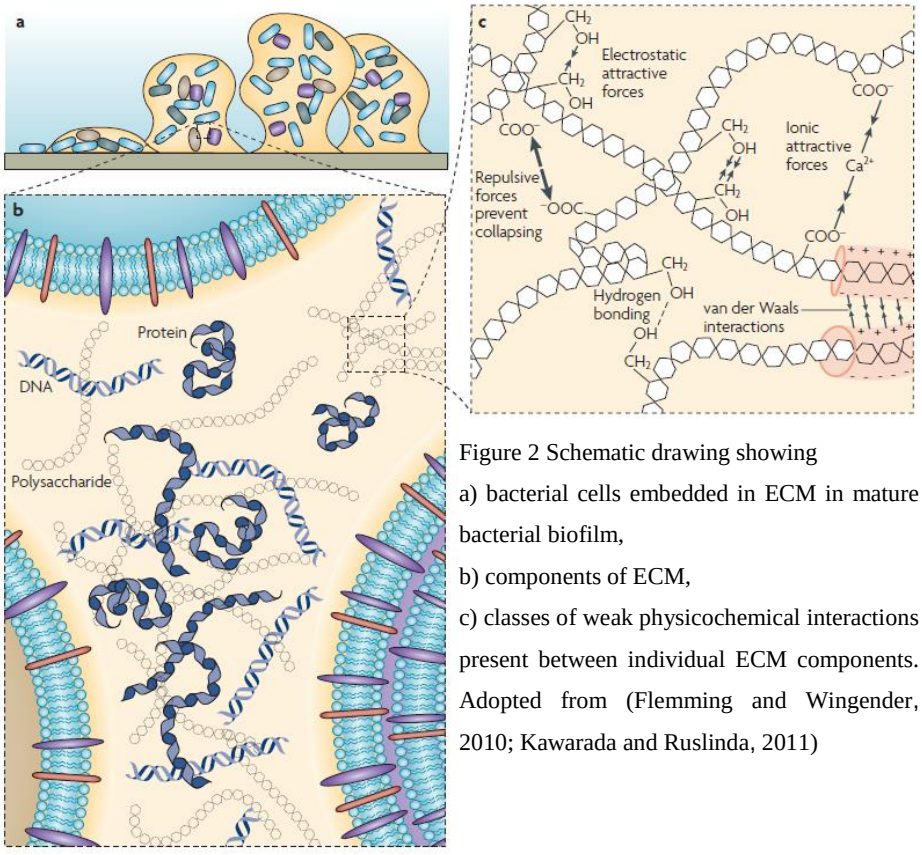

Figure 2 Schematic drawing showing
a) bacterial cells embedded in ECM in mature bacterial biofilm,
b) components of ECM,
c) classes of weak physicochemical interactions present between individual ECM components. Adopted from (Flemming and Wingender, 2010; Kawarada and Ruslinda, 2011)

(Zogaj *et al.*, 2001; Zogaj *et al.*, 2003; Shoda and Sugano, 2005; Beloin *et al.*, 2008), however the laboratory strain K-12, which was also used in this work, does not produce cellulose due to mutation in the crucial gene of the operon (Zogaj *et al.*, 2001). It was shown that degradation of these two polysaccharides by metaperiodate or β-hexosaminidase (for PGA) and cellulase (for cellulose), respectively, leads to total dispersion of the whole biofilm (Zogaj *et al.*, 2001; Romling, 2002; Zogaj *et al.*, 2003; Wang *et al.*, 2004; Itoh *et al.*, 2005; Da Re and Ghigo, 2006; Beloin *et al.*, 2008). Another substance often detected in *E. coli* biofilms is colanic acid (Beloin *et al.*, 2008). This polymer, composed of glucuronic acid, glucose, galactose and fucose, is produced only under specific environmental and growth conditions (Beloin *et al.*, 2008). For instance, it is not produced in rich medium at 37°C (Beloin *et al.*, 2008). Though colanic acid was reported to diminish initial bacterial attachment, it was also shown to participate in the development of the biofilm architecture (Danese *et al.*, 2000; Hanna *et al.*, 2003).

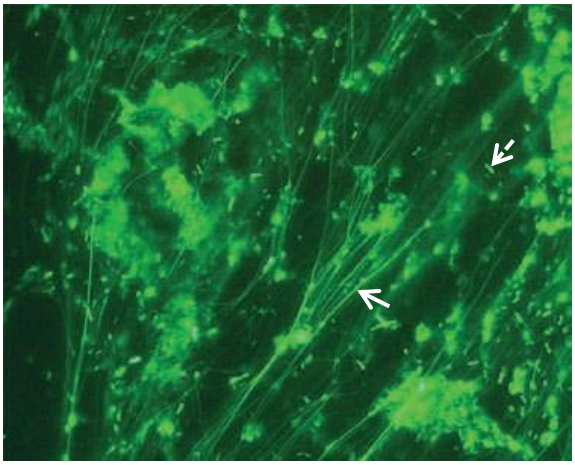

Figure 3 Extracellular DNA (fibrous structures – solid arrow) present in the biofilm matrix. The specimen was stained with SYTO9 strain which binds DNA. Apart from the extracellular DNA, bacteria are visible as small rods between the DNA strands (dashed arrow). Modified from (Flemming and Wingender, 2010).

3.1.1.3. Biofilm development

The formation of bacterial biofilm comprises three main stages: (1) attachment, (2) maturation and (3) detachment (Beloin *et al.*, 2008). Because this work is focused on bacterial adhesion to the surface of NCD films, the initial stages of biofilm formation are reviewed preferentially.

3.1.1.3.1. The primal adhesion and biofilm maturation

Prior bacterial attachment, many compounds form surrounding medium adhere to the surface.

These compounds (which can be salts, proteins etc.) form a layer called conditioning film (Stoodley *et al.*, 2002). Therefore, bacteria are not in direct contact with the bare surface but attach to this conditioning film.

Bacterial cells are driven to the surface proximity by Brownian motion, diffusion, gravitation (Boland Thomas, 2000) or even by chemotaxis (Kirov, 2003). Two processes contribute to bacterial

attachment: (1) non-specific physicochemical interactions between the cell surface and the surface of the substrate (based on charge, free energies, hydrophobicity etc. – see below) and (2) specific interactions between adhesive molecules present at the material surface and at the surface of bacteria (i.e. flagella, adhesins etc.)

The very first phase of the attachment is dependent mainly on physicochemical interactions. These interactions, which usually manifest when the cell is close enough to the surface, can be hydrophobic, electrostatic or chemical (e.g. hydrogen bonding) (Mayer *et al.*, 1999; Gottenbos *et al.*, 2002). Despite the fact that the exact mechanism of bacterial attachment to the surface is not known yet, there exist three theories describing these interactions (Katsikogianni M., 2004).

First is the thermodynamic approach, which compares the free energies between the interfacing surfaces. It can be described by equation

$$\Delta G_{adh} = \gamma_{SM} - \gamma_{SL} - \gamma_{ML}$$

where ΔG_{adh} is the total adhesion energy and γ_{SM} , γ_{SL} and γ_{ML} are interfacial energies between solid surface and the microorganism, solid surface and liquid medium and finally microorganism and liquid medium, respectively. This approach can be also used to calculate the microbial adhesion or co-adhesion of different microbial species (Bos *et al.*, 1999). The adhesion of bacteria is always more favourable if the total adhesion energy ΔG_{adh} is lower (Shao *et al.*, 2009).

The other theory is called Derjaguin-Landau-Verwey-Overbeek (DLVO) theory and can be described by following equation:

$$G_{adh} = G_{vdW} + G_{EL}$$

where ΔG_{adh} refers to the total adhesion energy, G_{vdW} to the van der Walls interactions and G_{EL} to the electrostatic interactions which origin from the negative charges of the cell and the surface to which the cell adheres (i.e. these interactions could be Coulomb interactions) (Katsikogianni M., 2004).

The interaction of a bacterial cell and a surface is described by this theory as a balance between repulsive (usually G_{EL}) and attractive forces (usually G_{vdW}).

Both, the DLVO theory and the thermodynamic approach, have several drawbacks: the DLVO theory does not take into account the interactions which would contribute to the attachment when the components of ECM or conditioning film are present and, also, it is not able to explain the different levels of attachment observed on different types of surfaces or in different solutions (Katsikogianni M., 2004). Whereas the thermodynamic approach does not allow for kinetic interpretation because the interaction energy is distance independent (Katsikogianni M., 2004). Anyway, either of these theories has been accurate in predicting bacterial attachment in various environments (Katsikogianni M., 2004).

The third, and also last, theory is the extended DLVO theory (Jucker *et al.*, 1998; Hermansson, 1999) which combines components of the DLVO theory with components from thermodynamic approach. The total adhesion energy (ΔG_{adh}) can be expressed as:

$$\Delta G_{adh} = \Delta G_{vdW} + \Delta G_{dl} + \Delta G_{AB} + \Delta G_{BR}$$

where ΔG_{vdW} and ΔG_{dl} are the classical van der Waals (vdW) and double layer (dl) interactions, ΔG_{AB} represents acid-base interactions and ΔG_{BR} Brownian motion (Katsikogianni M., 2004; Shao *et al.*, 2009).

Hence, all the theories count with individual components of energy. However, the estimation their real values is quite a complex problem in many real cases. In short, the individual parameters can be predicted usually from the surface energies of the bacterial cell, solid material and liquid. These can also have various components, which can sometimes be calculated from the data gained from contact angle measurements with various liquids (3.1.3.2). As thorough discussion on various approaches of counting these energies is beyond the scope of this thesis, for more information on this topic refer to the article of Bos *et al.* (1999).

The surface hydrophobicity (which is reflected by the contact angle value) and surface energies are ones from the most watched surface properties in studies focused on bacterial attachment to

solid surfaces of different materials, such as nanocrystalline diamond or diamond-like carbon films (3.3). However, for the exact estimation of ΔG_{adh}, also the information on hydrophobicity and surface energy of the bacterial cell is needed. However, obtaining the accurate values of these two parameters is very difficult especially because of the complex chemistry and hydration *in vivo* (Bos *et al.*, 1999).

After a bacterium approaches the solid surface and loosely adheres to it via nonspecific physical interactions, more specific chemical interactions start to play a role. There are many structures present on the bacterial surface which are of importance in cell-surface and cell-cell interactions crucial for stability of the whole biofilm: flagella, adhesins, fimbriae, curli, cell surface polysaccharides, ECM etc.

Flagella are important in bacterial adhesion, though their presence is not always required (Boland Thomas, 2000; Prigent-Combaret *et al.*, 2000). Also, the motility conferred by flagella probably enables to overcome the repulsive forces between the bacterium and the surface. Flagellar motion not only promotes easier attachment but also probably helps bacteria to spread along the material surface (Pratt and Kolter, 1999; Boland Thomas, 2000). Bacteria usually lose flagella during biofilm maturation (J.William Casterton, 1995). The renewal of flagellar synthesis, followed by restoration of swimming motility, is most probably connected to the detachment of the cells from mature biofilm (Pratt and Kolter, 1998; Bos *et al.*, 1999).

Other proteins involved in bacterial adhesion are pilins, especially FimH adhesin which is located at the tip of the type I pilus. FimH usually binds mannose oligosaccharides, but it was also reported to

bind nonspecifically to abiotic surfaces (Pratt and Kolter, 1998). Another adhesin, a self-organizing surface autotransporter Ag43, plays an important role in cell-cell interactions, which take place when the biofilm is getting thicker (Kjaergaard *et al.*, 2000).

Bacterial curli were also shown to be present in bacterial biofilms. These non-branching, fibrous, amyloid-like and β-sheet rich proteins (Barnhart and Chapman, 2006) bind to many components of eukaryotic ECM such as fibronectin, laminin, plasminogen (Olsen *et al.*, 1989; BenNasr *et al.*, 1996; Barnhart and Chapman, 2006). Also bacterial surface polysaccharides such as lipopolysaccharide (LPS) contribute to the primal adhesion process. *E. coli* strains, in the which synthesis of LPS was genetically supressed, showed lower ability to adhere to solid surfaces than wild type strains (Beloin *et al.*, 2008).

Once bacteria irreversibly attach to the surface, they start to grow and form microcolonies. Then the microcolonies start to unite and form seamless layer of bacterial cells tied together by ECM. The mature biofilm can be very structured – with apparent mounds, voids or water channels (Figure 4), which serve to nutrient and metabolite exchange between the biofilm and surrounding environment.

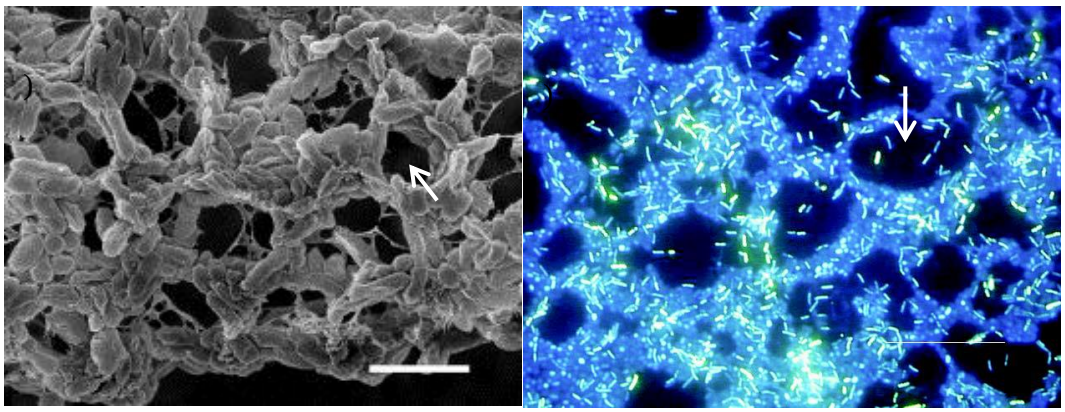

Figure 4 a - The SEM image of water channels (arrow) in biofilm of Haemophilus influenza. Scale bar = 2 μm. Modified from (Gallaher *et al.*, 2013); b – 14-day-old polymicrobic biofilm stained with DAPI and observed by fluorescence microscope. The water channels (arrow) are observable (Donlan, R. M., 2002).

3.1.1.3.2. The biofilm detachment

The detachment is the final stadium of biofilm development. During this phase, bacterial cells leave the biofilm. The detachment and releasing the cells to the environment can be caused by (1) physiological shift from sessile mode of living back towards the planctonic one. This is often connected with extracellular signalization and restored expression of flagellar genes (Flemming and Wingender, 2010) or (2) by physical forces – shearing (constant removal of small parts of biofilm), abrasion or sloughing (detachment of big portion of biofilm) (Donlan, R. M., 2002).

Surface physical properties, especially its wettability, seem to have substantial impact on biofilm detachment. In addition to purely mechanistic explanation, i.e. the fact that certain types of surfaces allow

tighter physical adhesion, it has been hypothesized that bacterial cells are able to sense the surface features and through specific signalization cascades trigger the biofilm detachment (Ploux *et al.*, 2007).

3.1.2. Factors, that influence biofilm formation

Bacterial biofilm formation is a quite complex process and can be influenced by many factors. One of these factors is the accessibility of nutrients. It has been shown in many studies, that nutrient deprivation promotes bacterial biofilm formation of *E. coli* (Dewanti and Wong, 1995; O'Toole George, 2000; Oh *et al.*, 2007). It appears that in low-nutrient medium *E. coli* is able to produce more ECM, which probably helps bacterial cells to adhere to the surface and to attach each other (Dewanti and Wong, 1995). For example, it was shown that the cultivation of *E. coli* on minimal medium (M9) supported fast biofilm formation (Oh *et al.*, 2007). However, some strains of *E. coli* were not able to form biofilm in minimal medium unless supplemented with amino-acids (Pratt and Kolter, 1998; Watnick, P. I. *et al.*, 1999). Also the carbon source can influence the biofilm formation (Figure 5). The cells of *Pseudomonas aeruginosa* cultivated on succinate dispersed over the whole surface while those cultivated on glucose formed discernible mounds. The biofilm grown on succinate was also flatter and showed more regular topology than the one cultivated on glucose (Karatan and Watnick, 2009).

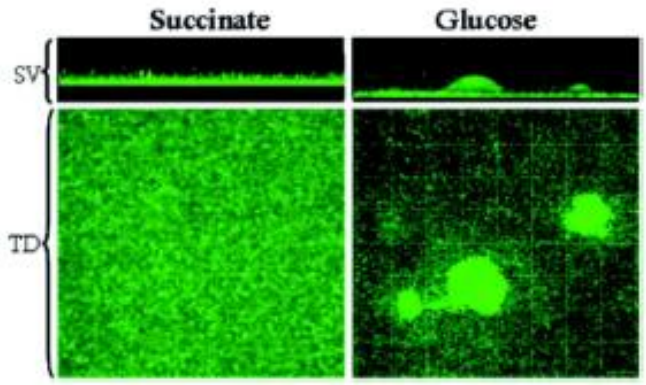

Figure 5 Different morphology of biofilm produced by *Pseudomonas aeruginosa* grown with succinate or glucose as a carbon source. (Karatan and Watnick, 2009).

Shear stress also influences the bacterial biofilm development (Figure 6). It could seem that the higher the flow is, the less bacteria are able to adhere to the surface but the experiments of Liu, Y. and Tay (2002) showed that there exists an optimal flow rate for biofilm formation as a balance between detachment and bacterium delivery to the surface. The higher sheer forces influence not only the number of attached bacterial cells but also the biofilm morphology: biofilms formed under more rapid flow are usually thinner and denser than those formed under static conditions (Chang *et al.*, 1991; Donlan, R. M., 2002). In response to different flow conditions, bacteria can alter their cell size, population density and metabolic activity (Liu, Y. and Tay, 2001; Liu, Y. and Tay, 2002).

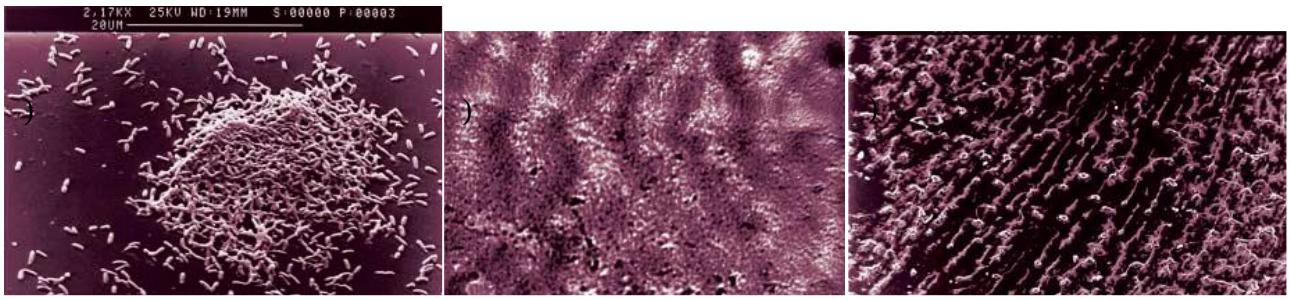

Figure 6 Different morphologies of biofilms (*P. aeruginosa*). a – "mound-like" structure of biofilm grown in low-sheer environment; b – ripple structure of biofilm grown in faster flow; c – biofilm streamers grown in high-sheer environment. Modified from (Hall-Stoodley *et al.*, 2004).

The properties of the solid surface to which the bacterium adheres is very important, too. The hydrophobicity (3.1.3.2) (Tegoulia and Cooper, 2002; Bakker *et al.*, 2004) and charge (Donlan, R. M., 2002; Li and Logan, 2004; Ploux *et al.*, 2007) of both the bacterium and the solid material surface plays substantial role in bacterial attachment and so it also influences the formation of the biofilm itself. Generally speaking, the bacteria with hydrophilic surface prefer hydrophilic substrates and those hydrophobic ones prefer hydrophobic material surfaces (Fletcher and Loeb, 1979; Taylor *et al.*, 1998; Katsikogianni M., 2004). Gram negative bacteria were reported to be rather hydrophobic due to presence of O-antigen in their LPS (Donlan, R. M., 2002). It was shown, that bacterium *Pseudomonas fluorescence* which lacked O-antigen attached more to hydrophilic surfaces (Williams, V. and Fletcher, 1996). Also, the strains of *E. coli* with longer LPS adhered better to solid surfaces than those with a shorter one (Li and Logan, 2004).

The surface roughness and morphology also influence the bacterial attachment. Bacteria adhere to rougher surfaces more easily than the smooth ones, probably due to their increased surface area (Taylor *et al.*, 1998; Katsikogianni M., 2004). It was also shown that bacteria adhere most likely to the surface irregularities which correspond with their cell size as was demonstrated by (Katsikogianni M., 2004) (Figure 7). This was confirmed by calculation of Edwards and Rutenberg (2001), who showed that bacterial attachment is the most favourable in grooves, which corresponds both with bacterial size and shape.

3.1.3.Methods of bacterial biofilm growth, observation and quantification

3.1.3.1. Biofilm cultivation methods

There have been many systems developed for *in vitro* cultivation of biofilms. They can be divided into two groups – batch systems and systems operated under continuous-flow conditions.

One of the methods is the cultivation in microtiter plates or well-plates (O'Toole and Kolter, 1998; Ceri *et al.*, 1999; Thuptimdang *et al.*, 2015). The cultivation is realized usually under static conditions, however the shear forces can be included if the dish is placed onto a rotary shaker (O'Toole and Kolter, 1998; O'Toole *et al.*, 1999; Zhao *et al.*, 2007).

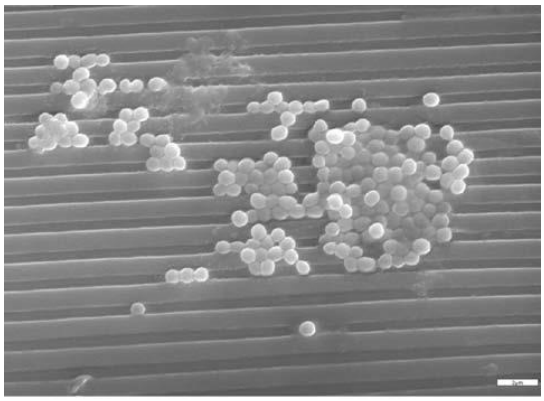

Figure 7 *Staphylococcus epidermidis* adhering to grooved polycaprolactone. The bacterial cells tend to attach especially into the grooves (Katsikogianni M., 2004).

The adhesion of bacteria to different surfaces, so called slide and bead methods can also be used. Slide methods are based on immersion of a slide of studied material into the bacterial culture (Bos *et al.*, 1999; Medina *et al.*, 2012). These cultures also can be grown under flow conditions in a shaker.

Very similar to slide methods are so called bead methods, which are based on (usually) glass beads immersed into the bacterial culture (Figure 8) (Bos *et al.*, 1999). The beads can be also placed into a column or a flask to simulate the development of bacterial biofilm in the soil (Ceri *et al.*, 1999). In contrast to slide methods, the bead methods are characterized by high substratum area relative to the bacterial culture volume (Bos *et al.*, 1999).

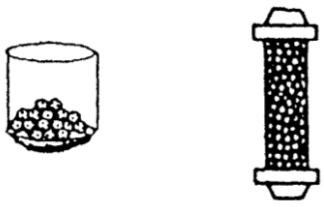

Figure 8 Schematic drawing of glass beads in a flask and in a column

However, the main drawback of the slide and bead methods represents the usually poorly characterized growth conditions. Therefore these methods are not practical for precise testing of bacterial adhesion. For these kinds of tests, flow systems are usually used to gain more accurate results. The most sophisticated device for the research of bacterial attachments are flow-chambers (Sjollema *et al.*, 1989; Dickinson *et al.*, 1995; Hanna *et al.*, 2003; Shao *et al.*, 2009) (Figure 9). These are small chambers with transparent surfaces which allow real-time observation of biofilm development. The nutrient supply is

provided by the continuous flow of fresh medium (Christensen *et al.*, 1999; Branda *et al.*, 2005). The *in situ* observation provides the possibility of quantifying nearly every parameter involved in the deposition process, including the kinetics of adsorption and desorption, as well as the spatial arrangements of the adhering microorganisms (Bos *et al.*, 1999). Also, the mass transport is usually very fast because it is independent on diffusion (Rijnaarts *et al.*, 1993) and can be easily controlled. However, this method is limited in number of samples which can be tested at once and therefore the method is quite time-consuming (Donelli, 2014).

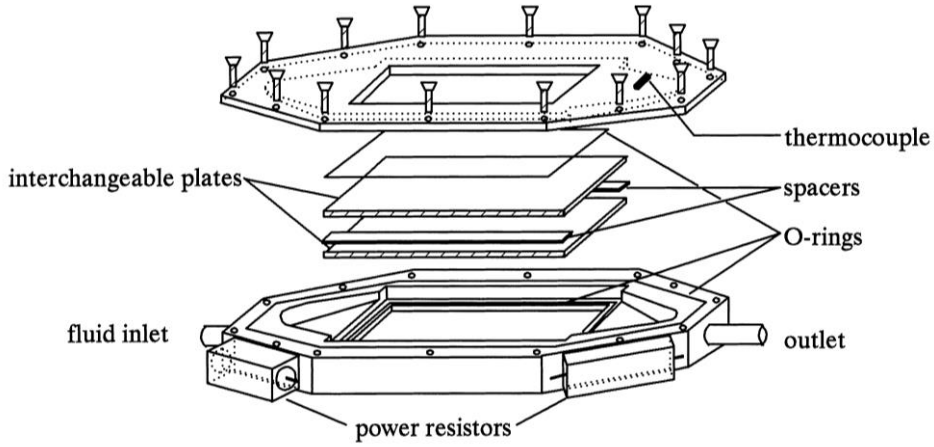

Figure 9 Schematic drawing of a flow chamber (Bos *et al.*, 1999).

To study the bacterial attachment to various materials at once, [1]CDC biofilm reactor (CDC Bioreactor) can be used instead (Lewis *et al.*, 2010; Thuptimdang *et al.*, 2015). This device was developed by Donlan, R *et al*. (2002).

The CDC Bioreactor (Figure 10a) consists of the main glass vessel with the side-arm discharge port and from the UHMW-polyethylene ported lid. The lid contains: slots for 8 sample holders (which can carry 3 round coupons each or one slide sample – Figure 10b), attached magnetic teflon stirrer, vents for air-exchange with a filter and the inlet for fresh medium influx. Because all the studied specimens can be inserted into the same bacterial culture, the errors caused by cultivation deviations are eliminated (Goeres *et al.*, 2005). This device was also used in this work for estimation of antiadhesive properties of NCD films.

3.1.3.2. Determination of the bacterial cell surface hydrophobicity

[1] CDC = Centre for disease control

http://www.google.com/url?url=http://www.jysco.com/product/download.php%3Fit_id%3D1217998050%26it_file%3D236991873_4a5c04ab_CDC_Operators_Manual.pdf&rct=j&q=&esrc=s&sa=U&ved=0CC8QFjAAahUKEwiUz-C3taTHAhVDBBoKHc7vCVs&usg=AFQjCNEMocX5uMJJZWqyfD19x5abDKXWpA

Contact angle measurement is a method widely used for surface hydrophobicity evaluation in general. It is usually used for evaluation of hydrophobicity of solid surfaces (Li and Logan, 2004; Zhao *et al.*, 2007; Liu, C. *et al.*, 2008; Marciano *et al.*, 2009b; Marciano *et al.*, 2009a; Marciano *et al.*, 2011; Beranova *et al.*, 2012; Beranova *et al.*, 2014) but can be also used for measuring the wetting properties of bacterial lawns (Shao *et al.*, 2009). The main advantage of this method lies in its simplicity: a drop of water is applied on the sample surface and the angle between the sample surface and a tangent line to the water droplet surface (at the point where the water droplet contacts the sample surface) is measured (Figure 11). The resulting angle is called the contact angle (θ) and reflects the degree of surface hydrophobicity – the higher the contact angle is, the more hydrophobic is the sample surface.

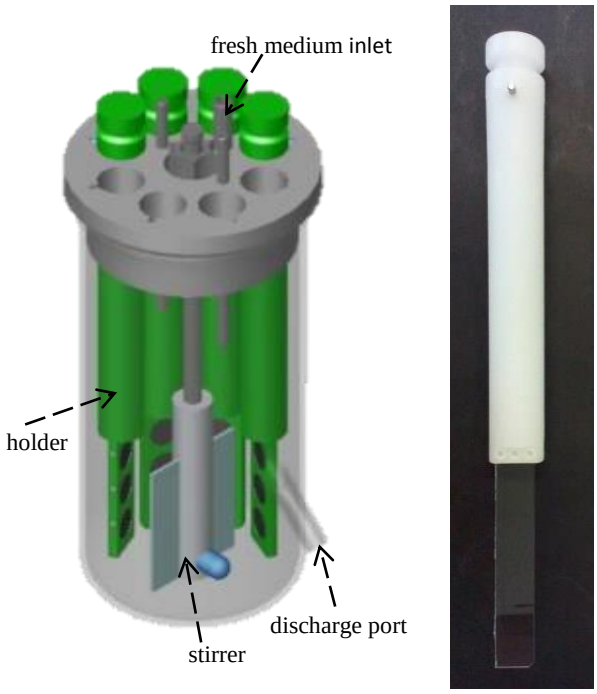

Figure 10 CDC biofilm reactor. a) schematic drawing of CDC Bioreactor with the lid, four inserted holders and magnetic stirrer, b) a holder with inserted glass sample. Source: CDC Biofilm manufacturer's manual

The determination of wetting properties of bacterial cell surface can be done by way of the method called microbial adhesion to hydrocarbons (MATH). This method was developed by (Rosenberg *et al.*, 1980) in 1980 and is based on adhesion of bacterial cells to various solvents, usually decane, hexane, chloroform and ethylacetate. Bacterial suspension is mixed thoroughly with a solvent. Because the solvents are not polar, they separate from the aqueous solution (bacterial culture) spontaneously after few minutes. The adherence of bacteria to various solvents is determined from absorbance before and after mixing. The equation for calculation adherence is:

$$\text{Adherence (\%)} = (1\text{-}A/A_0) \times 100$$

where A is absorbance after mixing and A_0 is absorbance before mixing. The absorbance is measured generally at the wavelength of 400 nm (BellonFontaine *et al.*, 1996).High affinity to decane and hexane signifies the hydrophobic character of bacterial cells. High affinity to hexadecane and chloroform shows to basic (electron-donor) character and high affinity to decane and ethyl acetate means acid (electron-acceptor) character of the cell surface (BellonFontaine *et al.*, 1996).

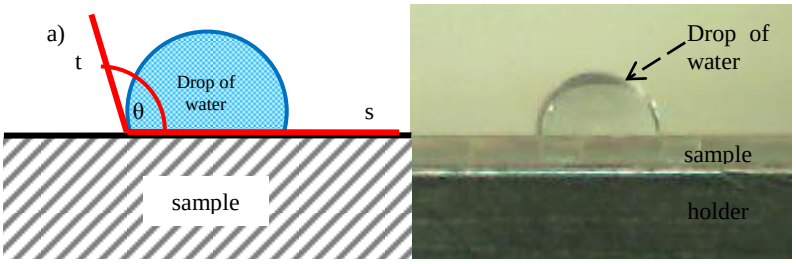

Figure 11 Contact angle measurement. a) Schematic drawing of contact angle measurement; s – surface, t – tangent line to the water drop at the point of contact between water and surface, θ – contact angle; b) droplet of water on the sample, contact angle was about 70°.

3.1.3.3. Methods used for biofilm analysis

Biofilms can be quantified by means of many methods. The solid material with the adherent bacteria can be sonicated and subsequently plated on agar plates (Zhao *et al.*, 2007; Hannig *et al.*, 2010; Medina *et al.*, 2012). Also biofilms can be stained with crystal violet followed by absorbance measurement (Stepanovic *et al.*, 2000; Thuptimdang *et al.*, 2015).

Very often, confocal laser scanning microscopy (CLSM) is used to visualize the structure of a biofilm (Branda *et al.*, 2005; Hannig *et al.*, 2010; Lewis *et al.*, 2010). It is often used for observation of the biofilm development in the flow chambers (Christensen *et al.*, 1999; Branda *et al.*, 2005; Romeo, 2008) and can be even used for observation of three-dimensional structure of thick biofilms (Figure 12) (Thormann *et al.*, 2004; Donelli, 2014).

For fluorescent microscopy, the appropriate staining is needed. One of the most used fluorescent dyes is DAPI (4',6-diamidino-2-phenylindole), which binds to AT rich regions of DNA of both vital and dead cells (Schwartz *et al.*, 2003). This stain is suitable for visualisation of the whole biofilm and also for calculation of the total cell number. However, no information on viability or bacterial species is provided, if this stain is applied (Hannig *et al.*, 2010).The differentiation of microbial species within multispecies biofilms is possible with the use of fluorescence *in situ* hybridization (FISH). Since this method is based on hybridization of oligonucleotide probe with rRNA, the bacteria need to be in good physiological state to be stained (Amann *et al.*, 2001).

For differential staining of live and dead bacteria, so-called live/dead staining techniques can be used. They are generally based on use of two fluorescent dyes with different ability to penetrate living cells. For life/dead staining of biofilms, dyes Syto9 and propidium iodide (PI) are often used (Ploux *et al.*,

2007; Peeters *et al.*, 2008). Syto9, since its molecules are small, can penetrate viable cells, while PI stains only the dead ones (Boulos *et al.*, 1999).

To achieve higher resolution, electron microscopic techniques can be used for biofilm visualisation.

The high resolution microscopic techniques overviewed here are scanning electron microscopy (SEM), transmission electron microscopy (TEM), and atomic force microscopy (AFM).

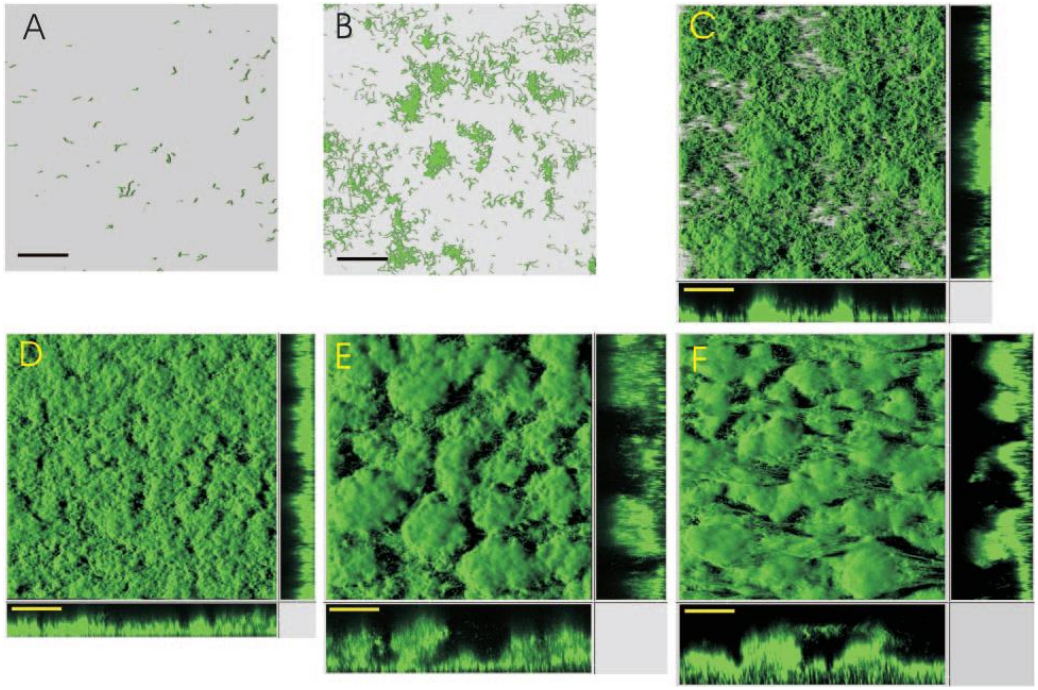

Figure 12 Visualisation of biofilm development by CLSM. x-z and y-z sagittal images at selected positions in the biofilm are shown at the bottom and right side of images C-F, respectively. Images were taken after 1, 8, 16, 24, 48, and 120 h (A-F, respectivelly). Scale bar = 80 µm. (Thormann et al., 2004)

SEM offers three-dimensional visualisation of the bacterial biofilm (Figure 13) and also solid surfaces. The principle of SEM is based on production of high-energetic electrons generated by a special cathode. These electrons are accelerated by extra high tension (EHT) and focused by magnetic lenses to

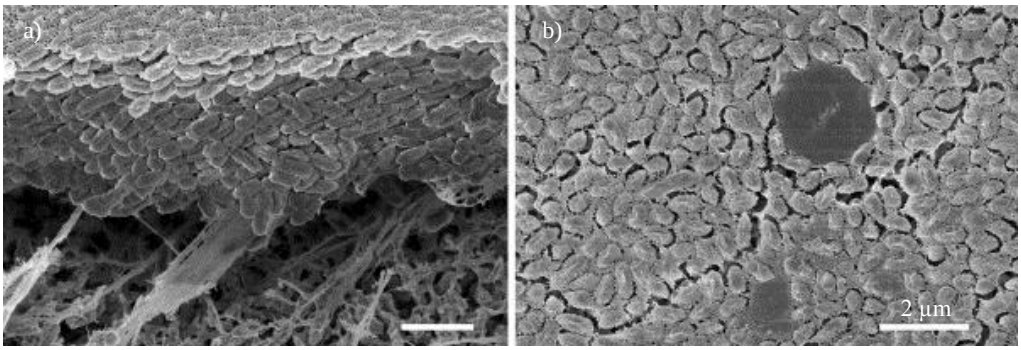

Figure 13 The SEM images of biofilms formed by *Haemophilus influenzae*. a – cross-section of thick biofilm with the base attached to the filter substrate, b – the top surface of the biofilm ECM covering the bacteria-free pockets. (Gallaher *et al.*, 2013)

one spot on the sample. The final signal, captured by the detector, comes from the electrons that result from the interaction of the electron beam with atoms on the sample surface. Conductive samples are preferable for this technique, because electrostatic charge can accumulate on the surface of electrically resistant samples (Kozak *et al.*, 2009b; Neykova *et al.*, 2012). Therefore, the biological samples need to be dehydrated and coated by a thin layer of conductive material as bacteria are non-conductive. This coating can be executed by gold sputtering (Bergmans *et al.*, 2005). Despite this disadvantage, SEM is very valuable method, especially for investigation of conditioning films (Hannig *et al.*, 2007).

TEM is a standard method in microbiology (Hannig *et al.*, 2010) and can be used also for visualisation of bacterial biofilms (Figure 14). The main advantage of this technique is its high resolution (down to 1.0 nm). However, the specimen preparation is a quite complex process, which includes steps as fixation by glutaraldehyd or osmium tetraoxide, dehydratation, embedding in acrylic resin, staining with heavy elements. Therefore, the method is quite time-consuming (Bergmans *et al.*, 2005; Hannig *et al.*, 2007).

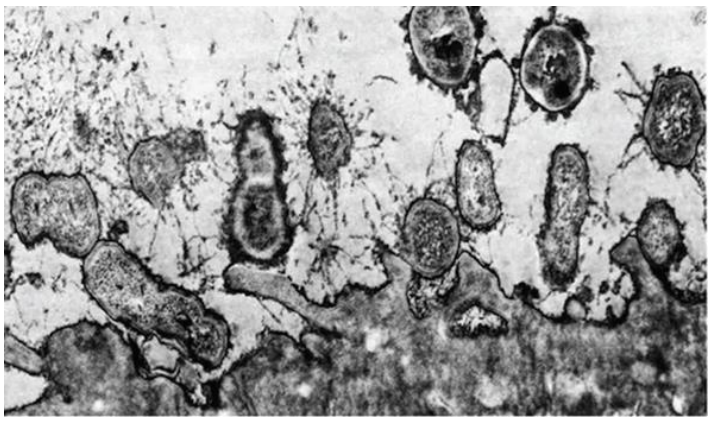

Figure 14 TEM image of biofilm of *Ruminococcus albus.* Modified from (Lappin-Scott *et al.*, 2014).

The main drawback of the electron microscopy (both SEM and TEM) is the danger of artefacts that can occur during specimen processing.

From the advanced microscopic techniques, the only one capable of validation of living cells is AFM (Figure 15), which also reaches high resolution (Dufrene, 2008). The principle of AFM is based on scanning of the material by a very sharp cantilever. The cantilever can be in direct contact with the analysed material (contact mode) or can oscillate above the material surface (tapping mode). During the contact mode, a laser beam detects the bending of the cantilever caused by unevenness of the examined surface. However, because the cantilever is in direct contact with the material surface, both the cantilever and the analysed material can be scratched easily and destroyed.

During tapping mode, the cantilever interacts with the sample surface by van der Walls interactions. Therefore, the change of amplitude of oscillation is measured. This mode is non-destructive for the analysed material and also for the cantilever.

Another great advantage of AFM over electron microscopic techniques (SEM and TEM) is the fact that it can be performed also in the atmospheric pressure (i.e. vacuum is not needed) or under water. The bacterial biofilm can be therefore immersed in buffer or medium for all the time of observation. This enables real-time observation of bacterial cells (Dufrene, 2008).

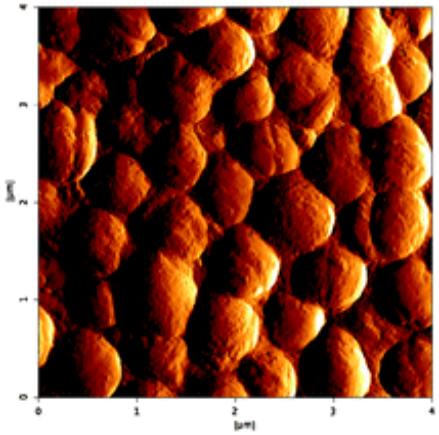

Figure 15 AFM image of biofilm of *Staphylococcus aureus.* (Abou Neel *et al.*, 2009)

3.2. Diamonds and other carbon nanomaterials

Carbon can be found in nature in three allotropic forms, shown in Figure 16: a) amorphous carbon, b) graphite and c) diamond. In amorphous carbon the atoms possess hybridizations sp, sp^2 and sp^3 and due to these different hybridizations it does not crystalize in any crystal lattice. In contrast, in graphite the carbon atoms are sp^2 hybridized and form three strong bonds with their neighbouring atoms. Consequently, graphite crystalizes in hexagonal crystal lattice where the carbon atoms are organized into covalently bonded layers which stack together through van der Waals interactions.

In diamond, the carbon atoms are sp^3 hybridized, where each atom forms four bonds and therefore diamond crystalizes in the facial centred cubic lattice. There are no layers formed in diamond and the material is very resilient.

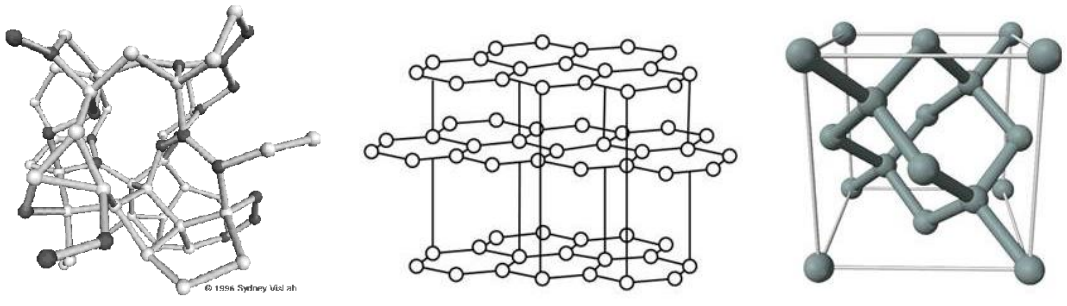

Figure 16 Three allotropes of carbon: of a) amorphous carbon; b) graphite; c) diamond. Source:
http://scmhardsoft.altervista.org/tag/curiosity
http://thefutureofthings.com/news/6677/harder-than-diamond.html
http://www.arch.mcgill.ca/prof/sijpkes/arch374/winter2002/psbmonro/

From these bulk materials, corresponding nanomaterials can be derived. Among the so-called graphitic nanomaterials belong graphene (single layer of carbon atoms), carbon nanotubes (CNTs) which can have just one layer (single-walled carbon nanotubes – SWCNTs) or more layers (multi-walled carbon nanotubes – MWCNT), and fullerenes (Figure 17). Diamond nanomaterials include diamond nanoparticles and nanocrystalline diamond (NCD) films. Also some nanomaterials derived from amorphous carbon exist, such as diamond-like carbon (3.2.1.3)

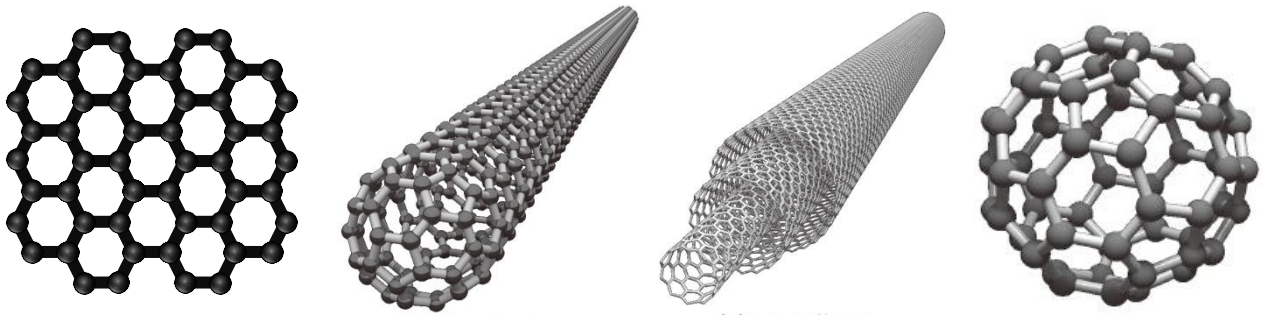

Figure 17 Structures of graphitic nanomaterials: a) graphene; b) single-walled carbon nanotube); c) multi-walled carbon nanotube; d) fullerene C_{60}. (Uo *et al.*, 2011)

3.2.1.Physical and chemical properties of bulk diamond a diamond nanomaterials

In the facial centred cubic lattice typical for diamond, the small carbon atoms are covalently bonded together over a short distance. In addition, these bonds are very strong. This is the reason for the diamond exceptional hardness and abrasion resistance. These properties make diamond the perfect material for fabrication of abrasive and cutting tools (Gracio *et al.*, 2010). Despite the fact that diamond cannot be scratched by almost any other material, it is quite brittle and so the edges can be damaged easily (Gracio *et al.*, 2010). From other properties of diamond, high thermal conductivity, unusual chemical inertness and its electrical properties are noteworthy (Gracio *et al.*, 2010).

The nanodiamond surface can be modified by many elements such as oxygen, hydrogen, fluorine, silicon, nitrogen etc. (Mochalin *et al.*, 2012). Such modifications (usually referred to as terminations) result in various functional groups, e.g. hydroxyl-, carboxyl-, amino-, etc., appearing on the material surface (Kawarada and Ruslinda, 2011; Mochalin *et al.*, 2012). To these functional groups, DNA or proteins or other functional molecules can be easily attached by linkers (Kawarada and Ruslinda, 2011; Meinhardt *et al.*, 2011).

The termination of the diamond surface itself is not complicated due to dangling bonds (Figure 18). The termination of such surface does not require modification of the crystal lattice as it is needed in the case of fullerenes, CNT and graphene which do not possess any dangling bonds and can therefore only be easily functionalized on their edges (Kawarada and Ruslinda, 2011; Mochalin *et al.*, 2012).

Especially electrical properties of diamonds are very technologically interesting. Wide bandgap (around 5.47 eV), large breakdown and high hole mobility are favourable properties for construction of high power and high-frequency electronic devices such as transistors, high-temperature diods etc. (Gracio *et al.*, 2010). The electronic properties of intrinsic diamond change distinctly with the surface termination. For example, the hydrogenated diamonds are more electrically conductive compared to oxidized NCD (Kozak *et al.*, 2009b; Gracio *et al.*, 2010; Kawarada and Ruslinda, 2011; Neykova *et al.*, 2012).

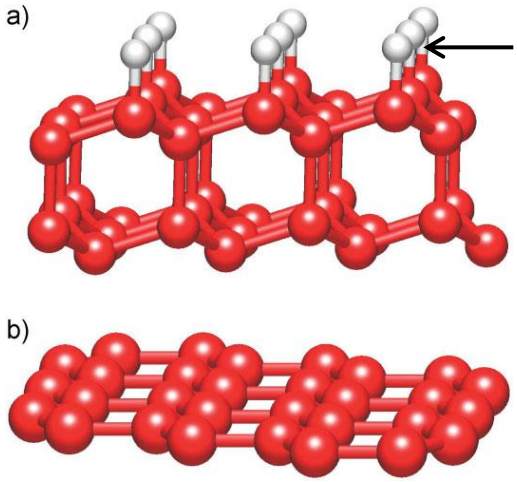

Figure 18 The difference in surface structure of diamond and graphitic nanomaterials: a) nanodiamond – white spheres represents hydrogen atoms bind to carbon (red spheres), so called "dangling" bonds (arrow); b) graphene – no dangling bonds are presented at the surface (Kawarada and Ruslinda, 2011).

Another property noticeably influenced by the termination of diamond material is its surface hydrophobicity. Hydrogenated and fluorinated diamonds are very hydrophobic with contact angles about 80-110° (3.3). On the contrary, oxidized diamonds are very hydrophilic (contact angles around 5° or less).

Bulk diamonds are usually called monocrystalline diamonds. The use of these materials is expensive and therefore diamond nanomaterials, such as micro- and nano-crystalline diamonds, are used instead. Micro and nano-crystalline diamonds are characterized by the size of their grains about 1 μm and less than 100 nm, respectivelly (Gibson *et al.*, 2011). Such diamond nanomaterials can be deposited on various substrates of large area.

Diamond nanomaterials possess similar mechanical and chemical properties as monocrystalline diamond and in addition they also possess some other beneficial properties, which cannot manifest in the bulk material. One of them is the extended surface area, due to which the effects of surface termination and functionalization is more observable.

3.2.1.1. Diamond nanoparticles

Diamond nanoparticles were synthetized for the first time in 1963 and introduced by (Danilenko, 2004). Because of the sp^3 hybridization of carbon atoms, the surface of nanoparticles must be stabilized by termination with other atoms or by forming a shell of sp^2-hybridized carbon atoms on the surface (Mochalin *et al.*, 2012; Lai and Barnard, 2015) (Figure 19). The ratio of sp^2 hybridized carbon and

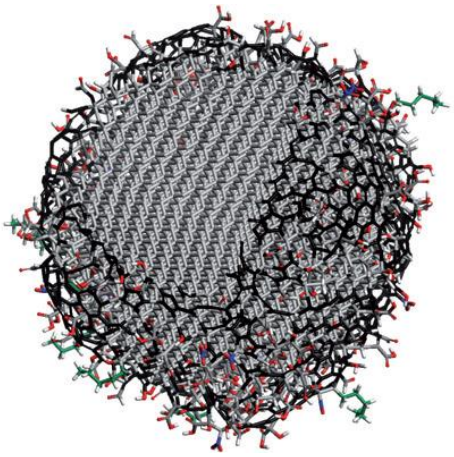

Figure 19 The schematic model illustrating the structure of diamond nanoparticle after oxygen purification. Part of the nanoparticle was cut along to illustrate the structure of diamond core (gray colour). The core is covered by the sp2 hybridized carbon (black colour) and functional groups (other colours)(Mochalin *et al.*, 2012).

surface terminated by non-carbon atoms can vary according to the size and purity of the nanoparticles. For instance, it was shown that buckydiamonds (i.e. diamonds fully covered by sp^2 shell) are energetically more feasible if the size of the particle reaches 3 nm (Schrand *et al.*, 2009). The diamond nanoparticles with negligible fraction of sp^2 hybridized carbon can be achieved by purification in acids (Dolmatov, 2001) or additional treatment in the air or hydrogen or oxygen plasma (Arnault *et al.*, 2011; Lai and Barnard, 2015).

Due to their small size, high biocompatibility and possibility of surface modification, diamond nanoparticles are one of the perspective materials in many biomedical applications, e.g. for drug delivery or bioimaging (Mochalin *et al.*, 2012; Lai and Barnard, 2015)

3.2.1.2. Nanocrystalline diamond films

Apart from the existence in form of individual nanoparticles, the diamond can be also crystalized on the surfaces of other material where it forms a seamless film of diamond crystals. These films are referred to as nanocrystalline diamond (NCD) films. The morphology can differ between various samples and depends strongly on the deposition conditions (Lewis *et al.*, 2010; Babchenko *et al.*, 2013). The NCD films are typically deposited on various surfaces by chemical vapour deposition method (4.1.2.1).

Nanocrystalline diamond coatings (Figure 20) are perspective for a wide range of electronic applications or as protective coatings (Erdemir *et al.*, 1999; Kawarada and Ruslinda, 2011). It is also an ideal material for bone engineering due to its high wear-resistance under sliding contact conditions (Erdemir *et al.*, 1999); it was also reported that NCD films promote adhesion of human osteoblast-like cells (Grausova *et al.*, 2009). In this study, I focus on its possible anti-adhesive properties against bacteria.

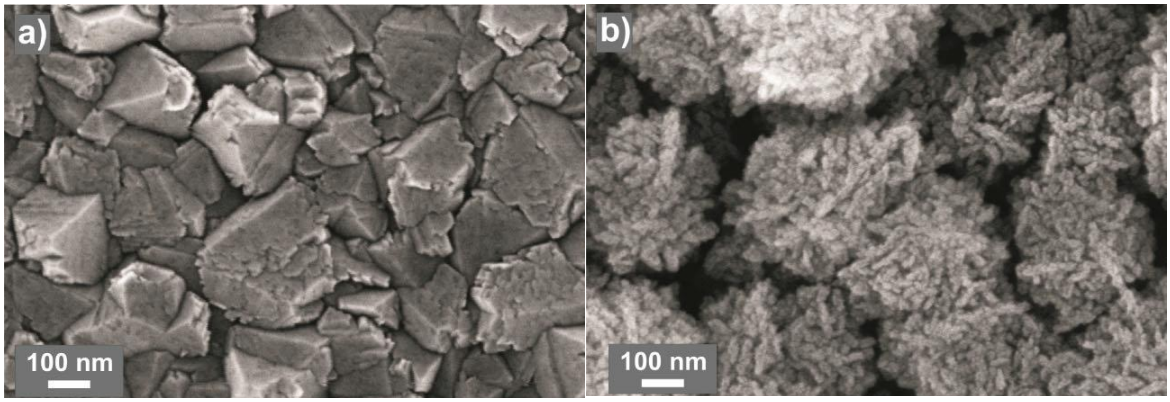

Figure 20 SEM images of different morphologies of NCD films. a – facetted NCD; b- porous NCD film (Babchenko *et al.*, 2013)

3.2.1.3. Diamond-like carbon films

Diamond-like carbon (DLC) films can be deposited on the substrate surface by CVD, the same as NCD films. In contrast to NCD, DLC represents amorphous carbon with high content of sp^3 hybridized carbon atoms. This feature provides the DLC films with similar physical properties as NCD films. Two basic types of DLC films exist: (1) a-C:H (from amorphous carbon) which contains hydrogen and where sp^3 fraction is usually smaller than 50 %, and (2) non-hydrogenated carbon films, also a-C or ta-C (tetrahedral carbon), which often contains more than 85 % of sp^3 hybridized carbon (Grill, 1999). a-C DLC films surpass a-C:H films in mechanical, optical and chemical properties, which are very similar to those of diamonds. The compatibility with eukaryotic cells is comparable between DLC and NCD films (Lifshitz, 1999). The functionalization and doping of these films by other elements often result in change of sp^2/sp^3 ratio which is hypothesized to influence the bacterial cell attachment (Shao *et al.*, 2009).

3.3. Antibacterial properties of diamond nanomaterials

Gram positive bacterium *E. coli* was reported to be inhibited by diamond nanoparticles with smaller diameter (5 nm) more than by those with a larger one (18, 24 and 50 nm) (Beranova *et al.*, 2014). Oxidation of the surface of diamond nanoparticles (which makes the surface more hydrophilic) resulted in loss of antibacterial activity of these nanoparticles. In contrast, gram positive bacterium *Bacillus subtilis* was inhibited by larger nanoparticles with average diameter about 18, 25 and 50 nm. The bacterial growth was inhibited by the smaller nanoparticles (with diameter about 5 nm) just if they were oxidized. Interestingly, the cultivation of *B. subtilis* with diamond nanoparticles also resulted in smaller and more circular colonies (Figure 21) (Beranova *et al.*, 2014).

Wehling *et al*. (2014) showed that antibacterial properties of diamond nanoparticles depend especially on the functional groups attached to the nanoparticle surface. The authors hypothesise, that reactive oxygen-containing surface groups cause interaction of the nanoparticle and bacterial surface components.

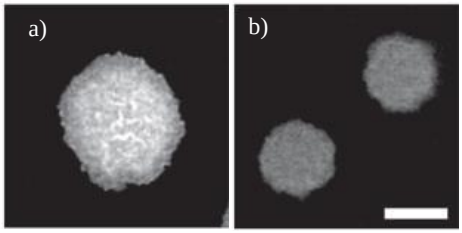

Figure 21 The change in morphology of colonies of B. subtilis; a - control colony cultivated without any diamond nanoparticles, b – colonies cultivated with diamond nanoparticles (Beranova *et al.*, 2014)

The topic of bacterial adhesion to nanodiamond or DLC surfaces has been addressed by rather few authors and therefore limited data are available in the literature. DLC films have comparable physical properties to those of NCD films and some antibacterial and anti-adhesive studies using this material have been made already. Several works investigated antiadhesive properties of these materials or "bactericidal effect" as the authors often call it, although they usually do not provide convincing data from any viability test. The results usually differ substantially between individual research teams: several authors often claim, that NCD and DLC possess antibacterial or at least antiadhesive properties (Jakubowski *et al.*, 2004; Ishihara *et al.*, 2006; Marciano *et al.*, 2009a; Marciano *et al.*, 2011). However, if the bacterial adhesion is correlated with the different physical properties of diamond nanomaterial, the results often contradict each other.Three main surface properties are commonly correlated with the change of bacterial attachment. The first is the roughness of the sample surface, second the hydrophobicity and third the surface free energy. Also, the effect of doping of DLC with different elements has been studied but the differences in experimental setups often hinder comparison between different research groups.

Doping of DLC films by various elements can influence the surface structure and roughness (Ishihara *et al.*, 2006; Liu, C. *et al.*, 2008; Marciano *et al.*, 2009b), hydrophobicity (Yokota T, 2007; Marciano *et al.*, 2009b; Shao *et al.*, 2009; Marciano *et al.*, 2011) and also bacterial attachment (Shao *et al.*, 2009). However, in some studies this change in surface properties due to doping did not occur (Zhao *et al.*, 2007).

More hydrophilic Si-doped DLC films were reported to inhibit attachment of gram positive bacterium *Pseudomonas aeruginosa* (Shao *et al.*, 2009) more than hydrophobic stainless steel. The bacterial cells (θ about 78°) used in this study surpassed in its hydrophobicity all materials used in the study (DLC with θ about 70° and Si-doped DLC films with θ down to 61°) except stainless steel (θ about 78°), which served as a control. This result is in agreement with results of Ishihara *et al.* (2006), who

showed, that gram negative bacterium *E. coli* preferred the un-doped DLC (θ about 70°) over F-doped DLC (θ about 91°).

In contrast, gram positive bacterium *Staphylococcus aureus* adhered more to hydrophilic surface of Si-doped DLC film (θ about 61°) than to almost un-doped DLC film with Si content of 1 % and θ about 72° (Zhao *et al.*, 2007). Unfortunately, the information on bacterial hydrophobicity has not been included in this article. However, the roughness of DLC films increased with the Si content. Therefore, the increased attachment of bacteria to DLC with higher content of Si could be caused by higher surface roughness (Zhao *et al.*, 2007). Interestingly, the bacterium *P. aeruginosa* was also reported to adhere more to smoother surfaces of N and Si-doped DLC than to those rough ones (Liu, C. *et al.*, 2008).

Marciano *et al.* (2009b) reported that both un-doped DLC (θ about 75°) and un-doped DLC terminated by oxygen (super hydrophilic with θ about 0°) inhibited adhesion of both *P. aeruginosa* and *S. epidermidis*. However, in contrast to results of Zhao *et al.* (2007), adhesion of S. aureus was inhibited comparably by both materials. *P. aeruginosa* was inhibited more by hydrophobic DLC films, which is in contradiction to the result of Shao *et al.* (2009).

Also surface free energy was examined as a parameter that may increase or decrease the attachment of bacteria. The higher surface free energy γ- was shown to inhibit attachment of *P. aeruginosa* to N and Si-doped DLC films (Liu, C. *et al.*, 2008) while increasing component γ_{SL} (solid-liquid interfacial free energy) was shown to promote the bacterial adhesion (Zhao *et al.*, 2007).

Concerning NCD films, the literature resources are even scarcer than those dealing with DLC films. The studied physical properties of these materials are similar to those of DLC films – e.g. surface hydrophobicity or surface roughness (and with it connected diamond grain size) (Ishihara *et al.*, 2006; Zhao *et al.*, 2007; Shao *et al.*, 2009; Medina *et al.*, 2012). The work of Medina *et al*. (2012) confirmed lower attachment of bacterium *P. aeruginosa* to NCD compared to stainless steel (Figure 22). Also, they compared NCD of different roughness and showed that bacteria adhered less to the smoother surface of NCD than to a rougher one. Also the experiment performed in CDC Bioreactor with NCD films of various morphologies (and thus also roughness) and stainless steel as control showed that bacteria settled

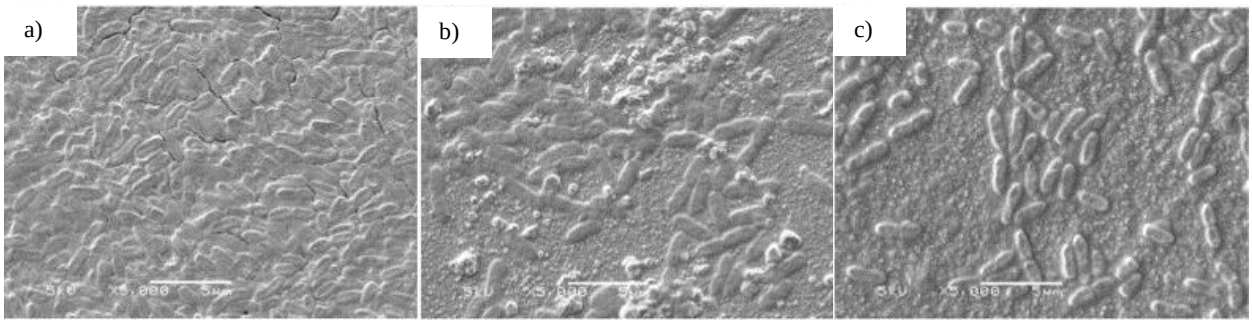

Figure 22 The different adhesion of P. aeruginosa to different materials. a - stainless steel; b – microcrystalline NCD; c – nanocrystalline NCD film. (Medina *et al.*, 2012)

preferably on stainless steel (Lewis *et al.*, 2010). However, no correlation between surface roughness and bacterial attachment was observed.

Due to apparent complexity of the problem and low amount of comparable experimental data, it is impossible to decide, which surface parameters, i.e. surface hydrophobicity, roughness or free energy are responsible for bacterial attachment. Most probably, it is a combination of these (and maybe also other additional) factors that underlie the desired "anti-fouling" property of a material. Whether DLC or NCD materials possess indeed such characteristic is not a trivial question that – also due to contradicting results of different research groups - has not been answered yet.

4. Material and methods

4.1. Nanomaterial samples preparation:

In my work, I used three different materials: untreated glass (which served as a negative control in majority of my experiments; its composition and properties are described in Table 1), glass coated with hydrogenated NCD film (NCD-H) and glass coated with oxidized NCD film (NCD-O).

All material samples were prepared in Institute of Physics of Academy of Science of the Czech Republic. In order to protect the samples against pollution and scratching, they were always handled wearing gloves and using tweezers.

Table 1 Composition and properties of silica-fused glass used as substrate for NCD deposition
Source: Manufacturer's web site, http://www.menzel.de

SiO_2	72.20%
Na_2O	14.30%
K_2O	1.20%
CaO	6.40%
MgO	4.30%
AL_2O_3	1.20%
Fe_2O_3	0.03%
SO_3	0.30%

Mean Coefficient of Expansion: 90.6 x 10^{-7} /ºC (20-300º C)
Strain Point log n 14.5: 513° C
Softening Littleton Point: 720° C

4.1.1. Substrates cleaning

Glass substrates (1.7×7.7 cm and 1.0×1.7 cm, silica fused glass, Menzel) were placed into a teflon holder and cleaned by isopropyl alcohol in the ultrasonic bath (Transsonic digital S or Transsonic T570/H, Elma GmbH) at 100 kHz for 10 minutes. Cleaned substrates were washed by moderate flow of deionized water for 10 min and dried by clean nitrogen gas.

4.1.2. Chemical vapour deposition of nanocrystalline diamond films

4.1.2.1. Theoretical background of chemical vapour deposition:

NCD films on glass microscope slides were grown by chemical vapour deposition (CVD) method. This method is one of the so-called "bottom-up" methods, during which atoms or molecules react together to form the final nanomaterial. (The opposite are "top-down" methods, which involve

disintegration - e.g. milling - of bulk material to gain nanoparticles of the same material.) During CVD, vapours of volatile precursors condensate on the substrate surface and form another chemical compound. In the case of NCD, the precursor compound is methane, whose molecules aggregate to form a layer of pure carbon. Under certain conditions, sp^3 hybridization is preferred and carbon crystalizes in the form of diamonds (Gracio *et al.*, 2010). The nanodiamond crystals grow until the CVD process is stopped.

4.1.2.2. Nucleation and growth of NCD films

Because diamond cannot be deposited on a non-diamond substrate *de novo,* crystallization of nanodiamonds on such surfaces requires a nucleation centre. In order to achieve compact covering of the substrate surface by nanodiamond crystals, it is necessary to substantially increase the density of nucleation centres. This process - called nucleation or seeding - is performed mostly by ultrasonic treatment of the substrate material in a suspension of diamond nanoparticles (Gracio *et al.*, 2010).

Cleaned and dried substrates were sonicated in the suspension of diamond nanoparticles in distilled water (4-5 nm, NanoAmando, New Metals and Chemicals Corp. Ltd., Kyobashi) for 45 min at 100 kHz. Mathematically calculated seeding density for the substrate surface coverage of 76 % and for the primary particle size of 5 nm was in the order of 10^{12} cm^{-2} (Kromka *et al.*, 2008a). This way, the growth of continuous, smooth and high quality NCD films is ensured (Kromka *et al.*, 2008b). Nucleated substrates were washed by deionized water for 5 min, dried by clean nitrogen gas flow and placed into the deposition system.

The growth of NCD films on glass substrates is not a trivial task due to low melting point of glass (700°C in our case), low adhesion of diamond to glass or damage of substrates during CVD (Costello *et al.*, 1994) However, the team of the Laboratory of diamond thin films and carbon nanostructures, lead by A. Kromka, possesses the necessary experience and equipment.

The growth of NCD films on glass substrates was performed in pulsed microwave plasma system with a linear antenna arrangement. The main advantages of this reactor are large distance between the high-density plasma region and the samples, and large (20×30 cm^2), scalable process area (Izak *et al.*, 2012). Thus, overheating of the substrate from plasma radiation is minimized. Schematic drawing and a photograph of the linear antenna microwave plasma enhanced chemical vapour deposition (PECVD) system AK400 (Roth and Rau) are shown in Figure 23. The growth of NCD films was realized as a two-step process.

The first step (formation of the supporting layer) lasted 5 hours and the gas flow was 100/30/5 in sccm (standard cubic centimetre) of $H_2/CO_2/CH_4$ mixture.

In the second step (formation on the functional layer) the gas composition was 200/20/5 in sccm of $H_2/CO_2/CH_4$ and the process lasted 20 hours. Both steps were performed under following parameters: the microwave power 2000W with on/off pulse cycle 6/3 ms, pressure 0.1 mbar and substrate temperature around 430°C.

The NCD films were deposited by Ing. Oleg Babchenko, PhD.

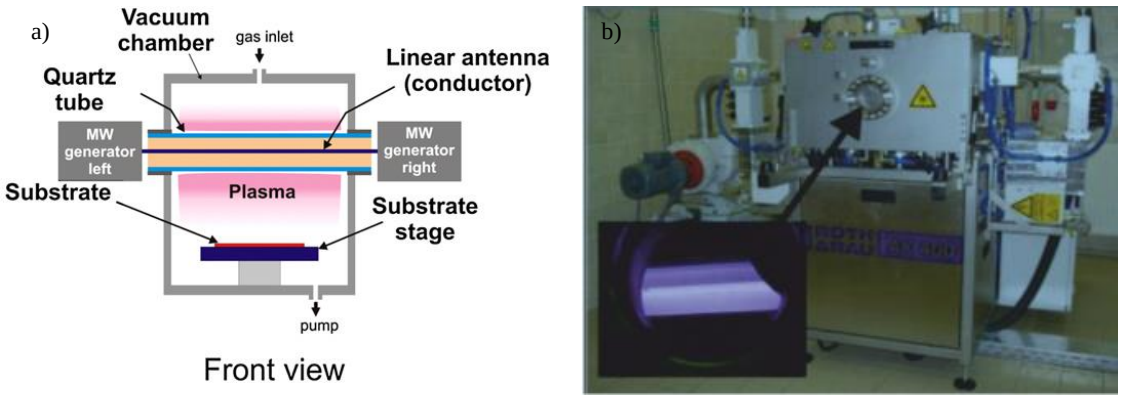

Figure 23 Schematic drawing (a) and a photograph (b) of linear antenna microwave PECVD system.

As discussed in chapter (3.2.1), the properties of nanodiamonds can be influenced by their surface termination. For antibacterial study I used two types of NCD surface terminations: hydrogen and oxygen plasma treated. As-grown NCD films prepared by CVD with previously described deposition conditions were hydrogenated (i.e. terminated by H atom) with hydrophobic surface properties. To achieve different termination, NCD films after deposition were plasmatically treated in pure oxygen to obtain hydrophilic surface terminated by oxygen (Kozak *et al.*, 2009a),(5.2.3). Oxidation of NCD films was performed in Femto PCCE system reactor (Diener) in 100% O_2 for 4 min under pressure of 1.1 mbar and at power of 100 W.

4.2. Nanomaterial samples characterization:

4.2.1.Scanning electron microscopy (SEM)

In my work, scanning electron microscopy was used to estimate the size of crystals in the grown NCD films and to obtain general information on their surface morphology.

The microscope used for characterization of NCD samples was SmartSEM V05.02.02 (Zeiss) with cathode ZrO/W (Schottky). The observing parameters were as follows: EHT 10 kV, aperture 20-30 µm, magnification was up to 100.000×, pressure about 10^{-2}-10^{-4} Pa and lower.

Ing. Karel Hruška and Ing. Vlastimil Jurka assisted me with operating the microscope.

4.2.2. Atomic force microscopy

Atomic force microscopy (AFM) was used to estimate the roughness of glass and NCD samples.

Our samples were analysed in the atmospheric pressure in tapping mode (50mV amp) on ICON atomic force microscope using new CF4 plasma treated Multi75AL cantilever.

1x1μm images were obtained. Z-scale was 50 nm, scan area was $1\times1\mu m^2$.

The microscope was operated by Ing. Egor Ukraintsev, PhD.

4.2.3. X-ray photo-electron spectroscopy

X-ray photo-electron spectroscopy (XPS) was used for chemical composition analysis of the NCD surface. In this method, the analysed material is irradiated by a beam of high energetic photons (x-ray). Photons provide energy to the atoms of the material and this energy is transformed into emission of electrons from these atoms. The energy of these emitted electrons correlates with different energy levels in the molecule. Based on the knowledge of energy levels typical for different atoms (that can practically serve as "fingerprints" of particular chemical elements), we can estimate the chemical composition of the analysed material. Because flying range of emitted electrons is only few nanometres, this method is suitable for surface composition analysis.

The XPS spectrometer used for our measurement consisted from multi-channel hemispherical electrostatic analyzer (Phoibos 150, Specs) and (Al/Mg) X-ray source (1 486.6 eV, Specs). Survey spectra were measured with pass energy of 40 eV and high resolution with pass energy of 10 eV at constant take-off angle 90°. The recorded spectra were then referenced to the peak at 285.1 eV as it corresponds to sp^3 hybridized carbon (Zemek *et al.*, 2006). CasaXPS software was used for curve fitting.

The measurement and data analysis was performed by Mgr. Anna Artemenko, Phd.

4.2.4. Raman spectroscopy

Raman spectroscopy is a method widely used for analysis of bulk material composition. In this study it was therefore used for composition analysis of NCD films, especially the ratio of sp^2 (graphitic) and sp^3 (diamond) hybridized carbon atoms.

Raman spectroscopy is based on so called Raman effect, which is an example of inelastic scattering.

If a material is illuminated by monochromatic light, part of the light is absorbed and the remaining part can be scattered. If the wavelength of the scattered light is the same as the wavelength of illumination, we speak about Rayleigh scattering, an example of elastic scattering. In contrast, the

minority of scattered photons can have different wavelength. This shift in wavelength is called Raman shift and was observed for the first time in 1928 by C. V. Raman and K.S. Krishnan (Moore, 1979).

The explanation of this phenomenon is that a photon of certain wavelength and corresponding energy interacts with a molecule of the material and excites it to virtual, non-discrete, energy level. During this process, the photon can either accept a quantum of energy from a certain molecule or pass it to another one. Resulting change of photon's energy becomes detectable as a shift in wavelength of the scattered light.

For Raman spectroscopy measurement the inVia Reflex Raman Spectroscope (Renishaw) was used The excitation wavelength was 422 nm. The collected data were processed by Origin 8.1 software.

The measurement was performed by Ing. Tibor Ižák, PhD.

4.2.5.Contact angle measurement

I investigated the wetting properties of NCD surfaces by a static wettability measurement with deionized water droplets at room temperature. A reflection goniometer (Surface Energy Evaluation (SEE) System) and CCD camera were used (Figure 11). A drop of deionized water (3 µl) was applied on the sample surface, the contact angle was measured and calculated by multipoint fitting of the drop profile using the SEE software. The sample was dried immediately after the measurement by pure nitrogen gass.

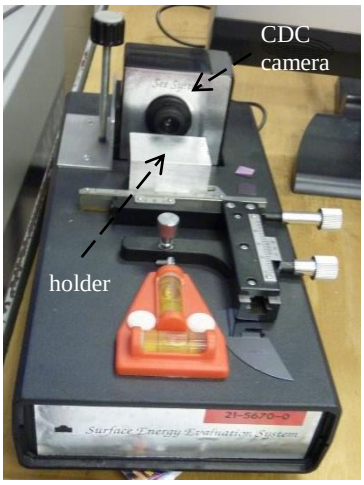

Figure 24 Reflection goniometer used in this work

4.3. Cultivation media and other solutions

4.3.1.Luria-Bertani medium

- Standard Luria-Bertani (LB) medium

Trypton (Oxoid)	10 g/l
Yeast extract (Oxoid)	5 g/l
NaCl (Penta)	10 g/l
pH	7.0

This medium was used for batch cultivation in Erlenmeyer flask and in the bioreactor.

- LB agar plates and slants

LB medium was solidified by addition of 2 % [w/v] of agar powder (Oxoid). Agar plates and slants were then left to dry in a sterile box.

- Saline-diluted Luria-Bertani

The standard LB medium was diluted 1:2 in 1% saline. (This way, the concentration of NaCl was the same as in standard LB medium.)

- Water-diluted Luria- Bertani medium

The standard LB medium was diluted 1:2 in distilled water.

4.3.2.Saline

NaCl	8.0 g/l

4.3.3.Hoechst 33342 staining solution

Hoechst 33342 stain is a fluorescent DNA stain which (similarly to DAPI) penetrates both living and dead cells. This stain binds into the minor groove of DNA. The excitation peak of this stain is around 350 nm and the emission peak is around 461 nm. In this study, this stain was used for detection of bacteria attached to the material sample surface 5 ml of solution was prepared by dilution of 1 g/l Hoechst 33342 (Invitrogen) in distilled water. Aliquots of the stock solution (0.4 ml) were stored at -20° C. Before use, the stock solution was diluted 10-times in saline.

4.4. Sterilization

Laboratory glass and razor blades (5.5) were sterilized by dry heat (300° C, 160 min).

Thermostable solutions, glass samples (1×1.7 cm), material samples (1.7×7.7 cm), CDC Bioreactor (4.6.2) and all hosepipes were sterilized by standard autoclaving (120° C, 100 kPa, 20 min).

The material samples (1.7 ×7.7 cm) were inserted into the holders before sterilization and sterilized inside the CDC Bioreactor. All openings of CDC Bioreactor and all hosepipe ends were covered with aluminium foil during sterilization.

After sterilization, the aluminium covering was removed and CDC Bioreactor was connected with stock and waste bottles by sterile hosepipes. The bioreactor assembling and all the other manipulations were performed in the sterile box.

Bigger volumes of cultivation medium needed for continuous cultivation in bioreactor (up to 10 litres), had to be autoclaved twice at higher temperature and longer time (130° C, 30 min) to guarantee complete sterilization.

Thermosensitive probe (part of the stirrer plate) was sterilized by UV light for 30 min from both sides and inserted into the CDC Bioreactor after addition of sterile LB medium right before the cultivation start.

4.5. Microrganism

In this study, a bacterium *Escherichia coli* strain K-12 (laboratory stock) was used. The stock culture was stored at -70 °C in glycerol solution (65% [w/v] glycerol, 0.1M $MgSO_4$, 25mM TrisCl, pH 8).

From the stock, slant LB agars were inoculated, incubated over-night at 37°C and stored in refrigerator for immediate use.

4.6. Bacterial growth

4.6.1.Batch cultivation in Erlenmeyer flasks

Agar plates and slants were incubated at 37°C in a temperated incubator (Memmert). For cultivation of liquid cultures, the orbital shaker (N-Biotek) was used with temperature set to 37° C and rotation speed to 180 rpm. The volume of the medium was always 30 ml in a 250-ml Erlenmayer flask covered with aluminium foil cap.

The optical density of the growing bacterial culture was measured at 450 nm (OD_{450}) in glass cuvette (10 mm) using spectrophotometer Beckman DU530. Distilled water was used as a reference. Background signal of cultivation medium was subtracted from the final value.

For the over-night culture, *E. coli* from the stock slants was inoculated into LB medium and incubated for 15 hours. Then it was diluted with fresh medium to OD_{450} = 0.05 and cultivated further. The growth was followed by OD measurement until the culture reached required density.

4.6.2. Bacterial biofilm growth

4.6.2.1. Repeated batch cultivation of E. coli on the glass surface in six-well plates

This method of cultivation was adopted from (Jakubowski *et al.*, 2004; Marciano *et al.*, 2011).

Each of the sterile material samples (1×1.7 cm) was incubated with *E. coli* in LB medium in the wells a of sterile six-well plate.

Fresh LB medium (9 ml of volume) in each well was inoculated by 1 ml of exponentially growing bacterial culture (OD_{450} = 0.5) to reach the final OD_{450} = 0.05, and the sterile material samples were immersed into the wells. The bacterial culture in the wells was cultivated for 24 hours at 37°C in the orbital shaker (rotation speed 110 rpm).

Than the samples, covered with early biofilm, were removed, rinsed three times by 1 ml of fresh sterile LB medium from both sides to wash away loosely adherent bacteria, and placed to a new well containing 10 ml of fresh LB medium. After another 24 hours of cultivation under the same conditions, the samples were removed, washed three times by 1 ml of sterile saline from both sides and used for further examination and evaluation (4.7.2, 4.7.1).

4.6.2.2. Cultivation of bacteria in CDC Bioreactor

For continuous cultivation, the commercially available CDC Bioreactor (BioSurface Technologies Corporation) was used (Figure 25).

The medium was pumped in by peristaltic pump (PCD 21M, Kouřil). To provide optimal stirring speed and temperation, the bioreactor was placed on a heated magnetic stirrer plate (RTC Basic, IKA) (Figure 25). The temperature of the medium inside the bioreactor was controlled by a thermosensitive probe immersed into the medium and connected directly to the stirrer.

Modus operandi was modified from (Hadi *et al.*, 2010) and CDC Biofilm manufacturer manual. The material samples (1.7×7.7 cm) were inserted into the bioreactor holders before sterilization. They were positioned in such a way that the surface of the sample coated with NCD film faced the centre of the CDC Bioreactor. For each experiment always 7 samples were inserted to the bioreactor. (The thermosensitive probe was inserted into the remaining port after sterilization.)

After sterilization, fresh LB medium (370 ml) was cautiously poured into the bioreactor, pre-warmed and inoculated from the batch bacterial culture (OD_{450} = 1.0) to reach the final OD_{450} = 0.025. The bacteria were cultivated 22 hours in the batch mode (without medium influx) at 200 rpm and 36°-37°C. After batch cultivation phase, the discharge was opened and the pump was switched on to

enable the medium exchange in the bioreactor. The medium inflow speed was 6.25 ml.min^{-1}. The duration of continuous phase of cultivation varied according to the respective experiment setup (see chapters 5.6.1 and 5.6.2).

At the end of cultivation, the material samples with grown biofilm were removed from CDC Bioreactor, washed with 5 ml of sterile saline solution from both sides, removed from the sample holders and placed to 50-ml plastic tubes containing 40 ml of fresh saline to prevent biofilms from drying. Then, the samples were either analysed by microscopy or sonicated and measured using ATP luminescence assay.

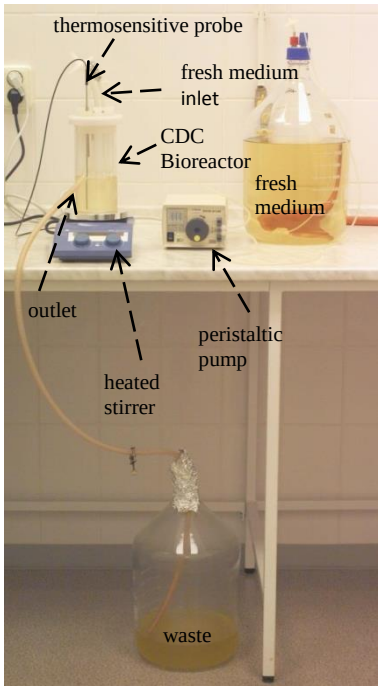

Figure 25 CDC Bioreactor real setup

4.7. Sample analysis

4.7.1.Fluorescence staining and microscopy

The material samples with grown biofilm were immersed into the solution of Hoechst 33342 for 20 min. The volume of staining solution was 5 ml for 1.0×1.7 cm samples and 40 ml for 1.7×7.7 cm samples.

The material samples were observed immediately after the staining with Olympus Cell-R fluorescent microscope. The excitation and emission wavelengths were 350 nm and 457 nm, respectively.

For some samples, differential interference contrast mode (DIC) was also used.

4.7.2.Sonication for bacterial detachment

In order to quantify the mass of grown bacterial biofilm, I needed to detach either all the living cells (for planned CFU count) or all destroyed biofilm (for ATP luminescence analysis –4.7.3). For this, sonication in ultrasonic bath and sonication using immersion probe were tested and optimized.

4.7.2.1. Sonication in ultrasonic bath

Sonication of material samples with grown biofilm in ultrasonic bath is widely used method for biofilm detachment (Elvers *et al.*, 1998; Davey and O'Toole, 2000; O'Toole George, 2000; Katsikogianni *et al.*, 2006; Zhao *et al.*, 2007; Liu, C. *et al.*, 2008; Bjerkan *et al.*, 2009; Akhavan and Ghaderi, 2010). The most frequently it is used for detachment of individual living bacterial cells for further examination or colony count. However, the sonication parameters greatly vary among different authors.

Some of the frequently used experimental set-ups are presented in

Table 2. Based on the

Table 2 An overview of sonication conditions used in work of different research groups for biofilm detachment from various materials.

Ref.	bacteria used	material	Sonication conditions		
			duration	temperature	solution
(Katsikogianni *et al.*, 2006)	*S. epidermidis*	PVC PVC+F PVC+DLC PVC+A	10 min	-	PBS
(Bjerkan *et al.*, 2009)	*S. aureus* *S. epidermidis* *E. fecalis* *P. acnes*	Ti Steel	5 min	37°C	saline
(Zhao *et al.*, 2007)	*S. aureus*	SS-DLC	10 min	warm	water
(Liu, C. *et al.*, 2008)	*P. aeruginosa*	SS-DLC +Si SS-Dlce+N	5 min	4°C	distilled water
(Elvers *et al.*, 1998)	*Pseudomonas alcaligenes* *Alcaligenes denitrificans* *Xanthomonas maltophilia* *Flavobacterium indologenes* *Rhodotorula glutinis* *Fusarium oxysporum* *Fusarium solani*	PVC surfaces	5 min	-	-
(Akhavan and Ghaderi, 2010)	*E. coli* *S. aureus*	graphene nano-sheets	1 h	37° C	-
(George O'Toole, 2000)	*E. coli*	polyurethane-DLC	2 h		
(Davey and O'Toole, 2000)	*E. coli*	SS-carbon	10 min		
(Stewart, C. R. *et al.*, 2012)	*L. pneumophila* *Klebsiella pneumoniae.* *Flavobacterium sp.* *Pseudomonas aeruginosa* *Pseudomonas fluorescens*	SS	3 cycles of 30-sec sonication		

Legend: PVC – poly-vinyl chloride, SS – stainless steel

literature data I chose the condition I was able to ensure with available ultrasonic bath (DT31H, Bandeline): temperature in range of 0°-4° C, time from 10 to 20 min (depending on the experiment – see chapter 5.5.2), fixed power of 35 kHz.

The glass samples (1.0×1.7 cm) with grown biofilm (4.6.2.1) were fully immersed into 10 ml of saline during whole sonication process.

After sonication, the resulted bacterial suspension in saline was serially diluted, plated on agar plates and cultivated over-night (18 h) in a temperated incubator (37°C). After that, the grown colonies were counted and colony forming units (CFU) per 1 ml were calculated.

4.7.2.1. Sonication by immersion probe

Sonication using a device with immersion sonication probe is destructive for bacterial cells, however this was no obstacle when biofilm growth was to be assessed via ATP quantification (4.7.3).

I used ultrasonic processor UP50H, (Hielscher, with Sonotrody MS2 probe; Figure 26). This method was applied on bacterial biofilms grown on tested material samples in CDC Bioreactor. Each material sample was sonicated in a 50-ml plastic tube containing 40 ml of saline. The optimization of this method is thoroughly described in the chapter 5.5.3. The samples were sonicated 4-times for 30 s with 100% amplitude and cycle 1 from both sides.

The resulting suspension was used for ATP analysis using BacTiter-Glo™ Microbial Cell Viability Assay kit (4.7.3).

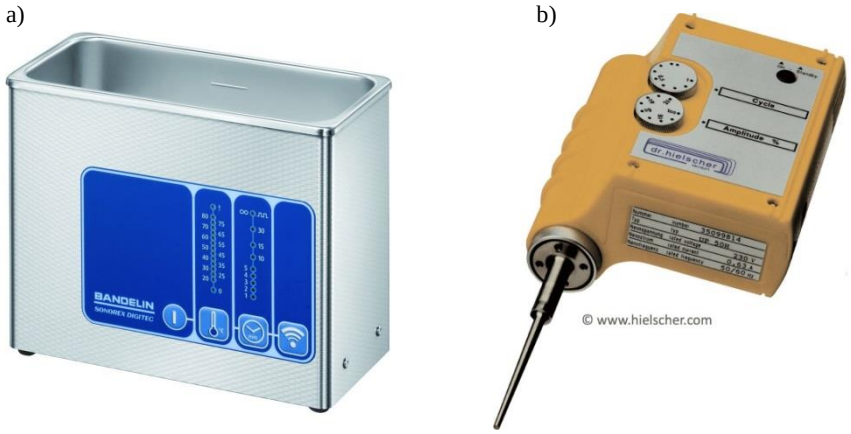

Figure 26 a - Ultrasonic bath DT31H, Bandelin. Source: Manufacturer's web site, http://bandelin.com/; b - Ultrasonic processor Hieschler UP520H. Source: Manufacturer's web site, www.hielscher.com

4.7.3.ATP assay

In order to quantify the growth of bacterial biofilm, I applied the determination of the overall ATP level in the detached biofilm.

The amount of bacteria attached to the sample surface was evaluated using BacTiter-Glo™ Microbial Cell Viability Assay kit (Promega) that enables ATP quantification. This method functions also with previously destroyed bacterial cells. This kit consists of proteins for cell destruction, luciferin and Ultra-Glo™ Recombinant Luciferase enzyme[2]. Luciferase uses ATP from destructed cells in reaction shown in Figure 27. In this reaction, luciferase produces oxy-luciferin from luciferin and ATP which is released from destructed bacteria. This reaction is accompanied by the emission of

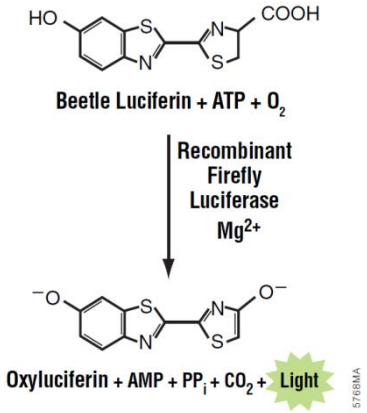

Figure 27 The principle of ATP assay by BacTiter-Glo™ Microbial Cell Viability Assay kit

Source: BacTiter-Glo™ Microbial Cell Viability Assay kit manufacturer web site

light. The light signal is proportional to the amount of ATP present in sample which is also directly proportional to the cell number in the sample.
(https://worldwide.promega.com/resources/protocols/technical-bulletins/101/bactiter-glo-microbial-cell-viability-assay-protocol/)

For construction of calibration curves, ATP stock solution in water and bacterial culture were serially diluted as indicated in Table 3.

Table 3 The construction of calibration curves for ATP assay

ATP calibration curve					
	1	2	3	4	5
ATP stock solution (1 nmol.l^{-1}) [µl]	100	10	1	0,1	0,01
distilled water [µl]	0	90	99	99,9	99,99
final ATP concentration [nmol.l^{-1}]	1	0.1	0.01	0.001	0.0001

bacterial culture calibration curve						
	1	2	3	4	5	6
Bacterial culture (1.98×10^8) [µl]	100	10	1	0,1	0,01	0,001
distilled water [µl]	0	90	99	99,9	99,99	99,999
final number of bacteria	$1.98 . 10^8$	$1.98 . 10^7$	$1.98 . 10^6$	$1.98 . 10^5$	$1.98 . 10^4$	$1.98 . 10^3$

[2] https://worldwide.promega.com/resources/protocols/technical-bulletins/101/bactiter-glo-microbial-cell-viability-assay-protocol/)

The bacterial suspension (1.98 $.10^8$ cells.ml^{-1},4.6.2.2) for calibration curve construction was taken from CDC Bioreactor vessel after 5 h of continuous cultivation (4.6.2.2).

The luminescence was measured in 96-well plate, the volume of the measured sample was 100µl on Varioskan™ Flash Multimode Reader (Thermo Fisher Scientific). The solutions were mixed for 10 s (600 rpm), the photons were collected for 1 s.

The ATP concentration was counted from the slope of linear phase of measured calibration curves (5.5.4).

If not stated differently, all presented data from luminescence experiments correspond to the luminescence intensity of the 100µl-aliquote.

5. Results and discussion

5.1. The scheme of experimental work

The flowchart of the originally planned experiments is presented in Figure 28.

The plan was to

(1) prepare hydrogen and oxygen terminated nanocrystalline diamond (NCD) films deposited on glass (uncoated glass substrates served as negative controls);

(2) characterize of the properties of all material samples;

(3) find the best method of sterilization of the NCD samples;

(4) grow bacterial biofilm on the surface of the samples, and finally

(5) qualitatively and quantitatively compare the biofilm growth on the NCD surfaces and control samples (glass).

For qualitative assessment of biofilm density and basic morphology, the fluorescence microscopy was employed. For quantitative analysis I planned to detach live cells from the sample surface and use the method of viable colony count. As this method failed to be reproducible, the measurement of the ATP level was used as an alternative method.

Each of these steps needed thorough optimization. All optimization experiments were carried out using uncoated glass. Based on the findings of these optimization experiments, final experiments using NCD-coated glass samples were performed.

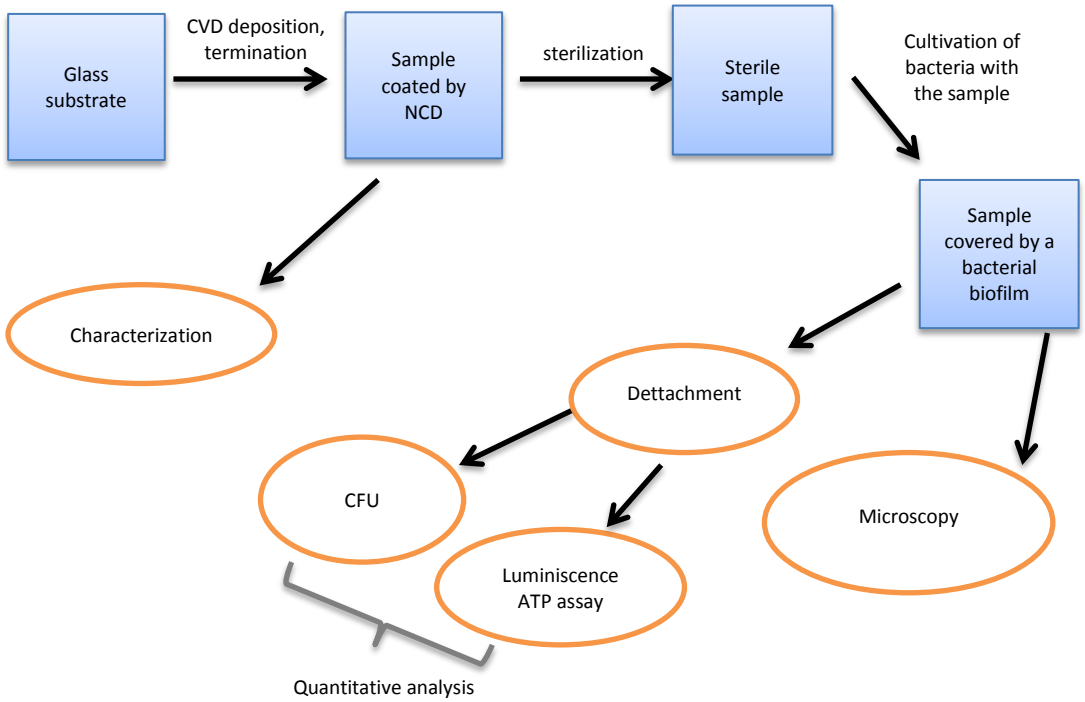

Figure 28 The flowchart of planned experiments

5.2. Theproperties of NCD films and glass substrates

Samples characterized in this section (and used later in experiments with bacteria) were uncoated glass, and glass coated by hydrogenated and oxidized NCD films.

5.2.1.The morphology of nanodiamond crystals

Scanning electron microscopy (SEM) images of NCD films are shown in Figure 29. It indicates typical surface morphology of nanocrystalline diamond films. The grain size was around 100 nm and did not exceed 200 nm. The NCD films were also fairly uniform within the whole surface.

The atomic force microscopy (AFM) was used for estimation of the roughness of NCD and glass surfaces.

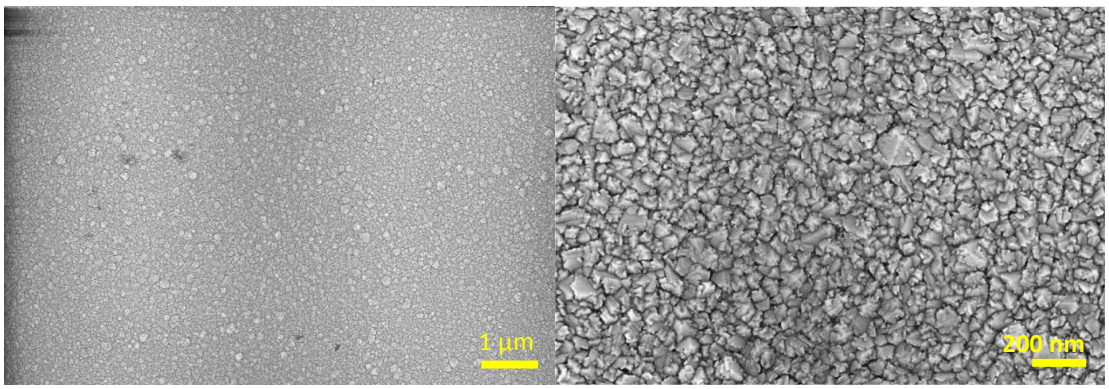

Figure 29 Representative SEM images of NCD films.

The Figure 30 shows the results of AFM analysis NCD film and uncoated glass. It is apparent that NCD films were rougher (RMS (root mean square) = 6.9 nm) than untreated glass (RMS = 0.9 nm). Even though the substrate glass was thoroughly cleaned before the AFM analysis, some impurities or particles of dirt can still be seen on the AFM image. However all the other attempts to clean the glass better were not successful. Therefore it appears that the glass is not the ideal reference material as it is difficult to characterize reproducibly. In many works other materials, which can be more easily defined, are used instead - for example silicon or stainless steel or titanium (Jakubowski *et*

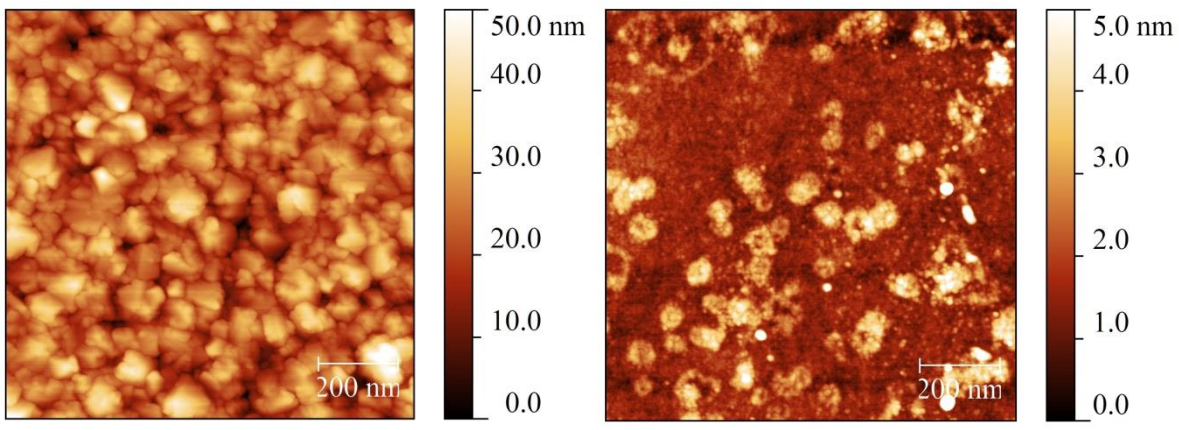

NCD film

Uncoated glass

Figure 30 Representative AFM images of NCD films and glass (note the different scale).

al., 2004; Goeres *et al.*, 2005; Zhao *et al.*, 2007; Shao *et al.*, 2009; Medina *et al.*, 2012). However, glass as a substrate was used in this work because transparent material was needed for further experiments that involved fluorescence microscopy. In the future experiments, we plan to switch to silicon substrates instead of glass and employ confocal microscope instead of inverted epifluorescence microscope to visualise bacterial biofilms on non-transparent materials.

5.2.2. Raman spectrum of NCD films

Representative Raman spectrum of NCD film is shown in Figure 31. It indicates the presence of three discernible peaks. First peak, around 1100 cm^{-1}, refers to trans-polyacetylene which can be present at the crystal boundaries (Ferrari and Robertson, 2001; Williams, O. A. *et al.*, 2008). Second, the most prominent peak at 1331 cm^{-1} corresponds to sp^3 hybridized carbon atoms (which are typical of diamond), while the lower peak at 1520 nm reflects sp^2 hybridization of carbon characteristic for graphite. The height of the diamond peak shows high proportion of crystalline diamond present on the surface of our samples. Certain fraction of sp^2 hybridized carbon is typical for CVD deposition process (Gracio *et al.*, 2010).

Because the Raman spectroscopy is rather volume sensitive method, there was no difference between hydrogenated and oxidized NCD films, so the spectrum presented in Figure 31 is identical for both hydrogenated and oxidized NCD films.

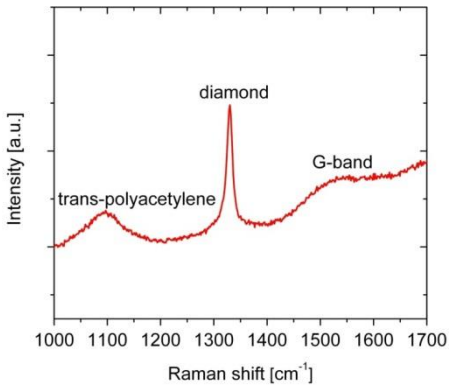

Figure 31 Representative Raman spectrum of NCD film. The intensity is expressed in arbitrary units.

5.2.3. Chemical composition NCD films determineded by XPS

The X-ray photoelectron spectroscopy is an ideal technique for quantitative analysis of the composition of the surface. The method is able to collect data to the depth of approximately 2 nm.

The results of XPS analysis are presented in Table 4. As expected, the hydrogenated NCD contained 10 % less of oxygen than oxidized NCD film. The content of 13 % oxygen on the oxidized NCD film surface and presence of the carbonyl groups (3 %) confirms the successful oxidation of the film (Beamson G., 1992) and is in perfect agreement with previously obtained data from XPS on NCD films (Kozak *et al.*, 2014).

The higher content of sp^2 hybridized carbon atoms on the surface of oxidized NCD film (23 %) in comparison with the hydrogenated one (7 %) is a consequence of partial graphitization of diamond surface after O_2 plasma treatment (Seth *et al.*, 1995).

Table 4 Chemical composition of H- and O-terminated NCD films estimated from XPS measurements

Sample	O [%]	C [%]		sp^2 [%]	sp^3[%]	C-O[%]	C=O[%]
NCD-H	3	97		7	77	16	-
NCD -O	13	87		23	59	15	3

5.2.4.Evaluation of the hydrophobicity of glass and NCD films

Contact angle (θ) serves as the measure of surface hydrophobicity, low contact angle signifies highly hydrophilic surface whereas high contact angle signifies high hydrophobicity of the surface.

As shown in the Figure 32, hydrogenated NCD films were very hydrophobic which is demonstrated by high contact angle around 80°. In contrast, oxidized NCD films were very hydrophilic with contact angles typically bellow 10°.

The uncoated glass exhibited contact angle in the range from 10° to 40°. This fluctuation was probably due to inhomogeneity of the glass surface. Also this problem could be probably solved if more homogenous material such as silicon is used.

The contact angles of oxidized (NCD-O) and hydrogenated (NCD-H) nanocrystalline diamond films are in perfect agreement with values measured for other nanodiamond materials (Marciano *et al.*, 2009b; Marciano *et al.*, 2011; Medina *et al.*, 2012).

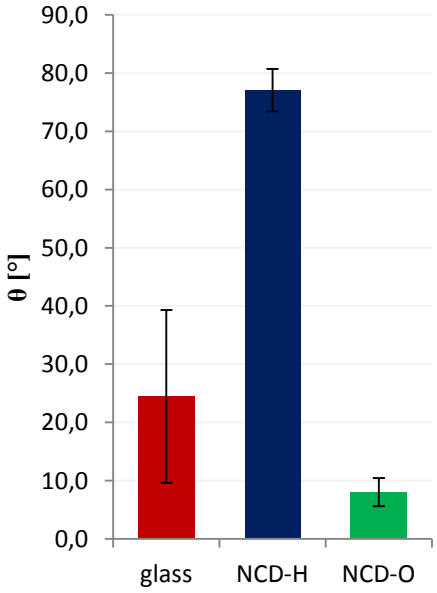

Figure 32 Contact angles of glass and NCD films. The graph shows mean values of at least three measurements with standard deviation.

5.3. The sterilization process optimization

Before use in further experiments, the NCD samples had to be sterilized.

It is known from the literature that hydrophilicity of oxidized DLC films did not endure the autoclaving process (Marciano *et al.*, 2009a), however, the impact of sterilization process on the NCD materials was not known. To investigate it, the following experiment was performed in which several sterilization methods were tested.

The stability of NCD films during different sterilization procedures was evaluated by contact angle measurement. Three standard sterilization methods were tested: autoclaving, dry heat sterilization and sterilization by UV light. Neither of sterilization methods physically damaged the samples; no visible signs of cracking or flaking of the NCD coating appeared. The contact angles were measured before and after the sterilization, the results are shown in (Figure 33).

Neither the sterilization by autoclaving nor the sterilization by UV light changed significantly the contact angle of hydrogenated or oxidized NCD films. In contrast, the dry heat sterilization substantially changed the surface of oxidized NCD films.

For further experiments I chose sterilization by autoclaving because autoclaving is definitely the most efficient way of sterilization (it eliminates bacteria and spores as well) and also because CDC Bioreactor used in my studies is whole autoclavable. This enabled to sterilize the whole CDC Bioreactor assembled together with the material samples and this way to minimize the risk of post-sterilization contamination.

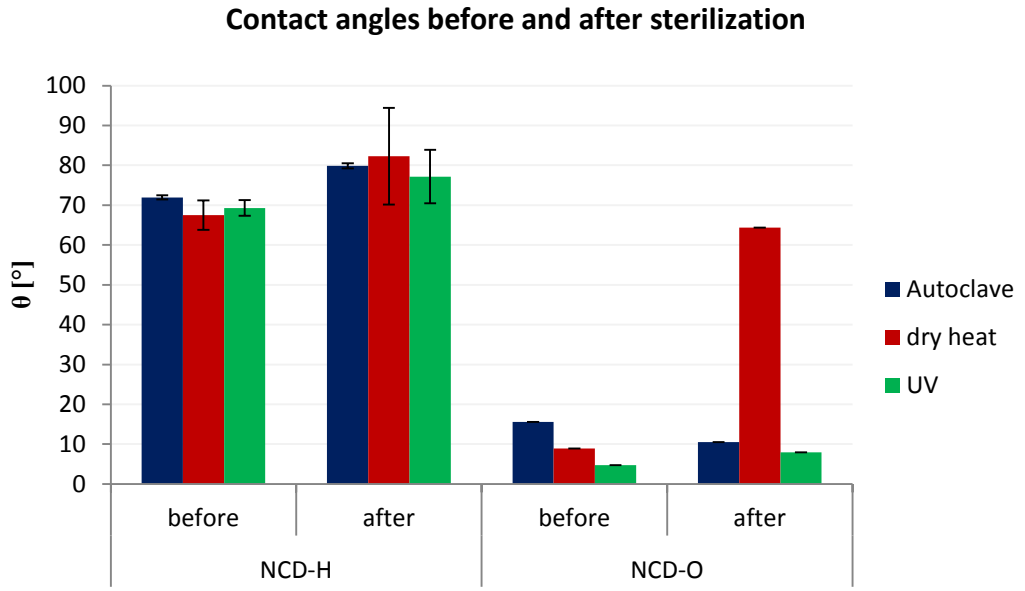

Figure 33 Change of contact angles of hydrogenated (NCD-H) and oxidized (NCD-O) films before and after sterilization by different sterilization method.

5.4. The optimization of cultivation of bacteria

5.4.1. Cultivation of bacteria in six-well plates

The growth of bacterial biofilm under static conditions is one from the most frequently used method (Maeyama *et al.*, 2004; Ploux *et al.*, 2007; Oh *et al.*, 2009). For the purpose of optimization of the parameters of cultivation, following scheme was used: bacterial culture (OD_{450} = 0.5) was diluted 10-times by fresh LB medium and applied into a six-well plate containing untreated glass (1×1.7 cm) samples in each well. Then, the biofilms were grown for 2 h, 6 h and 22 h.

The biofilm growth was evaluated by sonication in sonication bath (4.7.2.1) and following CFU count. However, this method showed to be poorly reproducible and unreliable because the sonicaton in ultrasonic bath was not able to detach bacterial biofilm properly (5.5.2). Therefore I do not show any data from this experiment. In the next experiments, the fluorescence microscopy and ATP assay was used to evaluate the biofilm growth. However, the result of this pilot experiment was not evaluable, it was obvious, that the chosen times were too short for more obvious and seamless covering of the sample by bacteria.

Thus, another experiment was performed: bacterial culture (OD_{450} = 0.5) was grown with glass samples for 24 h (1day), 48 h (2 days), 72 h (3 days) and 216 h (9 days). Every 24 h, the glass samples were removed from the medium, washed 3-times by 1 ml of fresh LB medium from both sides to detach loosely attached bacteria and placed to fresh pre-warmed medium. This experiment was evaluated by fluorescent microscopy. The results (Figure 34) of this experiment show well-developed biofilm which covered the whole surface of the sample.

After one day of biofilm growth, the individual cells were observed at the surface with no signs of biofilm formation. After two and three days of cultivation, bacteria formed thin biofilm. The biofilms grown for two days seemed more favourable for study of bacterial attachment and thus this set up was used in other experiments (5.5.2). After 9 days of cultivation, the biofilms were very thick and their staining with Hoechst 33342 was very problematic (most likely due to thicker ECM which is found in older bacterial biofilms (Donlan, R. M., 2002).

This experiment therefore showed that our strain *E. coli* K-12 is capable of biofilm formation on glass and provided a basic method for growing biofilms for other optimization studies (5.5.2).

5.4.2. Optimization of continuous cultivation of bacteria in CDC Bioreactor

The optimization of bacterial growth in CDC Bioreactor was crucial part of my work and so corresponding attention was payed to this problematics. It was necessary to (1) optimize stirring speed, (2) temperature setting and (3) to evaluate the parameters of bacterial growth in the bioreactor with and without fresh medium influx.

- Optimization of stirring speed

To find the stirring speed that would ensure the homogenous mixing and temperature distribution in the bioreactor vessel, an experiment simulating continuous cultivation was performed. In this experiment the possible temperature change in the vessel resulting from the non-temperated medium influx was monitored.

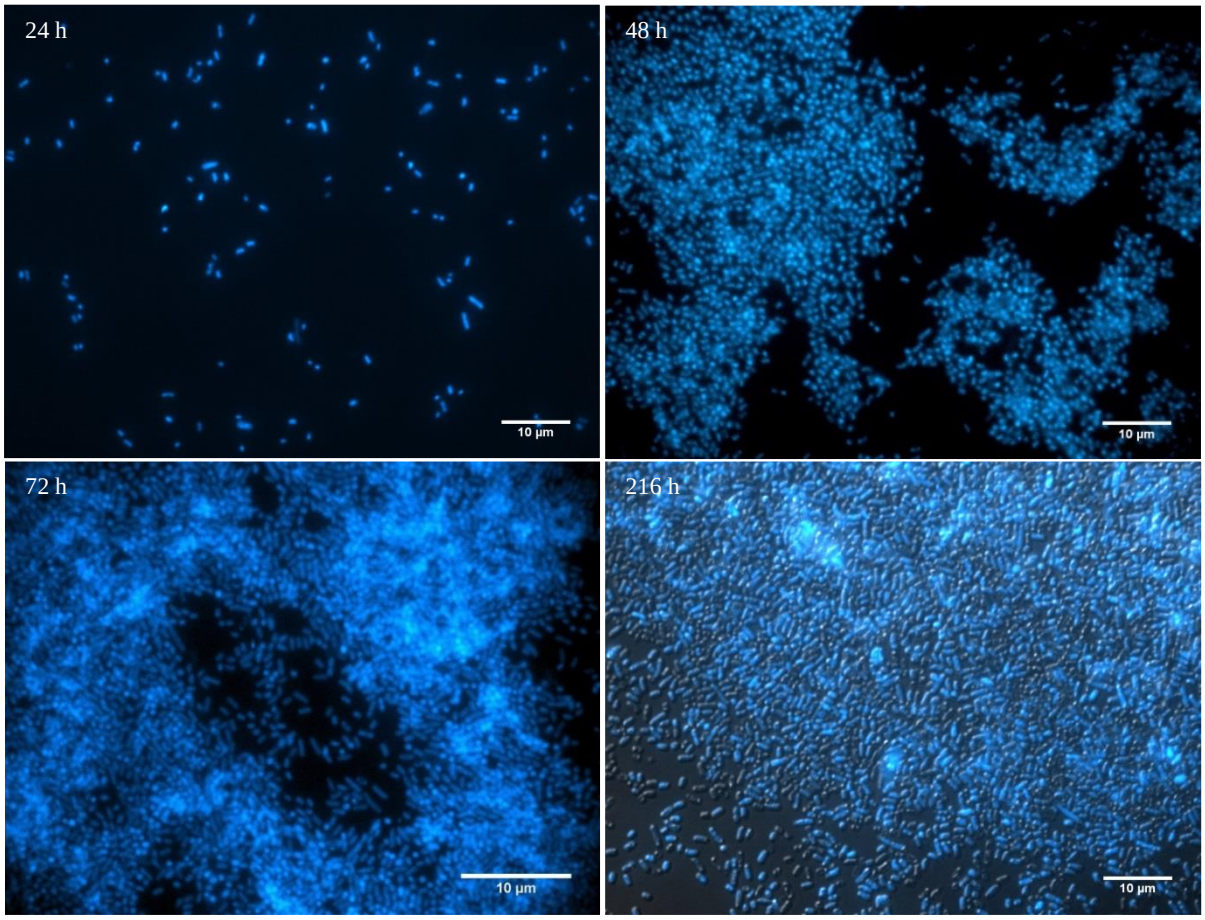

Figure 34 Representative images of glass samples covered by bacterial biofilm after various time of cultivation in six-well plates. (Stained by Hoechst 33342; image of the biofilm after 216 h is show also in DIC.)

Continuous cultivation in CDC Bioreactor was simulated using pre-warmed water poured into the bioreactor vessel (37° C).The continual inflow of fresh water at laboratory temperature simulated the future inflow of fresh LB medium. In order to simulate the cultivation conditions exactly, all holders with uncoated glass samples were also inserted into the CDC Bioreactor. The temperature inside the CDC Bioreactor was regulated via a thermo-sensitive probe connected to the heated magnetic stirrer. During this experiment, the actual temperature of the liquid in the vessel was also measured directly by a glass thermometer. The temperature was measured every minute and three stirring speeds were examined: 100 rpm, 150 rpm, and 200 rpm.

The results are shown in the Figure 35. It shows that all tested stirring speeds provided similar (and sufficient) temperature distribution. The temperature fluctuated in range of 1° C for all three

examined stirring speeds. In the all next experiments the stirring speed of 200 rpm was used as this speed ensured the most fluent stirring.

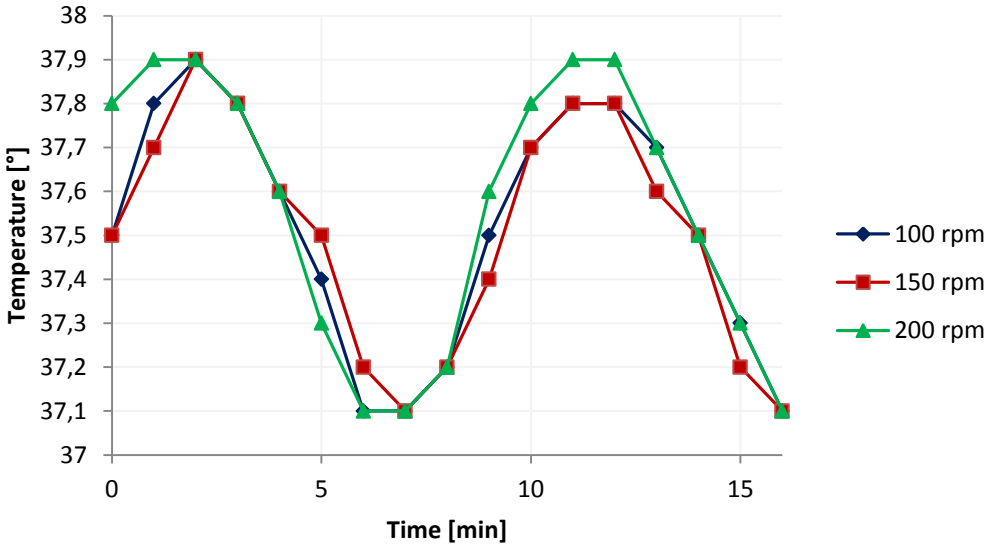

Figure 35 Fluctuation of the actual temperature in CDC Bioreactor. The temperation was ensured by external heated magnetic stirrer and three different stirring speeds were tested. Set temperature was 37°C and stirring speeds were 100, 150 and 200 rpm.

- The optimal temperature setting

When the temperature at the heated stirrer was set on 37° C, the temperature inside the vessel fluctuated between 37 and 38 °C. Therefore, in all other experiments the temperature was set on 36° C and the bacterial culture grew in the temperature between 36° and 37° C.

- Testing of the bacterial growth in diluted LB medium

As a stock medium for continuous cultivation I decided to use distilled water-diluted LB medium (4.3.1) The same medium was used in work of (Hadi *et al.*, 2010) for the cultivation of *Pseudomonas aeruginosa*. Lower concentration of nutrients was reported to promote adhesion to surfaces and biofilm formation also in the bacterium *E.coli* (Dewanti and Wong, 1995; Oh *et al.*, 2007).

Therefore, to examine whether it is possible to apply the experimental setup suggested by (Hadi *et al.*, 2010), the *E. coli* bacteria were cultivated in three different media:(1) in standard LB (control), (2) saline-diluted LB and (3) water-diluted LB medium. The saline-diluted medium was used as a control medium with lower concentration of nutrients while the concentration of NaCl remained the same as in standard LB medium (therefore the osmotic pressure remained unchanged). The batch cultivation in flasks was used (4.6.1). The results of this experiment are presented in the Figure 36.

All three cultures were inoculated from the same over-night culture (grown in standard LB). There was no observable lag phase in either of the cultures. As expected, the bacterial culture grown in

standard LB medium was able to reach higher OD than bacterial cultures grown in the media with lower content of nutrients, i.e. water-diluted and saline-diluted LB. This result is expectable, because bacteria use up all nutrients sooner in these two media. Nevertheless, in the continuous mode of cultivation this fact should not pose any problem, because the inflow of fresh stock medium should provide sufficient supply of nutrients needed for growth of the bacterial population.

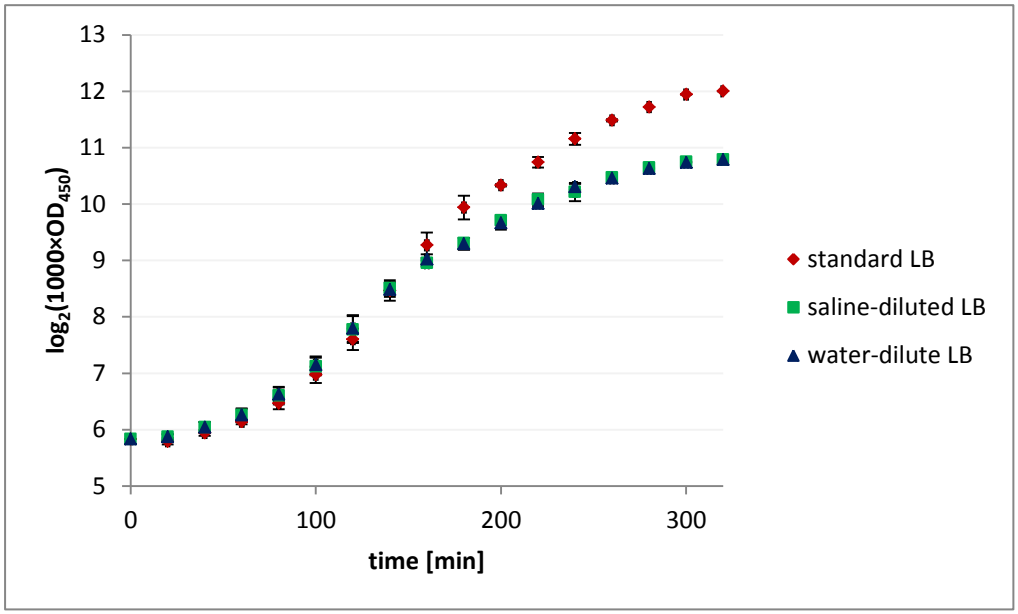

Figure 36 Growth curves of *E. coli* batch cultures grown in standard LB, saline-diluted LB and water-diluted LB medium. The data ale plotted in the semi-logarithmic mode. The graph shows mean values of three experiments with standard deviations.

From the exponential phase of the growth curves, the generation times were calculated for the respective cultures. The results are shown in Table 5. As expected, the cells grown in the standard LB medium exhibited somewhat shorter generation time compared to the bacterial cultures grown in low-nutrient alternatives of LB medium. Bacteria cultured in saline-diluted LB medium grew slightly faster than bacterial culture grown in water-diluted LB medium but the difference in generation times between these two cultures was insignificant. Therefore, as a stock medium for further cultivation in CDC Bioreactor, water-diluted LB medium was chosen.

Table 5 The generation times (T) of bacterial batch cultures grown in standard LB, saline-diluted LB and water-diluted LB medium. The values were calculated from the growth curves depicted in Figure 9.

	standard LB	saline-diluted LB	water-diluted LB
T [min]	25.8±0.8	32.2±2.3	31.8±1.5

- Bacterial growth in CDC Bioreactor

Cultivation process has been described in detail in chapter (4.6.2.2). The cultivation consists of two phases: batch (22 h) and continuous phase of various length (Figure 37).

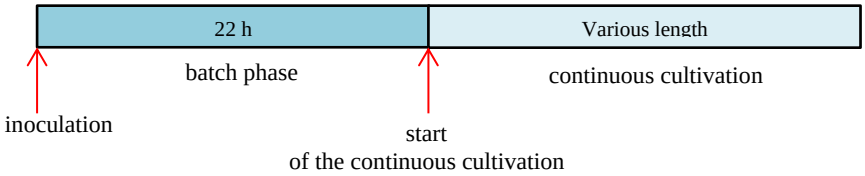

Figure 37 Experimental scheme of cultivation in CDC Bioreactor

To characterize the growth in CDC Bioreactor during both phases, the growth was followed turbidimetrically, OD was measured every 20 min or 30 min during batch and continuous phase, respectively.

The result is presented in Figure 38. In the batch phase, the bacterial culture grew with generation time 20.1±1.3 min. The growth slowed down after approximately 1 h of cultivation and was followed by the lag phase which lasted till the continuous flow was started. The continuous phase

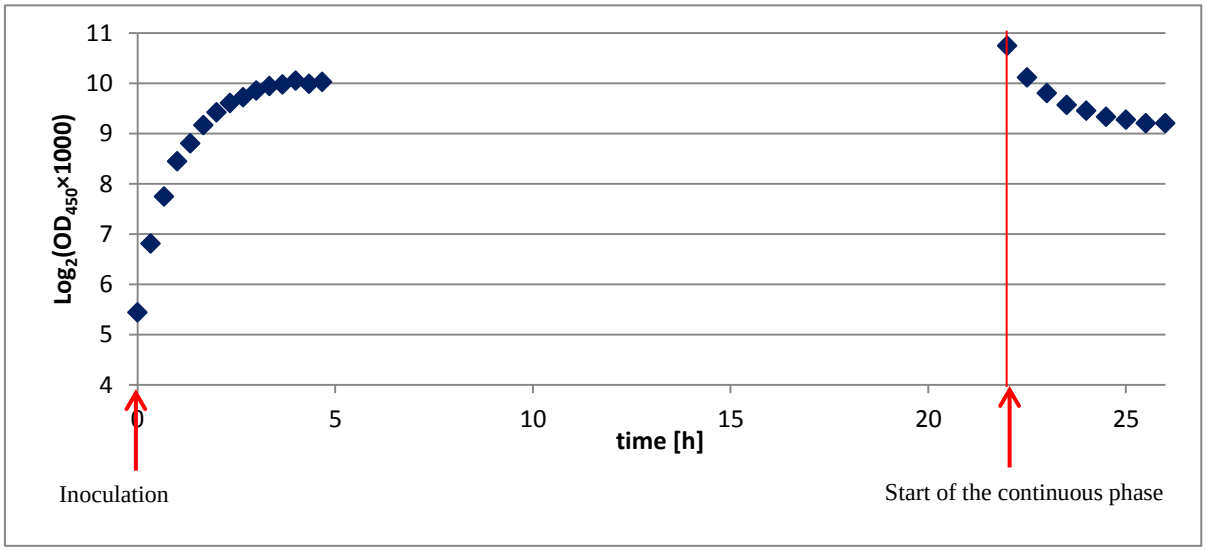

Figure 38 Growth of *E. coli* in CDC Bioreactor during batch phase and continuous phase of the cultivation. The graph shows mean values of three independent measurements. The data ale plotted in the semi-logaritmic mode.

of the cultivation is characterized by the initial dilution of the culture followed by the levelling of optical density at certain value. The bacterial culture reached this steady state after approximately 4 h of continuous cultivation. After these 4 hours, the culture maintained constant OD.

During cultivation, which would follow the experimental protocol described in CDC Bioreactor Manufacturer's manual[3], all unattached bacteria should be washed out by the fresh medium inflow.

[3]http://www.google.com/url?url=http://www.jysco.com/product/download.php%3Fit_id%3D1217998050%26it_file%3D236991873_4a5c04ab_CDC_Operators_Manual.pdf&rct=j&q=&esrc=s&sa=U&ved=0CC8QFjAAahUKEwiUz-C3taTHAhVDBBoKHc7vCVs&usg=AFQjCNEMocX5uMJJZWqyfD19x5abDKXWpA

This would need dilution speed about 12.4 $min.s^{-1}$. However, in our condition, it was impossible to ensure such fast diluting of the bacterial culture and therefore continuous cultivation in bioreactor was used as an improvement of cultivation in six-well plates. The advantages of continuous cultivation against cultivation in six-well plates are:

(1) no change in OD during longer cultivation and (2) limited but permanent supply of nutrient during the continuous phase of the cultivation.

5.5. The detachment of adherent bacteria and quantitative analysis of biofilm growth

5.5.1.Scraping by a razor blade

For viable colony count method, originally intended for biofilm quantification, a method was needed for reliable detachment of viable bacterial cells from the material sample surface. In the literature, the most used methods are: scraping by a teflon spatula (Dewanti and Wong, 1995) or cotton swab (Smeets *et al.*, 2003), sonication in ultrasonic bath (Elvers *et al.*, 1998; Katsikogianni *et al.*, 2006; Zhao *et al.*, 2007; Liu, C. *et al.*, 2008; Bjerkan *et al.*, 2009) or sonication by a sonicator with immersion probe (Stewart, C. R. *et al.*, 2012).

Many researchers (Smeets *et al.*, 2003) use scraping with a cotton swab as a method for quantitative detachment of bacteria. However, I do not consider this approach to be very exact because many bacteria remain in the swab and therefore cannot be washed out into the solution. This may significantly distort the results.

Another method (which I tested), scraping biofilm with a razor blade, seemed to be a more promising approach. The glass with grown biofilm was scraped with the blade once. However, as seen in Figure 39, the razor blade was not able to detach all the bacteria at once. The image shows the areas in the sample with a substantial portion of bacterial biofilm remains in near proximity of areas void of bacteria and also areas with traces of damaged bacterial cells.

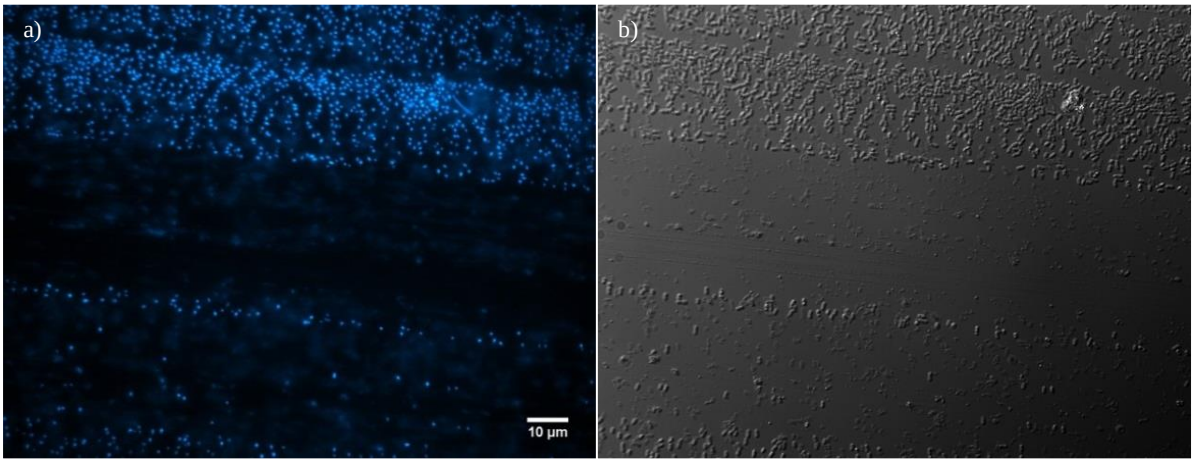

Figure 39 Representative images of the identical region of the glass sample with bacterial biofilm scraped by a razor blade and visualized by: a) fluorescent microscope (Hoechst 33342 staining); b) Differential interference contrast microscopy.

Therefore, neither this method was proved suitable for complete and reproducible detachment of viable bacterial cells.

5.5.2. Sonication in an ultrasonic bath

Sonication of the bacterial biofilm for the purpose of bacterial cells detachment is a widely used method and is claimed to be more reproducible than scraping (Bjerkan *et al.*, 2009).

- The effect of sonication in an ultrasonic bath on bacterial viability

To test the influence of sonication on bacterial cells (4.7.2) – especially the effect of the lower temperature and the sonication treatment itself – I performed following experiment: bacterial culture in exponential phase of growth was diluted ten times in saline. This suspension was divided into four sterile tubes (2 ml each): the first was appropriately diluted and plated immediately on LB agar, the second was left on the table at laboratory temperature (25°C) for 10 minutes, the third was cooled for 10 minutes (0-4° C) and the last was sonicated for 10 min (0-4° C, 35 kHz). After that, also these bacterial suspensions were appropriately diluted and plated on LB agar. The LB agar plates were cultivated over-night at 37°C, then the colonies were counted and the $CFU.ml^{-1}$ calculated.

The result of CFU count is presented in the Figure 40. The non-sonicated suspension incubated at room temperature exhibited the highest CFU count. The reason is probably the fact that the cell growth was not completely stopped in saline at room temperature and therefore the number of cell increased during the 10 min period of incubation. The cells in suspension incubated at low temperature had significantly lower CFU count due to growth inhibition by cold. The cooled + sonicated suspension exhibited comparable CFU count to the cooled suspension. This shows that the sonication itself was not harmful to bacterial cells. The reason why the sonicated culture did not grow to the same

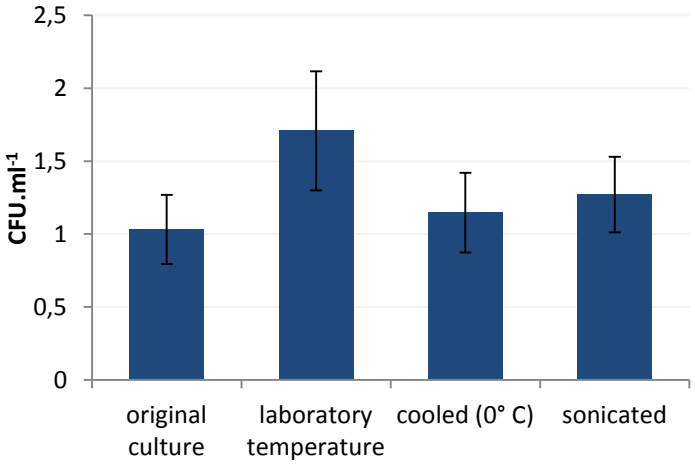

Figure 40 The effect of sonication on *E. coli* cells viability. The graph shows mean values of three independent experiments with standard deviations.

density as the non-cooled sample is probably only low temperature, not cell destruction during sonication. In summary, the sonication in ultrasonic bath was shown to be harmless for bacterial cells and can be used before CFU count.

- The efficiency of sonication in ultrasonic bath on bacterial detachment

The sonication process was subsequently tested with biofilms grown on glass. Bacterial biofilms grown in the six-well plates for 48 h were sonicated in saline for 20 min, than the saline with the detached bacteria was diluted and inoculated on LB agar for CFU count. After the sonication, the glass samples were investigated microscopically. It can be seen in the pictures (Figure 41), that the sonication was not able to detach all the adherent bacteria; there were large amounts of non-detached bacteria, comparable to the non-sonicated control samples.

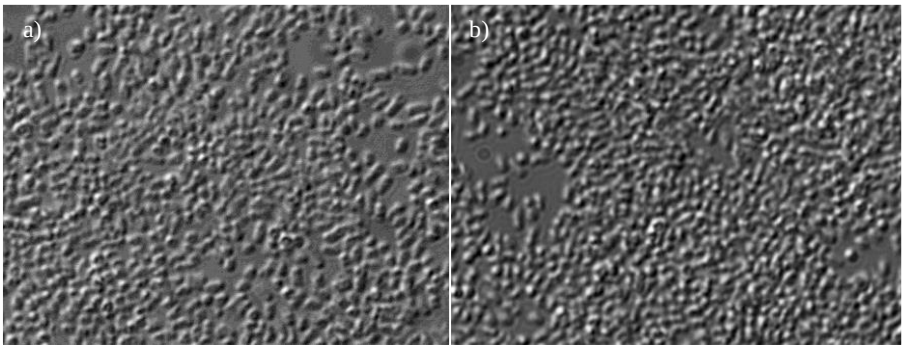

Figure 41 Result of sonication in ultrasonic bath: a – non-sonicated control; b- sample sonicated for 20 min. (DIC microscopy)

These results show that the sonication in the ultrasonic bath is sufficiently gentle to bacterial cells but at the same time is not efficient enough for complete detachment of living bacterial cells. Therefore, it is unfortunately not possible to use CFU count for quantitative analysis of the bacterial biofilm.

Hence, I also tested the sonication by a sonicator equipped with the immersion probe, which enables sonication at substantially higher power. However, such treatment damages the bacteria, and therefore the viable count method cannot be used for quantification. As an alternative method I therefore used the measurement of the ATP, released from the bacterial cells, with ATP luminescence assay (BacTiter-Glo® Viability Kit, Promega[4]). This assay contains also components for cell disruption and therefore also a solution containing both intact and destroyed cells can be easily analysed with this technique.

[4] https://worldwide.promega.com/resources/protocols/technical-bulletins/101/bactiter-glo-microbial-cell-viability-assay-protocol/

5.5.3.Sonication by a sonicator with immersion probe

To optimize the duration and amplitude of the sonication, I examined the impact of the set amplitude and number of sonication steps (one step = 30s of sonication, modified from (Stewart, C. R. *et al.*, 2012) on the effectivity of detachment of bacteria. The sonication effectivity was evaluated microscopically. The result of the sonication procedure was checked visually (Figure 42).

The biofilms were grown on uncoated glass samples in CDC bioreactor (5.4.2). Different sonication condition settings were examined: the amplitude (50 and 100 %) and number of sonication steps (1-4, 30s for each step).

Generally, the higher amplitude and longer time (i.e. more steps) ensured better bacterial detachment than the lower amplitude and shorter time of sonication. Sonication with 50% amplitude was not strong enough to detach the bacterial biofilm regardless the number of sonication steps.

Amplitude	100 %	100 %	50 %	50 %
n. of steps	1	4	1	4
duration of steps	30 s			

Figure 42 Effectivity of sonication-driven detachment of *E. coli* biofilm grown on glass (sonicator with the immersion probe)

With 100% amplitude I achieved better detachment than with the 50% amplitude. However, 100% applied just once for 30 was not sufficient enough for complete bacterial detachment from the glass surface. In the four-step sonication with 100% amplitude, there was visible glass cleaning in the proximity of the immersion probe already after the second step of sonication.

Based on this experiment, the sonication procedure was modified as follows: the sample with grown biofilm was sonicated twice for 30 s from each side: once at the top region of the glass sample and once at the bottom region to cover the whole sample area (Figure 43). After ultrasonic treatment the samples were also checked by fluorescent staining and microscopy. The result of the treatment was

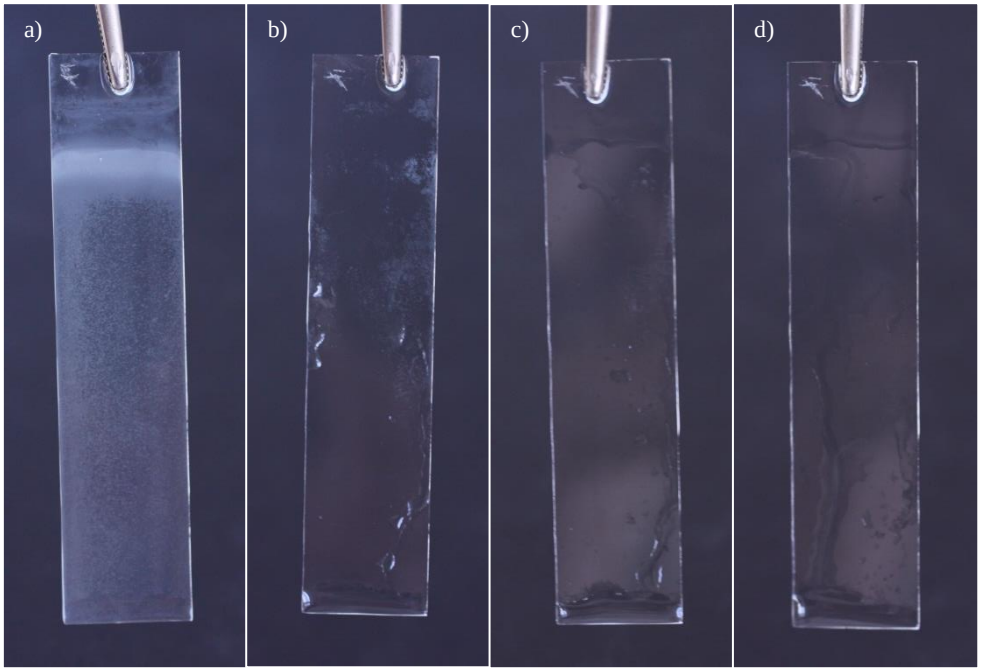

Figure 43 The gradual detachment of bacterial biofilm during the sonication process: a) before sonication b) 2× 30s c) 3× 30s d) 4×30s of sonication.

the glass almost completely free of bacteria only with a thin area covered with the biofilm remains on the edges of the glass (Figure 44 a).To detach also these remains, detergents Triton and SDS in concentration of 0.1 % and 1 % [w/v], respectively were added to the sonication solution (saline). Microscopic observation of so treated samples showed that Triton was less successful in detachment than SDS (Figure 44).

Figure 44 Sonication of sample a) without detergent ; b) with SDS; c) with Triton. Hoechst 33342 stain, scale bar: 10 µm

In the control experiment the ATP assay kit was tested with both ATP stock solution and sonicated-bacteria suspension in presence of detergents (Figure 45). The experiment unfortunately showed that chosen detergents, especially SDS, interfere with the luminescence measurement. The presence of detergents resulted in lower luminescence of both bacterial culture and ATP solution compared to negative control without detergent addition. The inhibition by Triton was not so distinctive but at the same time this detergent did not improve the biofilm detachment significantly. Therefore neither SDS nor Triton was applied in further experiments and the sonication was performed only in saline.

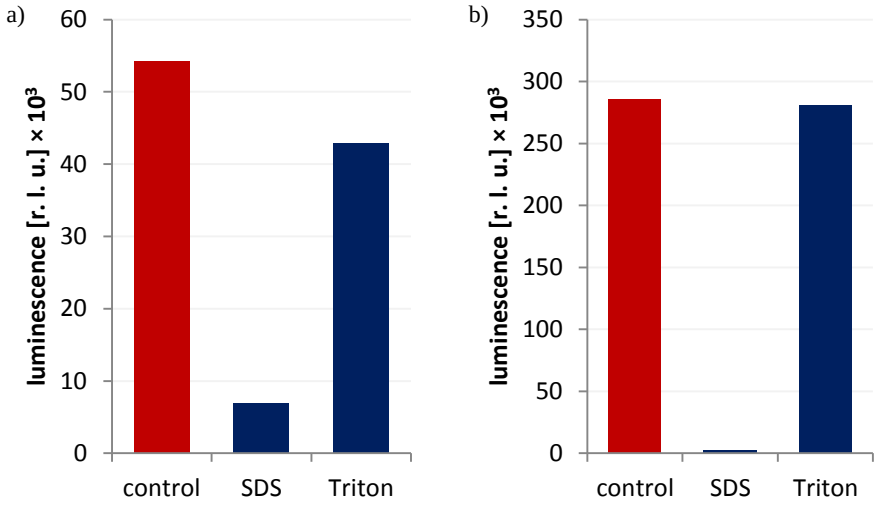

Figure 45 The effect of use of detergents on luminescence measurement. a – sonicated colution; b- ATP solution (1nmol.l^{-1})

5.5.4.Luminescence measurement

For quantitative analysis of the bacteria detached from the material samples, the ATP assay was performed using BacTiter-Glo® kit (Promega). First, the calibration curves for ATP and bacterial cells were constructed: (1) the dependence of luminescence intensity on ATP concentration, (2) the dependence of ATP concentration on the number of cells (Figure 46).

More diluted samples of the culture were difficult to measure due to low concentration of ATP. The threshold for measuring luminescence was determined to be around 100 r. l. u. (relative luminescence units). (The calibration curve for ATP was measured in every experiment and served as a reference.)

On the basis of these curves and CFU count of the bacterial culture, the concentration of ATP in a single cell was counted. One bacterial cell contained about 10.8 mmol.l^{-1} ATP, which is slightly more than the value determined by (Bennett et al., 2009), which was 9.6 mmol.l^{-1} ATP per 1 cell of *E.coli*.

Therefore, bacterial suspensions could be evaluated on the basis of ATP concentration measured by BacTiter-Glo® kit. However, because ATP content of bacterial suspensions, which were obtained after sonication of glass samples with grown biofilms by sonicator with immersion probe, could not be assayed immediately (from the technical reasons), the suspensions needed to be frozen. The stability of bacterial suspension during freezing (-20° C) was examined: after first ATP assay, the diluted samples were frozen for 5 days and then the assay and luminescence measurement was performed again. There was no decrease in the luminescence values compared to original measurement (data not shown). Hence in the following experiments, the bacterial suspensions after sonication could be frozen and stored several days for later ATP analysis if needed.

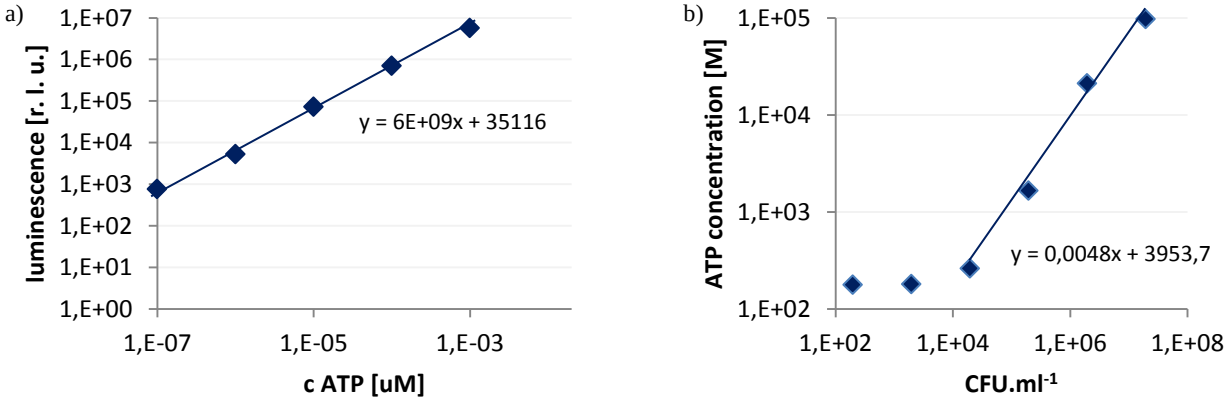

Figure 46 a - the dependence of luminescence intensity on ATP concentration; b- the dependence of ATP concentration on the number of cells.

The last step of the optimization of luminescence measurement was a pilot experiment with glass samples covered by bacterial biofilm grown in CDC Bioreactor. The glass samples (7.7×1.7 cm) were cultivated for 22 h in batch mode of cultivation and 24 h in continuous mode of cultivation. Then they were sonicated as described above (5.5.3) and the aliquots of resulting bacterial suspension were analysed with BacTiter-Glo® kit. The luminescence was around 31.10^3 r.l.u. which corresponds to ATP concentration of 40.10^3 mol.l^{-1}.

5.6. Adhesion of bacteria to nanocrystalline diamond films

5.6.1.Comparison of anti-adhesive properties of NCD films and glass

The main aim of this thesis was to verify the putative anti-adhesive properties of NCD films. For this purpose, three uncoated glass samples (controls), two hydrogenated and two oxidized NCD samples were cultivated with bacteria in the CDC biorector. The bacterial culture (OD_{450} = 0.1) was inoculated into the CDC Bioreactor (4.6.2.2) and cultivated first for 22 h in batch phase and then for

24 in continuous cultivation phase (Figure 47). At the end of cultivation all the samples were removed at once.

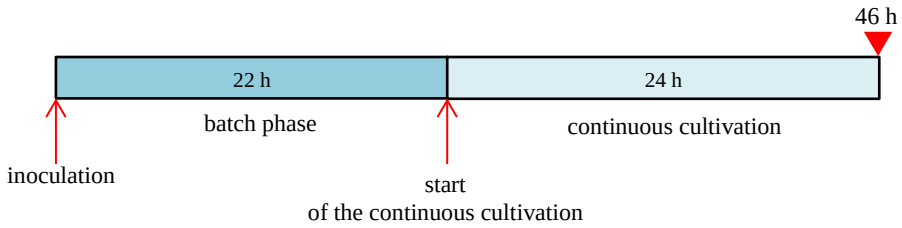

Figure 47 Schematic drawing of the experimental set-up. The moment of samples removal is marked with a red triangle.

One NCD-uncoated glass (control sample), one sample coated by hydrogenated NCD and one sample coated by oxidized NCD were stained with Hoechst 33342 stain and observed under fluorescence microscope (Olympus Cell-R). The whole experiment was repeated three times. Representative pictures are shown in the Figure 48.

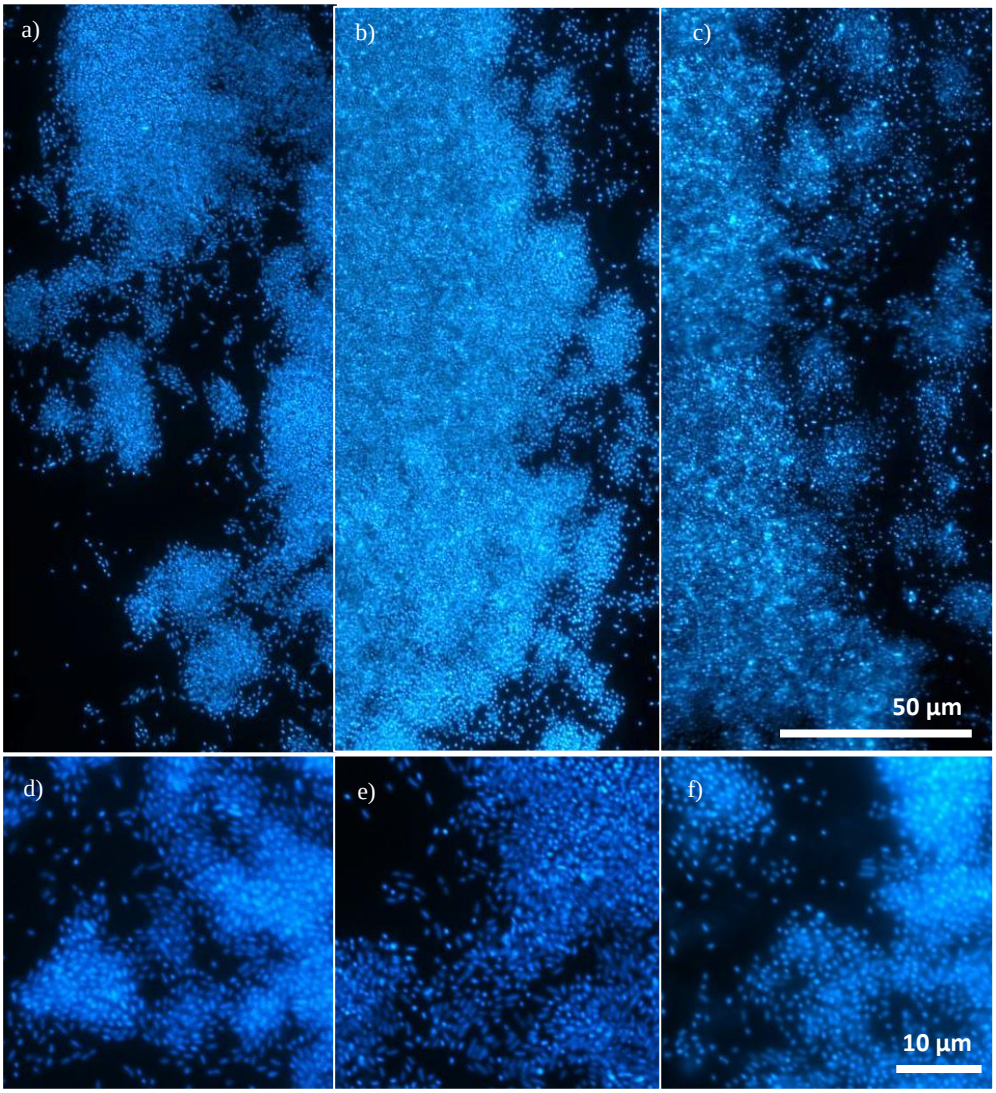

Figure 48 Representative pictures of *E. coli* attached to different materials: a, d – glass; b, e - hydrogenated NCD; c, f – oxidized NCD. The morphology of colonies is presented in the upper panel, the lower panel shows adhering bacteria in detail. Hoechst 33342 stain.

All the samples were covered by bacterial colonies. The samples were not covered uniformly, there were areas of bacteria growing in more layers as well as areas with low bacterial coverage. According to the images a)-c), from Figure 48, there are more bacteria attached to the hydrogenated NCD, which is also confirmed by results of ATP measurement (Figure 49).

The other three samples were sonicated following the protocol described in the chapter 4.7.2.1, the saline solutions with detached bacteria were frozen and the ATP concentration was measured the next day. The results (Figure 49) shows that bacteria attached preferably to hydrogenated NCD and adhered less to NCD-O and the uncoated glass. The differences between NCD-H and uncoated glass were not significant.

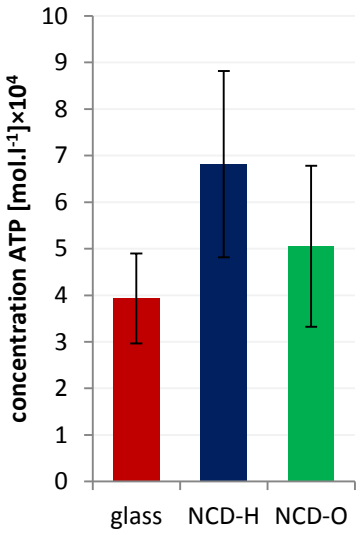

Figure 49 Quantification (ATP concentration) of ***E. coli*** biofilms grown on glass, NCD-H and NCD-O after 46h of cultivation. The graph shows mean values of three independent experiments with standard deviations.

5.6.2.Time-dependent growth of bacterial biofilm on NCD and glass in CDC Bioreactor

To estimate the dynamics of the *E. coli* biofilm development on the tested surfaces, the biofilm growth of was monitored over time. The samples used in this experiment were again glass samples (7.7 ×1.7 cm) coated either by hydrogenated or oxidized NCD films (3 samples) and uncoated glasses (4 samples) which served as the negative control. The bacterial culture (OD_{450} = 1.0) was inoculated into the CDC Bioreactor (4.6.2.2). After 22 h of batch cultivation, continuous cultivation phase started. In the course of cultivation, the samples (glass, NCD-H/NCD-O, one of each) were removed from the bioreactor at three given time points: (1) after 5 h of batch cultivation, (2) after 22 h of batch cultivation and (3) after 22 h of batch cultivation + 5 h of continuous cultivation (27 h in total) (Figure 50). The samples were sonicated immediately after removal and the saline with detached bacteria was frozen. The luminescence was measured the day after end of the cultivation. The experiment was repeated three times with hydrogenated and tree times with oxidized NCD samples.

The results (Figure 51) showed that after 5 h of batch cultivation the bacteria attached slightly more to hydrogenated NCD. After 22 h of batch cultivation, the bacteria adhered similarly to all three materials but after additional 5-h continuous cultivation (i.e. after 27 h of cultivation in total) the bacteria adhered more to NCD films than to glass. Also in this experiment, the bacteria seemed to prefer the hydrophobic surface (hydrogenated NCD) films over the hydrophilic one (oxidized NCD).

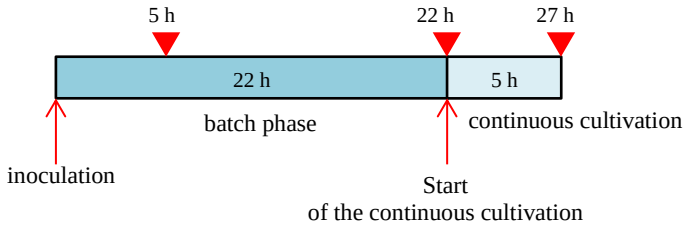

Figure 50 Schematic drawing of the experimental set-up. The moments of samples removal are marked with a red triangles.

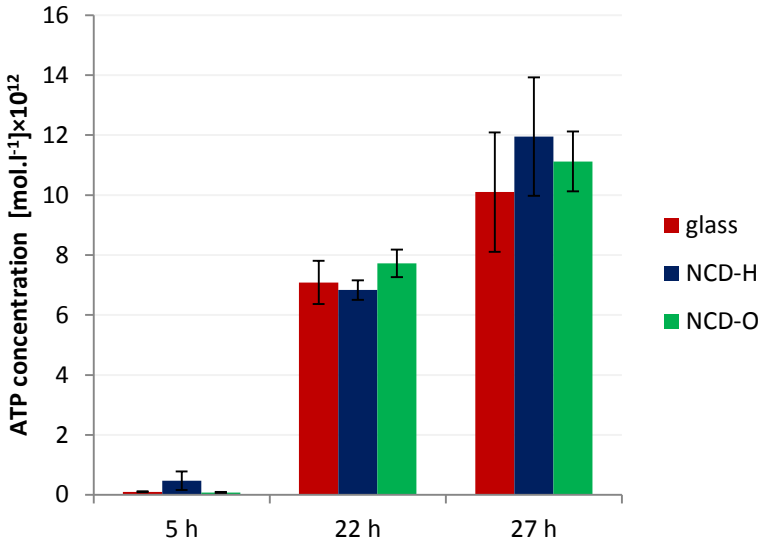

Figure 51 Quantification (ATP concentration) of *E. coli* biofilms grown on glass, NCD-H and NCD-O after 5, 22 and 27h of cultivation. The graph shows mean values of three independent experiments with standard deviations.

5.6.3.Discussion on the anti-adhesive properties of NCD films

In our experiments, the antibacterial potential of NCD films, as reported by (Medina *et al.*, 2012) was not confirmed. During the cultivation in bioreactor, both in the batch and continuous mode of cultivation, NCD coating was not able to prevent bacterial adhesion. On the contrary, with longer time of cultivation, bacteria adhered more to NCD films than to glass. One of the possible explanations of this effect can be the difference in surface roughness of compared materials. The AFM measurement (5.2.1) shown that NCD surface exhibit higher roughness compared to uncoated glass. This is in agreement with several published studies which report that increased surface roughness facilitates bacterial adhesion and settlement (Taylor *et al.*, 1998; Katsikogianni M., 2004).

The formation of conditioning film due to protein adherence on the surface of NCD material was observed by Grieten *et al.* (2011). In my experiments, Luria Bertani medium, i.e. the complex medium containing organic hydrolysates (yeast extract and peptone) was used. It is very probable that peptides and maybe other organic molecules present in the cultivation could bind to glass and NCD surface and promote bacterial adhesion. Therefore, I plan to repeat my experiments also in minimal medium in future.

Lewis *et al.* (2010) investigated the attachment and biofilm formation of *Pseudomonas fluorescens* to stainless steel and NCD films of different morphology. Their experiments were performed also in continuous perfusion environment of CDC Bioreactor and they used complex medium, which composition is comparable to that of Luria-Bertani medium used in my experiment. Their experiment indicated that the bacterial growth on the NCD surface was eliminated to 68%, 38% and 8%, depending on the morphology of the surface. The samples possessed different grain sizes but no correlation between grain size and anti-adhesive properties was observed. The bacterial biofilm was observable after 24 h of continuous cultivation and achieved thickness of about 20 μm on stainless steel. Also in my experiments, the bacterial biofilms were observable after 24 h of continuous cultivation.

The explanation of different bacterial colonisation of oxidized (hydrophilic) and hydrogenated (hydrophobic) NCD films could be based especially on different wetting properties of both materials. Hydrophobicity of both bacterial and material surface was reported to play important role in bacterial attachment (3.1.2) The cell surface of bacterium *E. coli* has been reported to have hydrophobic character (Donlan, R. M., 2002; Li and Logan, 2004) and therefore *E. coli* should adhere preferentially to rather hydrophobic surfaces (Fletcher and Loeb, 1979; Taylor *et al.*, 1998; Katsikogianni M., 2004). The results of my experiments are in accordance with these observations. The measurement of contact angles confirmed the higher hydrophobicity of hydrogenated NCD compared to highly hydrophilic oxidized NCD. During cultivation in continuous perfusion environment *E. coli* adhered more to hydrophobic surface of hydrogenated NCD than to the hydrophilic oxidized NCD.

Because the bacteria in my experiment adhered more to NCD, which are rougher, I hypothesise, that the bacterial attachment in my experiments was influenced mainly by surface roughness. The surface hydrophobicity played minor, but still not negligible, role, as there was slight decrease in the bacteria adhering to oxidized NCD.

Due to limited number of material samples I could not evaluate the hydrophobicity of *E. coli* cells from biofilms grown on glass and NCD. However, this experiment is planned for my future work on this topic. Also I would like to employ other bacterial species with different cell surface properties

(such as high hydrophobicity or cell wall structure). For example microorganism, which contain mycolic acid (such as *Corynebactrium*) were reported to have highly hydrophobic cell surface (Bendinger *et al.*, 1993). Also, *Bacillus subtillis* should be involved in my next experiments, since it is gram positive model organism or *Pseudomonas aeruginosa* as the most often used model organism for biofilm formation.

Another parameter that is hypothesised to influence the complex process of bacterial attachment is surface energy and charge, both of a bacterium and the substratum (Donlan, R. M., 2002; Li and Logan, 2004; Zhao *et al.*, 2007; Liu, C. *et al.*, 2008). However, these properties were not examined in my work.

The comparison of bacterial attachment to glass and NCD films was based on the ATP content in the solutions after biofilm sonication. Converting these values into numbers of cells was also considered. Finally, this conversion was not applied for the following reason. For such calculation, the dependence of ATP concentration on the number of cells is needed. Such calibration curve was constructed (5.5.4) and the ATP concentration in one cell was calculated as 10.8 $mmol.l^{-1}$. However, the bacterial suspension used for the calibration was a sample of the *E. coli* culture grown in suspension the CDC Bioreactor not cells from a resuspended biofilm grown on a solid surface. Due to procedure difficulties with biofilm disruption and following colony count (5.5.2), I was not able to measure a calibration curve with cells that would physiogically correspond to biofilm growers. Bacteria living in biofilms usually differ in their physiology, size etc. from those planctonic ones (O'Toole George, 2000; Liu, Y. and Tay, 2001; Donlan, R. M., 2002; Liu, Y. and Tay, 2002) Therefor also ATP level could differ between planctonic and biofilm-attached cells (Liu, Z. *et al.*, 2014). Consequently, the results of such conversion could be disputable.

In many works dealing with biofilms, the biofilm growth is quantified only using microscopic observation and consequent data analysis. However, I consider this method as more qualitative than quantitative. The reason is that the estimation of overall biomass and number of cells is difficult in the multilayer biofilms – which is the overwhelming majority of biofilms. Also, because thin biofilms usually does not cover whole surface of the sample, it is difficult to take representative image, the observation of several areas of the sample is needed. In my work, I used fluorescent microscopy to get the basic knowledge on the morphology and general coverage of the sample by the bacterial microcolonies. My aim was to introduce a method of biofilm cultivation and quantification, which would be useable for analysis of various nanomaterials in future.

ATP level measurement was chosen as a method for biofilm quantification as a seemingly easy, quick and reproducible method. However, even this approach seems to have certain limitations. If the

bacteria growing on different surfaces possess different physiology, the ATP levels could slightly differ as well (Ivanova *et al.*, 2006) and therefore comparison of such samples can be difficult.

When I compare the results of the two experiments with NCD and glass samples performed in CDC Bioreactor, the obtained values of concentrations of ATP are not logical: the higher value is obtained for shorter cultivation. However, it was obvious from microscopic observation of the biofilms grown for 46 h and 27 h (from pilot experiments with uncoated glass samples, data not shown), that there were notably more bacteria grown after 46 h compared to almost bacteria-free glass obtained after 27 h of cultivation.I hypothesise, that sonication by immersion probe could have detached biofilm from the samples, but did not disperse it completely. Therefore, there may remained a larger flocks of bacterial cells embedded in ECM. ECM could have protected the cells from certain components of BacTiter-Glo® kit, which led to incomplete release of cellular ATP to the solution and thus to lower luminescence signal.

The use of CDC Bioreactor was quite time-consuming and limited in number of samples which could be examined at once. However it has also some advantages (over the cultivation in a 6-well plates) such as more precise control of physiology of bacteria cultivated inside.

Also, glass showed up to be a rather unsuitable control material because of its complex chemistry which disables proper cleaning and XPS analysis. In the future, more suitable material, such as silicon, could be used (Scheuerman *et al.*, 1998). However, this would require the use of different microscope (CLSM, for instance), because the silicon is not transparent.

In summary, I managed to optimize basic methods for cultivation and analysis of bacterial biofilms and successfully used them for a study of anti-adhesive properties of nanocrystalline diamond and glass. Despite the NCD were not shown to possess anti-adhesive properties against E. coli, making a final conclusion on the bacterial attachment to NCD surfaces is quite difficult, due to quite contradicting data from the literature. Therefore, more information on this topic is needed.

6. Summary

Nanocrystalline diamond films (NCD) on glass were prepared and characterized:

- The main grain size was ca. 100 nm.
- Raman spectra indicated a formation of the NCD films with good structural properties.
- Hydrogenated and oxidized NCD films with hydrophobic and hydrophilic surface properties were prepared.
- The NCD surface oxidization was accompanied by the change in chemical composition and the substantial reduction in the surface hydrophobicity; the contact angle decreased from 77° (hydrogenated NCD, hydrophobic) to less than 10°C (oxidized NCD, hydrophilic).
- Several methods of NCD samples sterilization were tested (for the need of further experiments). Autoclaving was shown to be the most suitable non-destructive method for the NCD surface.

New laboratory methods were tested and optimized for bacterial biofilms cultivation and evaluation:

- Two alternatives of cultivation of *Escherichia coli* biofilm on the solid surface were tested and optimized: the cultivation in continuous perfusion environment of the CDC Bioreactor, where the conditions can be controlled with higher accuracy and the cultivation in 6-well plates.
- The methods for reproducible biofilm detachment were thoroughly tested:
    - Scraping of bacteria from the solid surface with the use of razor blade showed to be an unreliable method of bacterial detachment.
    - The ultrasonic bath was shown to be safe for planctonic bacteria but it was not able to detach bacteria from the solid surfaces. Therefore the method could not be used for bacterial detachment in my experiments.
    - The sonication of bacterial biofilms by a sonicator with the immersion probe resulted in the best biofilm detachment. After the optimization of this method, the sonicator was able to remove whole bacterial biofilm from the sample surface, with an exception of small area around the sample edges. It was not possible to improve this method by using detergents as they affect ATP level determination by ATP kit, which was used for the quantitative evaluation of the bacterial biofilm.

The anti-adhesive properties of NCD films were tested using the optimized methods:

- The antibacterial or anti-adhesive properties of NCD films were not confirmed.
- Both the hydrogenated and the oxidized NCD films slightly promoted bacterial settlement after 5, 22, 27 and 46 h of cultivation in comparison to uncoated glass. I hypothesise that this effect may be caused by higher surface roughness of the NCD samples.

- The bacteria adhered slightly more to hydrophobic surface of hydrogenated NCD than to highly hydrophilic surface of the oxidized NCD films.

7. References

Abou Neel, E. A., Pickup, D. M., Valappil, S. P., Newport, R. J. and Knowles, J. C. (2009). "Bioactive functional materials: A perspective on phosphate-based glasses." Journal of Materials Chemistry **19**(6): 690-701.

Agladze, K., Wang, X. and Romeo, T. (2005). "Spatial periodicity of *Escherichia coli* K-12 biofilm microstructure initiates during a reversible, polar attachment phase of development and requires the polysaccharide adhesin PGA." Journal of Bacteriology **187**(24): 8237-8246.

Akhavan, O. and Ghaderi, E. (2010). "Toxicity of graphene and graphene oxide nanowalls against bacteria." ACS Nano **4**(10): 5731-5736.

Amann, R., Fuchs, B. M. and Behrens, S. (2001). "The identification of microorganisms by fluorescence in situ hybridisation." Current Opinion in Biotechnology **12**(3): 231-236.

Arnault, J. C., Petit, T., Girard, H., Chavanne, A., Gesset, C., Sennour, M. and Chaigneau, M. (2011). "Surface chemical modifications and surface reactivity of nanodiamonds hydrogenated by CVD plasma." Physical Chemistry Chemical Physics **13**(24): 11481-11487.

Babchenko, O., Romanyuk, N., Jendelova, P. and Kromka, A. (2013). "Tailoring morphologies of diamond thin films for neural stem cells culturing." Physica Status Solidi B-Basic Solid State Physics **250**(12): 2717-2722.

Bakker, D. P., Busscher, H. J., van Zanten, J., de Vries, J., Klijnstra, J. W. and van der Mei, H. C. (2004). "Multiple linear regression analysis of bacterial deposition to polyurethane coating after conditioning film formation in the marine environment." Microbiology-(UK) **150**: 1779-1784.

Barnhart, M. M. and Chapman, M. R. (2006). Curli biogenesis and function. Annual review of microbiology. **60:** 131-147.

Beamson G., B. D. (1992). High resolution XPS of organic polymers: The scienta ESCA300 database. Chichester, John Wiley and Sons.

BellonFontaine, M. N., Rault, J. and vanOss, C. J. (1996). "Microbial adhesion to solvents: A novel method to determine the electron-donor/electron-acceptor or Lewis acid-base properties of microbial cells." Colloids and Surfaces B: Biointerfaces **7**(1-2): 47-53.

Beloin, C., Roux, A. and Ghigo, J. M. (2008). "Escherichia coli biofilms." Bacterial Biofilms **322**: 249-289.

Bendinger, B., Rijnaarts, H. H. M., Altendorf, K. and Zehnder, A. J. B. (1993). "Physicochemical cell-surface and adhesive properties of coryneform bacteria related to the presence and chain-length of mycolic acids." Applied and Environmental Microbiology **59**(11): 3973-3977.

BenNasr, A., Olsen, A., Sjobring, U., MullerEsterl, W. and Bjorck, L. (1996). "Assembly of human contact phase proteins and release of bradykinin at the surface of curli-expressing *Escherichia coli*." Molecular Microbiology **20**(5): 927-935.

Bennett, B. D., Kimball, E. H., Gao, M., Osterhout, R., Van Dien, S. J. and Rabinowitz, J. D. (2009). "Absolute metabolite concentrations and implied enzyme active site occupancy in *Escherichia coli*." Nature Chemical Biology **5**(8): 593-599.

Beranova, J., Seydlova, G., Kozak, H., Potocky, S., Konopasek, I. and Kromka, A. (2012). "Antibacterial behavior of diamond nanoparticles against *Escherichia coli*." Physica Status Solidi (b) **249**(12): 2581-2584.

Beranova, J., Seydlova, G., Kozak, H., Benada, O., Fiser, R., Artemenko, A., Konopasek, I. and Kromka, A. (2014). "Sensitivity of bacteria to diamond nanoparticles of various size differs in gram-positive and gram-negative cells." FEMS Microbiology Letters **351**(2): 179-186.

Bergmans, L., Moisiadis, P., Van Meerbeek, B., Quirynen, M. and Lambrechts, P. (2005). "Microscopic observation of bacteria: Review highlighting the use of environmental SEM." International Endodontic Journal **38**(11): 775-788.

Bjerkan, G., Witso, E. and Bergh, K. (2009). "Sonication is superior to scraping for retrieval of bacteria in biofilm on titanium and steel surfaces in vitro." Acta Orthopaedica **80**(2): 245-250.

Boland, T., Latour, R. A., Stutzenberger, F. J. (2000). Molecular basis of bacterial adhesion. Handbook of bacterial adhesion: Principles, methods, and applications, Humana Press.

Bos, R., van der Mei, H. C. and Busscher, H. J. (1999). "Physico-chemistry of initial microbial adhesive interactions - its mechanisms and methods for study." FEMS Microbiology Reviews **23**(2): 179-230.

Boulos, L., Prevost, M., Barbeau, B., Coallier, J. and Desjardins, R. (1999). "LIVE/DEAD® Baclight™: Application of a new rapid staining method for direct enumeration of viable and total bacteria in drinking water." Journal of Microbiological Methods **37**(1): 77-86.

Branda, S. S., Vik, A., Friedman, L. and Kolter, R. (2005). "Biofilms: The matrix revisited." Trends in Microbiology **13**(1): 20-26.

Ceri, H., Olson, M. E., Stremick, C., Read, R. R., Morck, D. and Buret, A. (1999). "The calgary biofilm device: New technology for rapid determination of antibiotic susceptibilities of bacterial biofilms." Journal of Clinical Microbiology **37**(6): 1771-1776.

Chang, H. T., Rittmann, B. E., Amar, D., Heim, R., Ehlinger, O. and Lesty, Y. (1991). "Biofilm detachment mechanisms in a liquid-fluidized bed." Biotechnology and Bioengineering **38**(5): 499-506.

Christensen, B. B., Sternberg, C., Andersen, J. B., Palmer, R. J., Nielsen, A. T., Givskov, M. and Molin, S. (1999). "Molecular tools for study of biofilm physiology." Biofilms **310**: 20-42.

Costello, M. C., Tossell, D. A., Reece, D. M., Brierley, C. J. and Savage, J. A. (1994). "Diamond protective coatings for optical-components." Diamond and Related Materials **3**(8): 1137-1141.

Costerton, J. W., Stewart, P. S. and Greenberg, E. P. (1999). "Bacterial biofilms: A common cause of persistent infections." Science **284**(5418): 1318-1322.

Da Re, S. and Ghigo, J. M. (2006). "A CsgD-independent pathway for cellulose production and biofilm formation in *Escherichia coli*." Journal of Bacteriology **188**(8): 3073-3087.

Danese, P. N., Pratt, L. A. and Kolter, R. (2000). "Exopolysaccharide production is required for development of *Escherichia coli* K-12 biofilm architecture." Journal of Bacteriology **182**(12): 3593-3596.

Danilenko, V. V. (2004). "On the history of the discovery of nanodiamond synthesis." Physics of the Solid State **46**(4): 595-599.

Das, T., Sharma, P. K., Busscher, H. J., van der Mei, H. C. and Krom, B. P. (2010). "Role of extracellular DNA in initial bacterial adhesion and surface aggregation." Applied and Environmental Microbiology **76**(10): 3405-3408.

Davey, M. E. and O'Toole, G. A. (2000). "Microbial biofilms: From ecology to molecular genetics." Microbiology and Molecular Biology Reviews **64**(4): 847-+.

Dewanti, R. and Wong, A. C. L. (1995). "Influence of culture conditions on biofilm formation by *Escherichia coli* O157: H7." International Journal of Food Microbiology. **26**(2): 147-164.

Dickinson, R. B., Nagel, J. A., McDevitt, D., Foster, T. J., Proctor, R. A. and Couper, S. L. (1995). "Quantitative comparison of clumping factor-mediated and coagulase-mediated *Staphylococcus aaureus* adhesion to surface-bound fibrinogen under flow." Infection and Immunity **63**(8): 3143-3150.

Dolmatov, V. Y. (2001). "Detonation synthesis ultradispersed diamonds: Properties and applications." Uspekhi Khimii **70**(7): 687-708.

Donelli, G. (2014). Microbial biofilms - methods and protocols. New York, Humana Press.

Donlan, R., Murga, R., Carpenter, J., Brown, E., Besser, R. and Fields, B. (2002). "Monochloramine disinfection of biofilm-associated legionella pneumophila in a potable water model system." American Society Microbiology

Donlan, R. M. (2002). "Biofilms: Microbial life on surfaces." Emerging Infectious Diseases **8**(9): 881-890.

Dufrene, Y. F. (2008). "Towards nanomicrobiology using atomic force microscopy." Nature Reviews Microbiology **6**(9): 674-680.

Edwards, K. J. and Rutenberg, A. D. (2001). "Microbial response to surface microtopography: The role of metabolism in localized mineral dissolution." Chemical Geology **180**(1-4): 19-32.

Elvers, K. T., Leeming, K., Moore, C. P. and Lappin-Scott, H. M. (1998). "Bacterial-fungal biofilms in flowing water photo-processing tanks." Journal of Applied Microbiology **84**(4): 607-618.

Erdemir, A., Fenske, G. R., Krauss, A. R., Gruen, D. M., McCauley, T. and Csencsits, R. T. (1999). "Tribological properties of nanocrystalline diamond films." Surface & Coatings Technology **120**: 565-572.

Ferrari, A. C. and Robertson, J. (2001). "Origin of the 1150-cm^{-1} Raman mode in nanocrystalline diamond." Physical Review B **63**(12).

Flemming, H. C. and Wingender, J. (2010). "The biofilm matrix." Nature Reviews Microbiology **8**(9): 623-633.

Fletcher, M. and Loeb, G. I. (1979). "Influence of substratum characteristics on the attachment of a marine pseudomonad to solid-surfaces." Applied and Environmental Microbiology **37**(1): 67-72.

Gallaher, T. K., Wu, S., Webster, P. and Aguilera, R. (2013). "Identification of biofilm proteins in non-typeable haemophilus influenzae." BMC Microbiology **13**.

Gibson, N. M., Luo, T. J. M., Brenner, D. W. and Shenderova, O. (2011). "Immobilization of mycotoxins on modified nanodiamond substrates." Biointerphases **6**(4): 210-217.

Goeres, D. M., Loetterle, L. R., Hamilton, M. A., Murga, R., Kirby, D. W. and Donlan, R. M. (2005). "Statistical assessment of a laboratory method for growing biofilms." Microbiology-(UK) **151**: 757-762.

Gottenbos, B., Busscher, H. J. and van der Mei, H. C. (2002). "Pathogenesis and prevention of biomaterial centered infections." Journal of Materials Science-Materials in Medicine **13**(8): 717-722.

Gracio, J. J., Fan, Q. H. and Madaleno, J. C. (2010). "Diamond growth by chemical vapour deposition." Journal of Physics D-Applied Physics **43**(37).

Grausova, L., Bacakova, L., Kromka, A., Potocky, S., Vanecek, M., Nesladek, M. and Lisa, V. (2009). "Nanodiamond as promising material for bone tissue engineering." Journal of Nanoscience and Nanotechnology **9**(6): 3524-3534.

Grieten, L., Janssens, S. D., Ethirajan, A., Vanden Bon, N., Ameloot, M., Michiels, L., Haenen, K. and Wagner, P. (2011). "Real-time study of protein adsorption on thin nanocrystalline diamond." Phys. Status Solidi A-Applications and Materials Science **208**(9): 2093-2098.

Grill, A. (1999). "Diamond-like carbon: State of the art." Diamond and Related Materials **8**(2–5): 428-434.

Hadi, R., Vickery, K., Deva, A. and Charlton, T. (2010). "Biofilm removal by medical device cleaners: Comparison of two bioreactor detection assays." Journal of Hospital Infection **74**(2): 160-167.

Hall-Stoodley, L., Costerton, J. W. and Stoodley, P. (2004). "Bacterial biofilms: From the natural environment to infectious diseases." Nature Reviews Microbiology **2**(2): 95-108.

Hanna, A., Berg, M., Stout, V. and Razatos, A. (2003). "Role of capsular colanic acid in adhesion of uropathogenic *Escherichia coli*." Applied and Environmental Microbiology **69**(8): 4474-4481.

Hannig, C., Huber, K., Lambrichts, I., Graeser, J., D'Haen, J. and Hannig, M. (2007). "Detection of salivary alpha-amylase and lysozyme exposed on the pellicle formed in situ on different materials." Journal of Biomedical Materials Research Part A **83A**(1): 98-103.

Hannig, C., Follo, M., Hellwig, E. and Al-Ahmad, A. (2010). "Visualization of adherent micro-organisms using different techniques." Journal of Medical Microbiology **59**(1): 1-7.

Hermansson, M. (1999). "The DLVO theory in microbial adhesion." Colloids and Surfaces B-Biointerfaces **14**(1-4): 105-119.

Ishihara, M., Kosaka, T., Nakamura, T., Tsugawa, K., Hasegawa, M., Kokai, F. and Koga, Y. (2006). "Antibacterial activity of fluorine incorporated dlc films." Diamond and Related Materials **15**(4-8): 1011-1014.

Itoh, Y., Wang, X., Hinnebusch, B. J., Preston, J. F. and Romeo, T. (2005). "Depolymerization of β-1,6-N-acetyl-D-glucosamine disrupts the integrity of diverse bacterial biofilms." Journal of Bacteriology **187**(1): 382-387.

Ivanova, E. P., Alexeeva, Y. V., Pham, D. K., Wright, J. P. and Nicolau, D. V. (2006). "ATP level variations in heterotrophic bacteria during attachment on hydrophilic and hydrophobic surfaces." International Microbiology **9**(1): 37-46.

Izak, T., Babchenko, O., Varga, M., Potocky, S. and Kromka, A. (2012). "Low temperature diamond growth by linear antenna plasma CVD over large area." Physica Status Solidi B-Basic Solid State Physics **249**(12): 2600-2603.

J.William Casterton, Z. L., Douglas E. Caldwell, Darren R. Korber, Hilary M. Lappin-Scott (1995). "Microbial biofilms." Annual Review of Microbiology.

Jakubowski, W., Bartosz, G., Niedzielski, P., Szymanski, W. and Walkowiak, B. (2004). "Nanocrystalline diamond surface is resistant to bacterial colonization." Diamond and Related Materials **13**(10): 1761-1763.

Jucker, B. A., Zehnder, A. J. B. and Harms, H. (1998). "Quantification of polymer interactions in bacterial adhesion." Environmental Science & Technology **32**(19): 2909-2915.

Karatan, E. and Watnick, P. (2009). "Signals, regulatory networks, and materials that build and break bacterial biofilms." Microbiology and Molecular Biology Reviews **73**(2): 310.

Katsikogianni, M., Spiliopoulou, I., Dowling, D. P. and Missirlis, Y. F. (2006). "Adhesion of slime producing *Staphylococcus epidermidis* strains to PVC and diamond-like carbon/silver/fluorinated coatings." Journal of Materials Science-Materials in Medicine **17**(8): 679-689.

Katsikogianni M., M. Y. F. (2004). "Concise review of mechanisms of bacterial adhesion to biomaterials and of techniques used in estimating bacteria-material interactions." European Cells and Materials **8**.

Kawarada, H. and Ruslinda, A. R. (2011). "Diamond electrolyte solution gate FETs for DNA and protein sensors using DNA/RNA aptamers." Physica Status Solidi A-Applications and Material Science **208**(9): 2005-2016.

Kirov, S. M. (2003). "Bacteria that express lateral flagella enable dissection of the multifunctional roles of flagella in pathogenesis." FEMS Microbiology Letters **224**(2): 151-159.

Kjaergaard, K., Schembri, M. A., Hasman, H. and Klemm, P. (2000). "Antigen 43 from *Escherichia coli* induces inter- and intraspecies cell aggregation and changes in colony morphology of *Pseudomonas fluorescens*." Journal of Bacteriology **182**(17): 4789-4796.

Kozak, H., Kromka, A., Ukraintsev, E., Houdkova, J., Ledinsky, M., Vanecek, M. and Rezek, B. (2009a). "Detecting sp^2 phase on diamond surfaces by atomic force microscopy phase imaging and its effects on surface conductivity." Diamond and Related Materials **18**(5-8): 722-725.

Kozak, H., Kromka, A., Ledinsky, M. and Rezek, B. (2009b). "Enhancing nanocrystalline diamond surface conductivity by deposition temperature and chemical post-processing." Physica Status Solidi A- Applications and Material Science **206**(2): 276-280.

Kozak, H., Babchenko, O., Artemenko, A., Ukraintsev, E., Remes, Z., Rezek, B. and Kromka, A. (2014). "Nanostructured diamond layers enhance the infrared spectroscopy of biomolecules." Langmuir **30**(8): 2054-2060.

Kromka, A., Potocky, S., Cermak, J., Rezek, B., Potmesil, J., Zemek, J. and Vanecek, M. (2008a). "Early stage of diamond growth at low temperature." Diamond and Related Materials **17**(7-10): 1252-1255.

Kromka, A., Rezek, B., Remes, Z., Michalka, M., Ledinsky, M., Zemek, J., Potmesil, J. and Vanecek, M. (2008b). "Formation of continuous nanocrystalline diamond layers on glass and silicon at low temperatures." Chemical Vapor Deposition **14**(7-8): 181-186.

Lacqua, A., Wanner, O., Colangelo, T., Martinotti, M. G. and Landini, P. (2006). "Emergence of biofilm-forming subpopulations upon exposure of *Escherichia coli* to environmental bacteriophages." Applied and Environmental Microbiology **72**(1): 956-959.

Lai, L. and Barnard, A. S. (2015). "Functionalized nanodiamonds for biological and medical applications." Journal of Nanoscience and Nanotechnology **15**(2): 989-999.

Lappin-Scott, H., Burton, S. and Stoodley, P. (2014). "Revealing a world of biofilms - the pioneering research of Bill Costerton." Nature Reviews Microbiology **12**(11): 781-787.

Lewis, J. S., Gittard, S. D., Narayan, R. J., Berry, C. J., Brigmon, R. L., Ramamurti, R. and Singh, R. N. (2010). "Assessment of microbial biofilm growth on nanocrystalline diamond in a continuous perfusion environment." Journal of Manufacturing Science and Engineering - Transactions of the ASME **132**(3).

Li, B. K. and Logan, B. E. (2004). "Bacterial adhesion to glass and metal-oxide surfaces." Colloids and Surfaces B: Biointerfaces **36**(2): 81-90.

Lifshitz, Y. (1999). "Diamond-like carbon — present status." Diamond and Related Materials **8**(8–9): 1659-1676.

Liu, C., Zhao, Q., Liu, Y., Wang, S. and Abel, E. W. (2008). "Reduction of bacterial adhesion on modified DLC coatings." Colloids and Surfaces B: Biointerfaces **61**(2): 182-187.

Liu, Y. and Tay, J. H. (2001). "Metabolic response of biofilm to shear stress in fixed-film culture." Journal of Applied Microbiology **90**(3): 337-342.

Liu, Y. and Tay, J. H. (2002). "The essential role of hydrodynamic shear force in the formation of biofilm and granular sludge." Water Research **36**(7): 1653-1665.

Liu, Z., Niu, H., Wu, S. Y. and Huang, R. (2014). "CsgD regulatory network in a bacterial trait-altering biofilm formation." Emerging Microbes & Infections **3**.

Maeyama, R., Mizunoe, Y., Anderson, J. M., Tanaka, M. and Matsuda, T. (2004). "Confocal imaging of biofilm formation process using fluoroprobed *Escherichia coli* and fluoro-stained exopolysaccharide." Journal of Biomedical Materials Research Part A **70A**(2): 274-282.

Marciano, F. R., Lima-Oliveira, D. A., Da-Silva, N. S., Diniz, A. V., Corat, E. J. and Trava-Airoldi, V. J. (2009a). "Antibacterial activity of DLC films containing tio_2 nanoparticles." Journal of Colloid and Interface Science **340**(1): 87-92.

Marciano, F. R., Bonetti, L. F., Da-Silva, N. S., Corat, E. J. and Trava-Airoldi, V. J. (2009b). "Wettability and antibacterial activity of modified diamond-like carbon films." Applied Surface Science **255**(20): 8377-8382.

Marciano, F. R., Bonetti, L. F., Mangolin, J. F., Da-Silva, N. S., Corat, E. J. and Trava-Airoldi, V. J. (2011). "Investigation into the antibacterial property and bacterial adhesion of diamond-like carbon films." Vacuum **85**(6): 662-666.

Mayer, C., Moritz, R., Kirschner, C., Borchard, W., Maibaum, R., Wingender, J. and Flemming, H. C. (1999). "The role of intermolecular interactions: Studies on model systems for bacterial biofilms." International Journal of Biological Macromolecules **26**(1): 3-16.

Medina, O., Nocua, J., Mendoza, F., Gomez-Moreno, R., Avalos, J., Rodriguez, C. and Morell, G. (2012). "Bactericide and bacterial anti-adhesive properties of the nanocrystalline diamond surface." Diamond and Related Materials **22**: 77-81.

Meinhardt, T., Lang, D., Dill, H. and Krueger, A. (2011). "Pushing the functionality of diamond nanoparticles to new horizons: Orthogonally functionalized nanodiamond using click chemistry." Advanced Functional Materials **21**(3): 494-500.

Mochalin, V. N., Shenderova, O., Ho, D. and Gogotsi, Y. (2012). "The properties and applications of nanodiamonds." Nature Nanotechnology **7**(1): 11-23.

Moore, W. J. (1979). Fyzikální chemie. Praha, SNTL - Nakladatelství technické literatury.

Morris, N. S., Stickler, D. J. and McLean, R. J. C. (1999). "The development of bacterial biofilms on indwelling urethral catheters." World Journal of Urology **17**(6): 345-350.

Neykova, N., Kozak, H., Ledinsky, M. and Kromka, A. (2012). "Novel plasma treatment in linear antenna microwave pecvd system." Vacuum **86**(6): 603-607.

O'Toole, G. A. and Kolter, R. (1998). "Initiation of biofilm formation in *Pseudomonas Fluorescens* WCS365 proceeds via multiple, convergent signalling pathways: A genetic analysis." Molecular Microbiology **28**(3): 449-461.

O'Toole, G. A., Pratt, L. A., Watnick, P. I., Newman, D. K., Weaver, V. B. and Kolter, R. (1999). "Genetic approaches to study of biofilms." Biofilms **310**: 91-109.

O'Toole, G., Kaplan, H. B., Kolter, R. (2000). "Biofilm formation as microbial development." Annual Review of Microbiology **54**: 49-79.

Oh, Y. J., Jo, W., Yang, Y. and Park, S. (2007). "Influence of culture conditions on *Escherichia coli* O157: H7 biofilm formation by atomic force microscopy." Ultramicroscopy **107**(10-11): 869-874.

Oh, Y. J., Lee, N. R., Jo, W., Jung, W. K. and Lim, J. S. (2009). "Effects of substrates on biofilm formation observed by atomic force microscopy." Ultramicroscopy **109**(8): 874-880.

Olsen, A., Jonsson, A. and Normark, S. (1989). "Fibronectin binding mediated by a novel class of surface organelles on *Escherichia coli*." Nature **338**(6217): 652-655.

Passerini, L., Lam, K., Costerton, J. W. and King, E. G. (1992). "Biofilms on indwelling vascular catheters." Critical Care Medicine **20**(5): 665-673.

Peeters, E., Nelis, H. J. and Coenye, T. (2008). "Comparison of multiple methods for quantification of microbial biofilms grown in microtiter plates." Journal of Microbiological Methods **72**(2): 157-165.

Ploux, L., Beckendorff, S., Nardin, M. and Neunlist, S. (2007). "Quantitative and morphological analysis of biofilm formation on self-assembled monolayers." Colloids and Surfaces B: Biointerfaces **57**(2): 174-181.

Pratt, L. A. and Kolter, R. (1998). "Genetic analysis of *Escherichia coli* biofilm formation: Roles of flagella, motility, chemotaxis and type I pili." Molecular Microbiology **30**(2): 285-293.

Pratt, L. A. and Kolter, R. (1999). "Genetic analyses of bacterial biofilm formation." Current Opinion in Microbiology **2**(6): 598-603.

Prigent-Combaret, C., Prensier, G., Le Thi, T. T., Vidal, O., Lejeune, P. and Dorel, C. (2000). "Developmental pathway for biofilm formation in curli-producing *Escherichia coli* strains: Role of flagella, curli and colanic acid." Environmental Microbiology **2**(4): 450-464.

Redfield, R. J. (2002). "Is quorum sensing a side effect of diffusion sensing?" Trends in Microbiology **10**(8): 365-370.

Rijnaarts, H. H. M., Norde, W., Bouwer, E. J., Lyklema, J. and Zehnder, A. J. B. (1993). "Bacterial adhesion under static and dynamic conditions." Applied and Environmental Microbiology **59**(10): 3255-3265.

Romeo, T., Ed. (2008). Bacterial biofilms, Springer.

Romling, U. (2002). "Molecular biology of cellulose production in bacteria." Research in Microbiology **153**(4): 205-212.

Rosenberg, M., Gutnick, D. and Rosenberg, E. (1980). "Adherence of bacteria to hydrocarbons - a simple method for measuring cell-surface hydrophobicity." FEMS Microbiology Letters **9**(1): 29-33.

Scheuerman, T. R., Camper, A. K. and Hamilton, M. A. (1998). "Effects of substratum topography on bacterial adhesion." Journal of Colloid and Interface Science **208**(1): 23-33.

Schrand, A. M., Hens, S. A. C. and Shenderova, O. A. (2009). "Nanodiamond particles: Properties and perspectives for bioapplications." Critical Reviews in Solid State and Materials Sciences **34**(1-2): 18-74.

Schwartz, T., Hoffmann, S. and Obst, U. (2003). "Formation of natural biofilms during chlorine dioxide and u.v. disinfection in a public drinking water distribution system." Journal of Applied Microbiology **95**(3): 591-601.

Seth, J., Babu, S. V., Ralchenko, V. G., Kononenko, T. V., Ageev, V. P. and Strelnitsky, V. E. (1995). "Lithographic application of diamond-like carbon films." Thin Solid Films **254**(1-2): 92-95.

Shao, W., Zhao, Q., Abel, E. W. and Bendavid, A. (2009). "Influence of interaction energy between Si-doped diamond-like carbon films and bacteria on bacterial adhesion under flow conditions." Journal of Biomedical Materials Research part A **93**(1): 133-139.

Shoda, M. and Sugano, Y. (2005). "Recent advances in bacterial cellulose production." Biotechnology and Bioprocess Engineering **10**(1): 1-8.

Sjollema, J., Busscher, H. J. and Weerkamp, A. H. (1989). "Real-time enumeration of adhering microorganisms in a parallel plate flow cell using automated image-analysis." Journal of Microbiological Methods **9**(2): 73-78.

Smeets, E., Kooman, J., van der Sande, F., Stobberingh, E., Frederik, P., Claessens, P., Grave, W., Schot, A., *et al.* (2003). "Prevention of biofilm formation in dialysis water treatment systems." Kidney International **63**(4): 1574-1576.

Stepanovic, S., Vukovic, D., Dakic, I., Savic, B. and Svabic-Vlahovic, M. (2000). "A modified microtiter-plate test for quantification of staphylococcal biofilm formation." Journal of Microbiological Methods **40**(2): 175-179.

Stewart, C. R., Muthye, V. and Cianciotto, N. P. (2012). "*Legionella pneumophila* persists within biofilms formed by *Klebsiella pneumoniae*, *Flavobacterium sp.*, and *Pseudomonas fluorescens* under dynamic flow conditions." PLoS One **7**(11).

Stewart, P. S. and Costerton, J. W. (2001). "Antibiotic resistance of bacteria in biofilms." Lancet **358**(9276): 135-138.

Stoodley, P., Sauer, K., Davies, D. G. and Costerton, J. W. (2002). "Biofilms as complex differentiated communities." Annual Review of Microbiology **56**: 187-209.

Sutherland, I. W. (2001). "The biofilm matrix - an immobilized but dynamic microbial environment." Trends in Microbiology **9**(5): 222-227.

Taylor, R. L., Verran, J., Lees, G. C. and Ward, A. J. P. (1998). "The influence of substratum topography on bacterial adhesion to polymethyl methacrylate." Journal of Materials Science-Materials in Medicine **9**(1): 17-22.

Tegoulia, V. A. and Cooper, S. L. (2002). "*Staphylococcus aureus* adhesion to self-assembled monolayers: Effect of surface chemistry and fibrinogen presence." Colloids and Surfaces B: Biointerfaces **24**(3-4): 217-228.

Thormann, K. M., Saville, R. M., Shukla, S., Pelletier, D. A. and Spormann, A. M. (2004). "Initial phases of biofilm formation in *Shewanella oneidensis* MR-1." Journal of Bacteriology **186**(23): 8096-8104.

Thuptimdang, P., Limpiyakorn, T., McEvoy, J., Pruss, B. M. and Khan, E. (2015). "Effect of silver nanoparticles on *Pseudomonas putida* biofilms at different stages of maturity." Journal of Hazardous Materials **290**: 127-133.

Uo, M., Akasaka, T., Watari, F., Sato, Y. and Tohji, K. (2011). "Toxicity evaluations of various carbon nanomaterials." Dental Materials Journal **30**(3): 245-263.

Wang, X., Preston, J. F. and Romeo, T. (2004). "The pgaABC locus of *Escherichia coli* promotes the synthesis of a polysaccharide adhesin required for biofilm formation." Journal of Bacteriology **186**(9): 2724-2734.

Watnick, P. and Kolter, R. (2000). "Biofilm, city of microbes." Journal of Bacteriology **182**(10): 2675-2679.

Watnick, P. I., Fullner, K. J. and Kolter, R. (1999). "A role for the mannose-sensitive hemagglutinin in biofilm formation by *Vibrio cholerae* El Tor." Journal of Bacteriology **181**(11): 3606-3609.

Wehling, J., Dringen, R., Zare, R. N., Maas, M. and Rezwan, K. (2014). "Bactericidal activity of partially oxidized nanodiamonds." ACS Nano **8**(6): 6475-6483.

Williams, O. A., Nesladek, M., Daenen, M., Michaelson, S., Hoffman, A., Osawa, E., Haenen, K. and Jackman, R. B. (2008). "Growth, electronic properties and applications of nanodiamond." Diamond and Related Materials **17**(7-10): 1080-1088.

Williams, V. and Fletcher, M. (1996). "*Pseudomonas fluorescens* adhesion and transport through porous media are affected by lipopolysaccharide composition." Applied and Environmental Microbiology **62**(1): 100-104.

Yokota T, T. T., Kobayashi T, Meguro T., Iwaki M. (2007). "Cell adhesion to nitrogen-doped DLCs fabricated by plasma-based ion implantation and deposition method using toluene gas."

Zemek, J., Houdkova, J., Lesiak, B., Jablonski, A., Potmesil, J. and Vanecek, M. (2006). "Electron spectroscopy of nanocrystalline diamond surfaces." Journal of Optoelectronics and Advanced Materials **8**(6): 2133-2138.

Zhao, Q., Liu, Y., Wang, C. and Wang, S. (2007). "Bacterial adhesion on silicon-doped diamond-like carbon films." Diamond and Related Materials **16**(8): 1682-1687.

Zogaj, X., Nimtz, M., Rohde, M., Bokranz, W. and Romling, U. (2001). "The multicellular morphotypes of *Salmonella typhimurium* and *Escherichia coli* produce cellulose as the second component of the extracellular matrix." Molecular Microbiology **39**(6): 1452-1463.

Zogaj, X., Bokranz, W., Nimtz, M. and Romling, U. (2003). "Production of cellulose and curli fimbriae by members of the family *Enterobacteriaceae* isolated from the human gastrointestinal tract." Infection and Immunity **71**(7): 4151-4158.